

AN UNCERTAINTY RELATION BASED STUDY OF QUANTUM CORRELATIONS

Ph.D. Thesis

by

Manju



Department of Physics
Indian Institute of Technology Ropar

Rupnagar, Punjab 140001, India

March 2024

An Uncertainty Relation Based Study of Quantum Correlations

By
Manju

Submitted
in fulfillment of the requirements for the degree
of
Doctor of Philosophy



Department of Physics
Indian Institute of Technology Ropar
March 2024

Manju: *An Uncertainty Relation Based Study of Quantum Correlations*

Copyright ©2024, Indian Institute of Technology Ropar

All Rights Reserved

This thesis is dedicated to
My Supervisors,
My Parents and My Family

Certificate

It is certified that the work contained in this thesis entitled “**An Uncertainty Relation Based Study of Quantum Correlations**” by **Ms. Manju**, a student in the Department of Physics, to Indian Institute of Technology Ropar, for the award of degree of **Doctor of Philosophy** has been carried out under my supervision and this work has not been submitted elsewhere for a degree.

March 2024



Dr. Asoka Biswas

Associate Professor

Department of Physics

Indian Institute of Technology Ropar



and

Dr. Shubhrangshu Dasgupta

Associate Professor

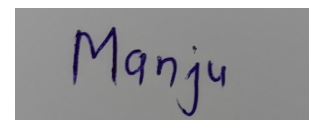
Department of Physics

Indian Institute of Technology Ropar

Declaration

I hereby declare that the work presented in the thesis entitled “**An Uncertainty Relation Based Study of Quantum Correlations**” submitted for the degree of **Doctor of Philosophy** in Physics by me to Indian Institute of Technology Ropar has been carried out under the supervision of **Dr. Asoka Biswas** and **Dr. Shubhrangshu Dasgupta**. This work is original and has not been submitted in part or full by me elsewhere for a degree.

March 2024

A rectangular box containing a handwritten signature in dark blue ink that reads "Manju".

Manju

PhD Research Scholar

Department of Physics

Indian Institute of Technology Ropar

Acknowledgements

First and foremost, I would like to express my sincere gratitude to my supervisors, Dr. Asoka Biswas and Dr. Shubhrangshu Dasgupta, for providing me with the opportunity to conduct my research work under their guidance. I am extremely grateful for their invaluable guidance throughout this journey. Their perpetual support, knowledge, and experience have been a sustaining pillar, providing me emotional strength whenever I needed it.

I would like to acknowledge the support of the members of my doctoral committee: Dr. Subhendu Sarkar, Dr. Rajesh V. Nair, and Dr. Sandeep Gautam from the Physics Department and Dr. Rohit Y. Sharma from the Electrical Engineering Department.

I am grateful to IIT Ropar, and Ministry of Human Resource and Development, Government of India for the financial support. I am thankful to the Department of Physics, IIT Ropar for providing the essential assistance, resources and computation facilities. I also appreciate the help from Mr. Anshu vaid, the lab assistants and the department's staff over these years.

I am thankful to my group members: Suman Chand, Chaten Waghela, Chayan Purkait, Nancy, Jatin, Ratnakaran, Parkhi, Shilpi, Monirul and Shivangi for their friendly nature and selfless help whenever I required it. I also appreciate the persistent support of my senior Devender Garg who always helped me to properly understand the nuances of the research.

I would take the opportunity to express my gratitude to the friends who have been a part of this journey. Each one of you has played a unique and significant role in making this chapter of my life truly memorable. Param has been there through the highs and lows of this journey. I am so thankful for the wonderful times Param, Nancy, Rajat and I have shared together during our tea breaks. Bipasha, Arzoo, Shagun, Monika and Kusum support and companionship have made this phase of life all the more enjoyable. I would

like to thank my labmates Daman, Rakhi, Raghav, Sanjay, Nitin, Pardeep, Sahil, Vasu and Mukesh for their wonderful friendship throughout the years.

Now, I would take a moment to express my deepest gratitude to my family. My parents, for their unconditional love, unshaken faith and support. I have experienced your guidance day by day. My brother, for always being there for me. My sisters for their love, support and encouragement. A special thanks to my father-in-law, mother-in-law and in-law's family for their support. I am immensely grateful for the love and companionship that my husband, Rohit, has brought into my life. Rohit has stood by me during the stressful moments of uncertainty. In times when I felt upset or discouraged, Rohit provided a listening ear and offered words of encouragement.

Finally, my gratitude and praise towards God, who has bestowed His grace and strength upon me throughout my life.

Manju
Indian Institute of Technology Ropar,
India-140001
March 2024

Abstract

Quantum mechanics has long been a subject of fascination and intense study, challenging our classical intuition and offering unique insights into the behavior of particles at the smallest scales. Among its fundamental principles, the uncertainty principle, as articulated by Heisenberg, lays the groundwork for understanding the limitations of simultaneous measurements of complementary observables. Quantum correlations, such as entanglement, and the emerging concept of quantum synchronization, represent intriguing phenomena that transcend classical boundaries and have the potential to revolutionize information processing and communication technologies. This thesis delves into the multifaceted world of quantum correlations, entanglement and quantum synchronization, using the framework of uncertainty relations as a guiding light. The first part of this study explores the effect of linear and quadratic coupling on the entanglement and quantum synchronization between two indirectly coupled mechanical oscillators in a double cavity optomechanical system. Our investigation revealed that the quadratic coupling, in particular, plays a pivotal role in preserving both entanglement and quantum synchronization simultaneously. Following this findings, in the second part of the thesis, we do a similar analysis in a more generic optomechanical system. This analysis is expected to provide some insight into correlated behavior of synchronization and entanglement. By employing uncertainty-based synchronization measure and entanglement criterion, we probed the generalized relation between entanglement and quantum synchronization. This approach unveils the intricate connections between the two independent phenomena, offering insights into how the presence of entanglement can facilitate the complete quantum synchronization. The final part of our research delves into generalized uncertainty relations that extend beyond the traditional position-momentum pair. These extended uncertainty inequalities serve as a foundational tool in understanding the inherent limitations governing quantum systems. Moreover, we employ these relations to formulate a stronger uncertainty-based entanglement criterion, providing a fresh perspective on the characterization of entangled bipartite mixed states.

Keywords: quantum synchronization, entanglement, uncertainty relation, cavity optomechanics

Contents

1	Introduction	1
1.1	Cavity Quantum Optomechanics : Basic Theory	2
1.2	Generic Model of an Optomechanical System	3
1.2.1	Generic Optomechanical Hamiltonian	4
1.2.2	Quantum Langevin Equation	6
1.2.3	Dissipation	7
1.2.4	Input Fluctuation	7
1.2.5	Input-Output Theory	8
1.2.6	Optomechanical Equations of Motion	11
1.3	Synchronization	14
1.3.1	Pearson Factor	16
1.3.2	Synchronization error	17
1.4	Entanglement	18
1.4.1	Peres-Horodecki Criterion	19
1.4.2	Entanglement Witness	20
1.4.3	Peres-Horodecki Criterion for Continuous Variable	21
1.4.4	Uncertainty Principle based Entanglement Criterion	22
1.5	Outline of Thesis	25
2	Quantum synchronization and entanglement between two indirectly cou-	

pled oscillators	29
2.1 Motivation	29
2.2 Model	33
2.3 Langevin equations	35
2.4 Simultaneous Entanglement and Synchronization	37
2.4.1 Numerical Results and Discussion	42
2.4.2 Effect of indirect coupling and quadratic coupling	44
2.5 Conclusion	45
3 Entanglement boosts quantum synchronization between two oscillators	49
3.1 Motivation	49
3.2 Theoretical Model	53
3.2.1 Solution in mean-field approximation	57
3.2.2 Numerical results	60
3.3 Analytic solution of fluctuations	62
3.3.1 Asymptotic solutions of first moments	62
3.3.1.1 Obtaining the Fourier coefficients of Q_- and P_-	63
3.3.1.2 Obtaining the Fourier coefficients $A_{-1,0,1}$	64
3.3.1.3 Obtaining the Fourier coefficients of Q_+ and P_+	65
3.3.2 Frequency spectrum of fluctuations	66
3.3.2.1 Derivation of mean square fluctuations	68
3.3.3 Generic relation between entanglement and quantum synchronization	71
3.3.4 Numerical results	72
3.4 Conclusion	74
4 Strong entanglement criteria for bipartite mixed states	77
4.1 Motivation	77
4.2 Wigner-Yanase Skew Information	80

4.3	Entanglement criteria based on the uncertainty relations	82
4.3.1	Modified uncertainty relations	82
4.3.2	Relation to the entanglement criteria	85
4.4	Examples	86
4.4.1	Two qubit pure states	86
4.4.2	Two qubit mixed states	87
4.4.2.1	Werner state	87
4.4.2.2	Werner derivative	90
4.4.2.3	An example of mixed non-maximally entangled state . . .	92
4.4.3	Two qutrit mixed states	93
4.4.3.1	Two-qutrit Werner state	93
4.4.4	Discussions	95
4.5	Conclusions	96
5	Summary and Outlook	99

List of Figures

1.1	Schematic diagram of basic optomechanical system	4
1.2	Schematic diagram of the single side cavity with the cavity field, the input and output fields	8
2.1	Schematic diagram of the two coupled cavity optomechanical systems. Each mechanical oscillator is suspended inside its respective cavity. The two cavity modes are externally coupled with each other via a coupling constant J	35
2.2	Variation of (a) the mean values of \bar{q}_1 (red) and \bar{q}_2 (blue), (b) the mean values of \bar{p}_1 (red) and \bar{p}_2 (blue), (c) complete synchronization S_q , (e) entanglement E_D , with respect to time (in the units of $\tau = 1/\omega_{m1}$). Parameters chosen are $\omega_{m1} = -\Delta_{c1} = 1$, $\omega_{m2} = -\Delta_{c2} = 1.005$, $\bar{n}_{mj} = 0$, $g_1 = 0.005$, $g_2 = 0$, $\gamma_{mj} = 0.005$, $\kappa_j = 0.15$, $E = 100$, $\eta_D = 1$, $\Omega_D = 1$ and $J = 0.04$. The inset shows the steady-state behavior of the oscillation of S_q and E_D	40
2.3	Variation of (a) the mean values of \bar{q}_1 (red) and \bar{q}_2 (blue), (b) the mean values of \bar{p}_1 (red) and \bar{p}_2 (blue), (c) synchronization S_q , and (e) entanglement E_D , with respect to time (in the units of $\tau = 1/\omega_{m1}$). Here we have chosen $g_2/g_1 = 1 \times 10^{-2}$, while all the other parameters are the same as in Fig. 2.2. The inset shows the steady-state behavior of the oscillation of S_q and E_D	41

2.4	(a) A parametric plot of the variation of time-averaged values of synchronization \bar{S}_q with the entanglement \bar{E}_D , when the number of thermal phonons \bar{n}_m varies from 0 to 5. The inset shows the zoomed version of the same plot in the regions of parameters when $\bar{E}_D \leq 0.25$. (b) Variation of time-averaged values of synchronization \bar{S}_q and entanglement \bar{E}_D between the mechanical oscillators with respect to frequency difference $\delta_m = \omega_{m2} - \omega_{m1}$ of the mechanical oscillators. The other parameters are the same as in Fig. 2.3.	42
3.1	Schematic illustration of a driven optical cavity with one oscillating end mirror (acting as a mechanical oscillator) and a membrane in the middle (acting as the second mechanical oscillator). The two oscillators indirectly interact with each other through their common coupling to the same cavity field via radiation pressure force. The optical cavity is driven by a strong amplitude-modulated blue-detuned laser drive to achieve self-sustained oscillations and synchronization of these oscillators.	53
3.2	(a) Limit-cycle trajectories in the $Q_1 \rightleftharpoons P_1$ (red) and $Q_2 \rightleftharpoons P_2$ (blue) spaces, Variation of (b) the mean values Q_1 (red) and Q_2 (blue), (c) the mean values P_1 (red) and P_2 (blue), (d) synchronization S_q , (e) entanglement E_D , with respect to time (in the units of $\tau = 1/\omega_{m1}$). The parameters chosen are $\omega_{m1} = -\Delta = 1$, $\omega_{m2} = 1.005$, $\bar{n}_{mj} = 0.5$, $g_1 = 5 \times 10^{-5}$, $g_2 = g_1 \times 10^{-2}$, $g_3 = 10^{-6}$, $\gamma_{mj} = 0.009$, $\kappa = 0.1$, $E = 250$, $\eta_D = 4$ and $\Omega_D = 1$. All frequencies are normalized with respect to ω_{m1} . (f) Evolution of time-averaged values of synchronization \bar{S}_q (blue) and entanglement \bar{E}_D (red) with respect to the frequency difference $\delta_m = \omega_{m2} - \omega_{m1}$ of the mechanical oscillators. [all the other parameters are the same as in (a)-(e) above].	59

3.3	Variation of (a) K from Eq. (3.48), (b) quantum synchronization S_q , (c) entanglement E_D between the mechanical oscillators as a function of modulation amplitude η_D and modulation frequency Ω_D with $E = 250$ and $\bar{n}_m = 0.5$. The other parameters are the same as in Fig. 3.2.	70
3.4	Variation of (a) quantum synchronization S_q and (b) entanglement E_D between the mechanical oscillators as a function of the driving field intensity E and the average number of thermal phonons \bar{n}_m with $\eta_D = 4$ and $\Omega_D = 1$. The other parameters are the same as in Fig. 3.2.	72

Chapter 1

Introduction

The urge to explore quantum correlations has motivated physicists for many years. The study of quantum correlations is important for advancing our understanding of quantum mechanics, developing new quantum technologies, exploring physics at the foundational level, and enabling practical applications that leverage the unique properties of quantum systems. It plays a pivotal role in the ongoing development and realization of quantum information science and technologies. It has practical implications for various real-world applications. For example, quantum cryptography relies on the security offered by quantum correlations [1], ensuring secure communication and data transmission. Quantum sensors utilizing quantum correlations [2] can offer enhanced sensitivity for precise measurements, impacting fields such as healthcare [3], and environmental monitoring [4].

In the quantum realm, the study of synchronization is relatively recent and has gained significant attention due to its potential implications for various fields, such as quantum information processing and communication [5, 6]. The phenomenon of spontaneous synchronization was first observed by Huygens in the 17th century [7]. A nice and detailed discussion of the generic nature of synchronization can be found in [8]. The phenomenon of spontaneous synchronization is universal and has been widely investigated in classical systems [9, 10, 11, 12, 13].

It is envisaged that quantum synchronization is a manifestation of certain correlations which are of purely quantum origin. There are some recent studies that explore the relation between quantum synchronization and different measures of quantum correlations [14, 15, 16, 17].

Entanglement [18] is one of the most well-known and extensively studied forms of quantum correlation. It lies at the heart of many intriguing and counter-intuitive phenomena in quantum physics and plays a crucial role in various areas. In this thesis, we will explore the phenomenon of quantum synchronization and its connection with entanglement. This thesis exclusively deals with this issue and attempts to develop a generic understanding of their inherent relation. Exploring these connections sheds light on the underlying mechanisms and implications of quantum synchronization. Optomechanical systems [19], which involve coupling mechanical oscillators to electromagnetic fields inside an optical cavity, provide a suitable platform for studying synchronization and its connection with entanglement. The coupling in these systems is nonlinear, leading to limit-cycle oscillations known as optomechanical self-oscillations. There are a number of excellent review articles [19] and books covering various aspects of cavity quantum optomechanics. In the following, we are going to discuss briefly only those facets of cavity quantum optomechanics that are relevant to the present thesis.

1.1 Cavity Quantum Optomechanics : Basic Theory

Cavity quantum optomechanics is a field of great research interest in physics [19, 20]. This field of research utilizes the tools of quantum optics in a variety of physics systems. Optomechanics studies the interaction between light and mechanical motion in a system consisting of a cavity that contains light and a mechanical resonator that can vibrate at certain frequencies. There are mechanical systems, such as cantilever, beams etc, on micro and nano scale, that can vibrate in the frequency range of kHz to GHz. The so-called radiation pressure induced interaction between photons and mechanical motion is

at the heart of cavity optomechanics [21]. The radiation pressure force, arising due to the momentum carried by light, can displace a movable end mirror of the cavity. This in turn changes the length of the cavity, resulting in the modification of the cavity frequency. The interaction between light and mechanical motion is nonlinear in nature. This nonlinear interaction has led to the exploration of a wide variety of interesting phenomena, such as squeezing of the light field and mechanical motion, synchronization between mechanical modes [14, 22, 23, 24, 25], entanglement between optical [26] and mechanical modes [27, 28], optomechanical normal mode splitting [29, 30], optomechanically induced transparency [31, 32], and so on, both theoretically and experimentally.

1.2 Generic Model of an Optomechanical System

Basic optomechanical system consists of an optical cavity with two mirrors, one fixed and the other movable, separated by some distance (say L) [19] as shown in Fig. 1.1. The cavity is driven by a laser source of amplitude E and frequency ω_l . When a light field is injected into a cavity, the cavity enhances the intensity of the light due to multiple reflections. As the intracavity photons interact with the cavity's mechanically-adaptable end mirror, the radiation pressure force exerted by the photons results in a continuous transfer of momentum to the mirror. This transfer of momentum gives rise to mechanical degrees of freedom associated with the mirror's motion. The mirror behaves as a mechanical oscillator with harmonic modes of vibration. One can then focus on that single optical mode of the cavity (say with frequency $\omega_c = \frac{n\pi c}{L}$ with mode number n) which is close to the laser frequency. This in turn changes the length of cavity and modifies the cavity resonance frequency. Suppose Q is the displacement made by the mechanical mirror, the modified cavity resonance frequency is, as follows:

$$\omega_c(Q) = \frac{n\pi c}{L + Q} = \frac{\omega_c}{1 + \frac{Q}{L}} \approx \omega_c \left(1 - \frac{Q}{L}\right) \quad (1.1)$$

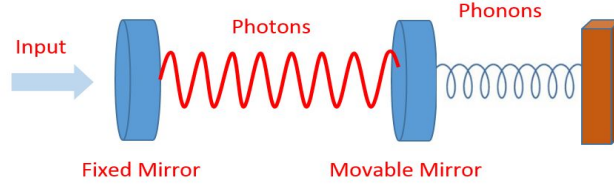


Figure 1.1: Schematic diagram of basic optomechanical system

1.2.1 Generic Optomechanical Hamiltonian

The generic total Hamiltonian H of the optomechanical system consists the optical contribution, mechanical contribution, interaction between optics and mechanics, laser drive and transfer of phonons and photons to and from environment. A very basic assumption to start with, is that these optical and mechanical modes can be represented as quantum harmonic oscillators with frequency ω_c and ω_m respectively. The Hamiltonian H of the system can then be written as follows:

$$H = \hbar\omega_c(Q)a^\dagger a + \frac{P^2}{2m} + \frac{m\omega_m^2}{2}Q^2 \quad (1.2)$$

On substituting (Eq. (1.1)), we get

$$H = \hbar\omega_c a^\dagger a + \frac{P^2}{2m} + \frac{m\omega_m^2}{2}Q^2 - \hbar g_l a^\dagger a Q \quad (1.3)$$

where $a^\dagger(a)$ is the creation (annihilation) operator of the optical mode, satisfying the commutation relation $[a, a^\dagger] = 1$, Q and P are the position and momentum operators of the mechanical oscillator with the commutation relation $[Q, P] = i\hbar$, which are defined as $Q = q_{zpf} (b + b^\dagger)$, $P = i\hbar m\omega_m q_{zpf} (b^\dagger - b)$ and g is the linear coupling constant between cavity and mechanical oscillator, which is defined as $g_l = \frac{\partial\omega_c}{\partial Q} = \frac{\omega_c}{L}$. Here $q_{zpf} = \sqrt{\frac{\hbar}{m\omega_m}}$ is the zero-point fluctuation of the mechanical mirror (of mass m). Typical order of q_{zpf} is

of 10^{-15} m. A detailed derivation of the Hamiltonian can be found in [33].

From the Hamiltonian (Eq. (1.3)), one can note the following points: Firstly, the optomechanical coupling between optical mode and mechanical mode is essentially nonlinear in nature. Secondly, this nonlinear coupling is weak in nature i.e., $g_l \ll \omega_m$ and, therefore is not able to show the desired quantum effect. However, one can achieve the strong effective optomechanical coupling by applying the strong drive to the cavity. To do so, we now add the coherent laser drive to the cavity which describes the addition of photon at laser frequency and its Hermitian conjugate inside the cavity. Thus, the total Hamiltonian takes the following form:

$$H = \hbar\omega_c a^\dagger a + \frac{P^2}{2m} + \frac{m\omega_m^2}{2} Q^2 - \hbar g_l a^\dagger a Q + \iota \hbar E (a^\dagger e^{-\iota\omega_l t} - a e^{\iota\omega_l t}) \quad (1.4)$$

Define the dimensionless position and momentum operators q and p as

$$\begin{aligned} q &= \sqrt{\frac{m\omega_m}{\hbar}} Q, \\ p &= \sqrt{\frac{1}{m\hbar\omega_m}} P, \end{aligned} \quad (1.5)$$

On substituting Eq. (1.5) in Eq. (1.4), we get

$$H = \hbar\omega_c a^\dagger a + \frac{\hbar\omega_m}{2} (q^2 + p^2) - \hbar g a^\dagger a q + \iota \hbar E (a^\dagger e^{-\iota\omega_l t} - a e^{\iota\omega_l t}) \quad (1.6)$$

where ω_l and E is the frequency and amplitude of the laser drive and $g = \frac{\omega_c}{L} \sqrt{\frac{\hbar}{m\omega_m}}$ is the scaled linear coupling constant. The driving amplitude E can also be written as, $E = \sqrt{\frac{P_l \kappa}{\hbar\omega_l}}$, where P_l is the power associated with laser field and κ is the decay rate of the cavity field. Note that the adopted mode corresponds to the ideal case of the one-sided cavity i.e., there is only one input-output port of the cavity and there is no additional photon loss. The explicit time-dependence in the above Hamiltonian can be removed by

switching to the rotating frame of laser frequency ω_l . The Hamiltonian (Eq. (1.6)) can be written in the following manner:

$$H = \hbar\Delta_c a^\dagger a + \frac{\hbar\omega_m}{2} (q^2 + p^2) - \hbar g a^\dagger a q + \imath\hbar E (a^\dagger - a) \quad (1.7)$$

where $\Delta_c = \omega_c - \omega_l$ is the detuning of cavity mode from the respective laser field. A typical order of cavity frequency (ω_c) is of 10^{15} Hz, whereas the order of mechanical frequency ω_m lies in the range of MHz to GHz. Therefore, the laser frequency is adjusted in such a way that its detuning Δ_c , from the cavity frequency, is comparable to mechanical frequency ω_m . Since the order of cavity frequency is very high, the effect of the thermal photons entering the cavity can therefore be safely neglected and the cavity can be considered to be coupled with a reservoir at zero temperature. However, the laser field introduces the noise into the system dynamics. On the other hand, thermal phonons plays an important role in the dynamics of mechanical mode. We will explore these environmental effects systematically in our thesis. Using the Hamiltonian (Eq. (1.7)), one can discuss the underlying physics of the cavity optomechanical system.

1.2.2 Quantum Langevin Equation

Optomechanical systems, like many other quantum systems, are considered open quantum systems. This means they interact with their surrounding environment, leading to fluctuations, dissipation, and the introduction of environmental noise into the system [34, 35]. This interaction with the environment can result in several effects like decay of cavity mode, damping of mechanical mode and insertion of noise from environment. Therefore, understanding and characterizing these effects are crucial for optimizing the performance of optomechanical systems and mitigating their impact on quantum correlations.

1.2.3 Dissipation

Since the photons and phonons are coupled to the environment, they experience losses. These losses define the cavity decay rate κ and the mechanical damping rate γ , respectively. The cavity decay rate and the mechanical damping rate determines the cavity quality factor $Q_c = \frac{\omega_c}{\kappa}$ and the mechanical quality factor $Q_m = \frac{\omega_m}{\gamma}$. The quality factor Q_c defines the total number of oscillation of a single photon inside the cavity before moving out. Similarly, Q_m defines the life time of phonon.

1.2.4 Input Fluctuation

As discussed before, environment adds noises to the the system and influences the system dynamics. However, the environment is modelled by a thermal bath of non-interacting harmonic oscillators. Therefore, the noise entering the system can be best approximated as Markovian, δ - correlated and zero-mean. Note that a system can be termed as Markovian if the present state of system does not depend on the past history. a_{in} and ξ are the input optical and mechanical noise operators, which in the Markovian approximation, satisfies the following two-time correlations [34, 36]:

$$\begin{aligned} \langle a_{in}(t) a_{in}^\dagger(t') \rangle &= \delta(t - t') , \\ \langle a_{in}^\dagger(t) a_{in}(t') \rangle &= 0 , \\ \langle \xi(t) \xi(t') \rangle &= \frac{\gamma_m}{2\pi\omega_m} \int \omega e^{-i\omega(t-t')} \left[1 + \coth \left(\frac{\hbar\omega}{2k_B T} \right) \right] d\omega , \end{aligned} \quad (1.8)$$

where k_B is the Boltzmann constant. The thermal bath is assumed to be in thermal equilibrium at a temperature T . The mechanical mode coupled to the thermal bath is influenced by a Brownian stochastic force described by $\xi(t)$. For the case of large quality factor of the oscillator i.e., $\omega_m \gg \gamma$, the Brownian noise operator can be approximated

as:

$$\langle \xi(t) \xi(t') \rangle = \gamma_m (2\bar{n}_m + 1) \delta(t - t') , \quad (1.9)$$

where $\bar{n}_m = 1/[\exp(\hbar\omega_m/k_B T) - 1]$ is the mean phonon number of the mechanical oscillator at oscillator frequency ω_m and bath temperature T .

1.2.5 Input-Output Theory

Input-output theory is formulated on the basis of Heisenberg equations of motion, describing the time evolution of optical field (a) inside the cavity. Assume the cavity has only one transmitting mirror. This mirror will couple the single cavity mode with the external multi mode field. The interaction between the output field modes and the cavity mode is influenced by the shape of the cavity and the properties of the mirror material [37]. The Hamiltonian for this can be written as

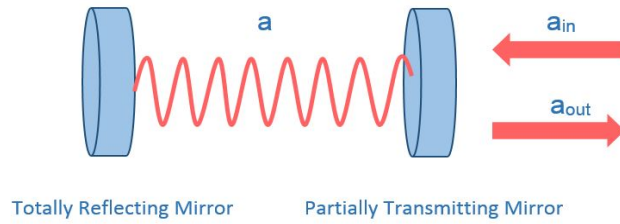


Figure 1.2: Schematic diagram of the single side cavity with the cavity field, the input and output fields

$$H = \hbar\omega_c a^\dagger a + \int d\omega \omega a_\omega^\dagger a_\omega + i\hbar\sqrt{\frac{\kappa}{\pi}} \int d\omega (a a_\omega^\dagger - a^\dagger a_\omega) \quad (1.10)$$

Here, it is assumed that the electromagnetic environment as an infinite number of harmonic oscillators over the entire frequency range. a_ω and a_ω^\dagger are the annihilation and creation operators of the environment oscillator mode at a frequency ω . $\sqrt{\kappa/\pi}$ is the cou-

pling between the mechanical oscillators and the cavity field. Calculate the Heisenberg equation of motion for cavity mode and the environment mechanical mode:

$$\dot{a} = -i\omega_c a - \sqrt{\frac{\kappa}{\pi}} \int a_\omega d\omega \quad (1.11)$$

$$\dot{a}_\omega = -i\omega a_\omega + \sqrt{\frac{\kappa}{\pi}} a \quad (1.12)$$

Now, integrate the equation of motion for a_ω , from some past time t_0 to the current time t .

$$a_\omega(t) = e^{-i\omega(t-t_0)} a_\omega(t_0) + \sqrt{\frac{\kappa}{\pi}} \int_{t_0}^t e^{-i\omega(t-\tau)} a(\tau) d\tau \quad (1.13)$$

Enter the value of a_ω into the a equation of motion:

$$\dot{a} = -i\omega_c a - \sqrt{\frac{\kappa}{\pi}} \int \left[e^{-i\omega(t-t_0)} a_\omega(t_0) + \sqrt{\frac{\kappa}{\pi}} \int_{t_0}^t e^{-i\omega(t-\tau)} a(\tau) d\tau \right] d\omega \quad (1.14)$$

Define the input field $a_{in}(t) = \frac{1}{\sqrt{2\pi}} \int d\omega e^{-i\omega(t-t_0)} a_\omega(t_0)$ and use the relations $\int d\omega e^{-i\omega t} = 2\pi\delta(t)$ and $\int_{t_0}^t d\tau a(\tau) \delta(t-t_0) = \frac{1}{2}a(t)$

Using the definition of a_{in} in the first term of equation and changing the order of integration in the second term between the τ and ω .

$$\int \int_{t_0}^t e^{-i\omega(t-\tau)} a(\tau) d\tau d\omega = \int_{t_0}^t a(\tau) \int e^{-i\omega(t-\tau)} d\omega d\tau = \pi a(t) \quad (1.15)$$

Final expression can be written as:

$$\dot{a} = -i\omega_c a - \sqrt{\frac{\kappa}{\pi}} \left(\sqrt{2\pi} a_{in} + \sqrt{\pi\kappa} a \right) \quad (1.16)$$

On simplifying

$$\dot{a} = -(i\omega_c + \kappa) a - \sqrt{2\kappa} a_{in} \quad (1.17)$$

The output field is defined as $a_{out}(t) = \frac{1}{\sqrt{2\pi}} \int d\omega e^{-i\omega(t-t_1)} a_\omega(t_1)$ for a distant future time t_1 . In this time integrate the differential equation backward in time from t_1 to t to obtain the equation of motion for a in terms of output field a_{out} . So, for $a_\omega(t)$ one have

$$a_\omega(t) = e^{-i\omega(t-t_1)} a_\omega(t_1) + \sqrt{\frac{\kappa}{\pi}} \int_{t_1}^t e^{-i\omega(t-\tau)} a(\tau) d\tau \quad (1.18)$$

Using above equation in \dot{a} , we have

$$\dot{a} = -i\omega_c a - \sqrt{\frac{\kappa}{\pi}} \int \left[e^{-i\omega(t-t_1)} a_\omega(t_1) + \sqrt{\frac{\kappa}{\pi}} \int_{t_1}^t e^{-i\omega(t-\tau)} a(\tau) d\tau \right] d\omega \quad (1.19)$$

Final expression can be written as:

$$\dot{a} = -i\omega_c a - \sqrt{\frac{\kappa}{\pi}} \left(\sqrt{2\pi} a_{out} - \sqrt{\pi\kappa} a \right) \quad (1.20)$$

So

$$\dot{a} = -(i\omega_c - \kappa) a - \sqrt{2\kappa} a_{out} \quad (1.21)$$

Now equating the equations [Eq. \(1.17\)](#) and [Eq. \(1.21\)](#), we have

$$-(i\omega_c - \kappa) a - \sqrt{2\kappa} a_{out} = -(i\omega_c + \kappa) a - \sqrt{2\kappa} a_{in} \quad (1.22)$$

Therefore,

$$a_{out} = a_{in} + \sqrt{2\kappa} a \quad (1.23)$$

We can measure the output field to extract information about the cavity.

1.2.6 Optomechanical Equations of Motion

Considering the Hamiltonian of the system derived in equation (Eq. (1.7)), dissipation and fluctuation, the time evolution of system operator can be described by the Heisenberg equation of motion with the addition of corresponding damping term and noise term as follows [34]:

$$\begin{aligned}\frac{d}{dt}q &= -\frac{\iota}{\hbar}[q, H] , \\ \frac{d}{dt}p &= -\frac{\iota}{\hbar}[p, H] - \gamma p + \xi(t) , \\ \frac{d}{dt}a &= -\frac{\iota}{\hbar}[a, H] - \kappa a + \sqrt{2\kappa}a_{in} ,\end{aligned}\tag{1.24}$$

Here, the first term on the R.H.S. describe the coherent evolution of the system operators, the second term takes the decay κ and damping γ of optical and mechanical mode into account and the last term describes the noise entering the system due to its coupling to the thermal bath. On solving above equation, we got

$$\begin{aligned}\frac{d}{dt}q &= \omega_m p , \\ \frac{d}{dt}p &= -\omega_m q + ga^\dagger a - \gamma p + \xi(t) , \\ \frac{d}{dt}a &= -\iota\Delta a + \iota gqa - \kappa a + E + \sqrt{2\kappa}a_{in} ,\end{aligned}\tag{1.25}$$

It can be seen from the above equations, there is a frequency shift in the optical mode by the mechanical position and changes the optical amplitude, which in turn changes the mechanical mode amplitude. Both these phenomenon depends upon the strength of optomechanical coupling constant g . To understand the quantum regime of optomechanics in a better way, let us first study the classical regime. Such a behaviour can be studied from the Quantum Langevin equation (Eq. (1.25)) by rewriting the QLEs for the complex field amplitudes $\alpha = \langle a \rangle$, $\bar{q} = \langle q \rangle$ and $\bar{p} = \langle p \rangle$. When the cavity is strongly driven,

the number of photons inside the cavity increases which in turn enhances the radiation pressure. In such cases, one can use mean-field approximation i.e., the system can be described by the linearized dynamics, even for small value of optomechanical coupling. In the large mean field approximation, we can expand the system operators as a sum of their classical mean amplitudes and quantum fluctuations around these classical values as follows: $a = \alpha + \delta a$, $q = \bar{q} + \delta q$ and $p = \bar{p} + \delta p$. Considering the time-averaged properties of the noise operators, we obtain the coupled set of equations for classical amplitudes from equations (Eq. (1.25)) as,

$$\begin{aligned}\frac{d}{dt}\bar{q} &= \omega_m \bar{p}, \\ \frac{d}{dt}\bar{p} &= -\omega_m \bar{q} + g|\alpha|^2 - \gamma \bar{p}, \\ \frac{d}{dt}\alpha &= -(\kappa + \iota\Delta')\alpha + E,\end{aligned}\tag{1.26}$$

Where $\Delta' = \Delta - g\bar{q}$ is the effective detuning. The classical equations of motion described in (Eq. (1.26)) leads to many interesting phenomenon. The coupled Langevin equations for quantum fluctuation can be obtained from equation (Eq. (1.25)) as:

$$\begin{aligned}\frac{d}{dt}\delta q &= \omega_m \delta p, \\ \frac{d}{dt}\delta p &= -\omega_m \delta q + g(\alpha^* \delta a + \alpha \delta a^\dagger) - \gamma \delta p + \xi(t), \\ \frac{d}{dt}\delta a &= -(\kappa + \iota\Delta')\delta a + \iota g_0 \delta q + \sqrt{2\kappa} a_{in},\end{aligned}\tag{1.27}$$

Here, $g_0 = g\alpha$ is the effective optomechanical constant. Thus, we can see that optical amplitude enhances the optomechanical coupling strength. Since the amplitude of fluctuations is small, therefore we have ignored the higher order terms in δa and δq under the linearization approximation. By defining the fluctuation quadrature for the optical mode $\left(\delta X = \frac{1}{\sqrt{2}}(\delta a^\dagger + \delta a), \delta Y = \frac{\iota}{\sqrt{2}}(\delta a^\dagger - \delta a)\right)$ and the noise operators $\left(X_{in} = \frac{1}{\sqrt{2}}(a_{in}^\dagger + a_{in}), Y_{in} = \frac{\iota}{\sqrt{2}}(a_{in}^\dagger - a_{in})\right)$ above equation (Eq. (1.27)) can be writ-

ten in the matrix form as:

$$\dot{R}(t) = MR(t) + N(t) , \quad (1.28)$$

where $R(t)^T = (\delta q, \delta p, \delta X, \delta Y)$, $N(t)$ is given by $N(t)^T = (0, \xi, \sqrt{2\kappa}X_{in}, \sqrt{2\kappa}Y_{in})$ and M is the 4×4 coefficient matrix. The solution of the equation (Eq. (1.28)) can be written as:

$$R(t) = MR(0) + \int_0^t ds F(s)N(t-s) , \quad (1.29)$$

where $F(t) = \exp(Mt)$. One of the fascinating phenomena that can occur in optomechanical systems is the observation of macroscopic quantum behavior. In these systems, mechanical oscillators can exhibit quantum effects at a macroscopic scale. An important ingredient in the calculation of figure of merit defining these phenomenon is the covariance matrix [38]. The time evolution of covariance matrix follows the following linear differential equation:

$$\dot{C} = MC + CM^T + D , \quad (1.30)$$

where the elements of C can be defined as $C_{ij} = \frac{1}{2}\langle R_i R_j + R_j R_i \rangle$ and D is the diffusion matrix given as:

$$D = \text{diag}[0, \gamma(2\bar{n}_m + 1), \kappa, \kappa] , \quad (1.31)$$

It is important to note here that stability of the solution is necessary to obtain the dynamical form of covariance matrix. This analysis can be done by applying the Routh-Hurwitz criterion [39], according to which the solution of equation (Eq. (1.28)) reaches its steady state if the eigenvalues of matrix M have negative real part. With this, let us briefly introduce the quantum phenomenon which we will study in our thesis.

1.3 Synchronization

Synchronization is a widespread phenomenon in daily life, occurring in various natural and social systems. It can be experienced in daily life like in flashing of fireflies [40], biological rhythms [41] and many more. It showcases the inherent tendency of systems to synchronize their behavior or states, leading to coordination and collective dynamics. It was first observed by Huygens in the earliest 17th century in a classical pendulum system with a common support [7]. He noticed that when two pendulum clocks were placed on the same wall, their swing periods would synchronize over time. Since then, it is experienced in various aspect of physical, biological and chemical systems [7]. Different scenario of classical synchronization can be considered in the context of self-sustaining oscillators. Frequency locking of a self-sustained oscillator driven by a harmonic force is a fundamental scenario in classical synchronization [7, 42]. The Van der Pol (VdP) oscillator is the most famous known example of self-sustained oscillator. In the absence of external driving force, dynamics of the VdP is governed by the following classical equation of motion:

$$\ddot{x} + \omega_0^2 x - \epsilon (1 - x^2) \dot{x} = 0 \quad (1.32)$$

where x represents the displacement of the oscillator, $\epsilon > 0$ and ω_0 is the natural frequency of the VdP oscillator. The VdP is a nonlinear dynamical system with two kinds of damping terms: negative damping ($-\dot{x}$) and nonlinear damping ($x^2\dot{x}$), combination of which leads to the self-sustained oscillations (known as limit cycle) in the steady state. If the additional harmonic drive is added to the self oscillator, there is a finite range of detuning (difference between oscillator's natural frequency and frequency of driving force) for which the oscillator is frequency locked to the drive, and noise can reduce or destroy this range of synchronization. There are also the regimes of frequency entertainment in which the observed frequency of driven oscillator differs from both the natural frequency of oscillator

and the force frequency. The VdP oscillator is the simplest model exhibiting these effect [7]. The second setting consists of two coupled self oscillating systems synchronizing their motion due to mutual interaction. For example, orbital resonances (synchronization) in planetary motion or synchronization of muscle cells in mammal hearts. In the case of two mutually coupled oscillators, synchronization (phase locking) occurs when the coupling strength reaches above a critical value [7]. This critical coupling strength required for phase locking to occur depends on frequency detuning between the oscillators. The term "Arnold tongue" is used to describe the region of coupling and detuning values in which phase locking occurs. A third well-studied case is of large ensemble of coupled limit-cycle oscillators with random frequencies: Kuramoto model [43, 44]. In the Kuramoto model, each oscillator is represented by a phase variable, denoted by θ_i , where i ranges from 1 to N , representing the total number of oscillators in the system. The dynamics of each oscillator is described by the following equation:

$$\frac{d}{dt}\theta_i = \omega_i + \frac{K}{N} \sum_{j=1}^N \sin(\theta_j - \theta_i) \quad (1.33)$$

where, K is the coupling strength, determining the influence of neighboring oscillators on the dynamics of each oscillator. An order parameter is defined to measure the degree of synchronization

$$re^{i\psi} = \frac{1}{N} \sum_{j=1}^N e^{i\phi_j} \quad (1.34)$$

where ψ is the average phase. The order parameter $r(t)$, with $0 \leq r(t) \leq 1$, is a measure of phase coherence or synchronization. Detailed explanation of Kuramoto's model can be found in [44]. The model's applicability to a wide range of systems led to its adoption in various fields. For example, in physics, the Kuramoto model has been used to study the synchronization of coupled oscillators in areas such as Josephson junctions [45] and

optoelectronic devices.

While classical nonlinear dynamical systems have been extensively studied for synchronization, there is a growing interest in observing similar phenomena in quantum systems. Among theoretical models, both linear and non-linear oscillators have been considered to study synchronization in quantum domain. The Van der Pol oscillator describes self-sustained oscillations in systems with nonlinear dynamics and has been studied in quantum regimes [46, 47, 48, 49] to understand its synchronization properties. The Van der Pol oscillator in the quantum regime has been studied in the context of phase locking [46] and frequency entertainment [47] under the influence of external driving forces. The VdP oscillator exhibits self-sustained oscillations and spontaneous synchronization, which arise due to coherent coupling [46] or dissipative coupling [48, 49]. Physical platforms operating in the quantum regime, such as trapped ions [46] and optomechanical oscillators [49], have been suggested as potential systems to realize the Van der Pol oscillator. In the study of self-sustained oscillators, such as VdP oscillators, in the quantum regime, the nonlinearity of these systems poses challenges for exact analysis. As a result, the analysis is often limited to specific cases and requires various approximations to make progress. An exact analysis can be performed in linear systems like harmonic networks [50, 17, 51].

The classical notion of synchronization, which is based on the dynamics of phase space trajectories and classical variables, cannot be directly applied to quantum systems due to the fundamental differences between classical and quantum mechanics. So, when extending the concept of synchronization to microscopic domain, a first question is about what defines this phenomenon. To answer this question, different approaches are reported for quantum synchronization.

1.3.1 Pearson Factor

The Pearson correlation coefficient, commonly known as the Pearson factor, is a statistical measure that quantifies the linear relationship between two variables. Calling X_1 and X_2 ,

two variable, it is defined as

$$C_{X_1, X_2}(t, \Delta t) = \frac{\overline{\delta X_1 \delta X_2}}{\sqrt{\overline{\delta X_1^2} \overline{\delta X_2^2}}} \quad (1.35)$$

where $\delta X_i = X_i - \bar{X}_i$ and $\bar{X}_i = \frac{1}{\Delta t} \int_t^{t+\Delta t} X_i(t') dt'$. The value of C_{X_1, X_2} ranges from +1 to -1 corresponding to complete synchronization and complete anti-synchronization. In classical synchronization problems [7, 52], the Pearson correlation coefficient is commonly used to quantify the temporal correlation between two classical trajectories. In the quantum framework the classical trajectories X_i can be replaced with the expectation values of the quantum operators describing the dynamical behavior of the quantum system. This measure was first adopted in the framework of a quantum system to study the mutual synchronization of two linearly coupled harmonic oscillators dissipating to a common bath using the expectation values of second-order moments of position and momenta of oscillators in [50]. the same measure of synchronization was also applied to study the synchronization behavior of an extended network of linear oscillators [17]. Pearson correlation coefficient has been a commonly adopted measure to study synchronization in a variety of quantum systems [53, 54, 55, 56].

1.3.2 Synchronization error

Two subsystems initialized into different states acquire identical trajectories under the effect of mutual interaction between subsystems. The two subsystems are then said to be completely synchronized. In a similar way, two coupled harmonic oscillators (two continuous variable systems) characterized by the displacement $q_j(t)$ from their respective equilibrium positions and the linear momenta $p_j(t)$, where $(j \in 1, 2)$, are said to be completely synchronized if they maintain $q_-(t) = \{q_1(t) - q_2(t)\}/\sqrt{2} \rightarrow 0$ and $p_-(t) = \{p_1(t) - p_2(t)\}/\sqrt{2} \rightarrow 0$, at long times. This corresponds to complete classical synchronization.

One can note that extension of the above concept to the quantum system is not possible due to Heisenberg's uncertainty principle. According to Heisenberg's uncertainty principle, position and momentum quadratures cannot be measured simultaneously, so it is not possible to make generalized positions $q_j(t)$ and linear momenta $p_j(t)$ ($j \in 1, 2$) equal at the same time t . With this, the best estimate of the quantum synchronization therefore corresponds to a state of two oscillators, for which the sum of uncertainty in $q_-(t)$ and $p_-(t)$ becomes minimum.

To turn this argument into a quantitative statement, Mari et al. introduced the following figure of merit [14]:

$$S_c(t) = \langle q_-^2(t) + p_-^2(t) \rangle^{-1} \quad (1.36)$$

in terms of synchronization errors $q_-(t)$ and $p_-(t)$ to gauge the level of quantum complete synchronization between the two coupled oscillators. Here $\langle \dots \rangle$ denotes the expectation (or mean) values of the corresponding operators. Expanding $q_-(t)$ and $p_-(t)$ around mean values, $q_-(t) = \bar{q}_-(t) + \delta q_-(t)$, $p_-(t) = \bar{p}_-(t) + \delta p_-(t)$, and using the limit $\bar{q}_-(t) = 0, \bar{p}_-(t) = 0$ as time approaches large enough, a modified form of quantum synchronization measure can be obtained as:

$$S_q = \frac{1}{\langle \delta q_-^2(t) + \delta p_-^2(t) \rangle} \leq 1 \quad (1.37)$$

Note that Heisenberg uncertainty relation ($\langle \delta q_-^2(t) \rangle \langle \delta p_-^2(t) \rangle \geq 1/4$) sets the upper limit of S_q and $S_q = 1$ corresponds to complete quantum synchronization.

1.4 Entanglement

The concept of entanglement [18] is indeed a fundamental and intriguing aspect of quantum physics with profound philosophical and practical implications. Entanglement refers

to a quantum phenomenon where two or more particles become correlated in such a way that their properties are interdependent, regardless of the distance separating them. Entanglement is a captivating and complex phenomenon that underpins many aspects of quantum physics and has the potential to revolutionize various technological fields. Entanglement has several intriguing properties and has been the subject of extensive research and exploration due to its potential applications in various fields, including quantum computing, quantum communication, quantum cryptography [57], quantum teleportation [58]. These applications rely on the presence of entanglement among participating subsystems. As a result, the detection and characterization of entanglement within a quantum system's state hold paramount importance. Here, we discuss briefly the entanglement criteria that are related to our thesis work.

1.4.1 Peres-Horodecki Criterion

In the past, several criterion for detection of entanglement have been proposed. One of the most important criterion for entanglement detection is provided by Peres and Horodecki, which is known as positive partial transpose (PPT) criterion [59]. The Peres-Horodecki criterion is a necessary condition for the joint density matrix ρ of two systems A and B to be separable. In the 2×2 and 2×3 dimensional cases the condition is also sufficient [60]. The description and the principle underlying the criterion is given below. First, note that for every physical system, the density matrix must be positive-semidefinite. Next, consider a separable state,

$$\rho = \sum_{j=1}^n p_j \rho_{1j} \otimes \rho_{2j} \quad (1.38)$$

Let T be an operator performing transposition. Then to perform partial transposition on the second subsystem is equivalent to operate $I \otimes T$ on the whole system (I is the identity

operator). This gives,

$$\rho^T = (I \otimes T)\rho = \sum_{j=1}^n p_j I(\rho_{1j}) \otimes T(\rho_{2j}) = \sum_{j=1}^n p_j \rho_{1j} \otimes \rho_{2j}^T \quad (1.39)$$

ρ will be a separable state if all the eigenvalues are positive. In other words, according to Peres criterion, the joint density matrix ρ of a bipartite entangled system after partial transpose (PT) in the basis of one of the system exhibits negative eigenvalues. There are other known entanglement criterion like computable cross norm [61] and the reduction criterion [62]. These criteria require the reproduction of density matrix using quantum state tomography to test experimentally. Also, the PPT criterion doesn't provide a complete characterization of all entangled states, especially in higher-dimensional systems.

1.4.2 Entanglement Witness

Let's delve into a different class of criteria for identifying separability in quantum systems. Above discussed criteria relies on the initial assumption that the density matrix is already known. They rely on performing specific operations on the density matrix to determine whether a state is entangled or not. However, there exists a comprehensive entanglement criterion that operates in terms of directly measurable observables, known as entanglement witness [60, 63]. In the following, we will introduce this concept. In mathematical terms, an entanglement witness is typically defined as an operator that has different expectation values for separable states and entangled states. If the expectation value of this operator exceeds a certain threshold, then the state is identified as entangled. This provides a practical way to experimentally verify the presence of entanglement without necessarily fully characterizing the quantum state itself.

1.4.3 Peres-Horodecki Criterion for Continuous Variable

The Peres-Horodecki criterion is a well-known criterion used to test the separability of bipartite quantum systems. It was originally formulated for discrete variable systems but can be extended to continuous variable systems as well [64]. Quantum state ρ of a two-mode continuous variable system can be expressed in terms of a Wigner function as:

$$W(x_1, p_1, x_2, p_2) = \left(\frac{1}{\pi}\right)^2 \int \int dy_1 dy_2 e^{2i(y_1 p_1 + y_2 p_2)} \times \sum_j p_j \langle x_1 - y_1 | \rho_{1j} | x_1 + y_1 \rangle \otimes \langle x_2 - y_2 | \rho_{2j} | x_2 + y_2 \rangle \quad (1.40)$$

Here x_1, x_2, p_1 and p_2 are the quadrature variables. Performing partial transposition on second subsystem, it will become,

$$W^{PT}(x_1, p_1, x_2, p_2) = \left(\frac{1}{\pi}\right)^2 \int \int dy_1 dy_2 e^{2i(y_1 p_1 + y_2 p_2)} \times \sum_j p_j \langle x_1 - y_1 | \rho_{1j} | x_1 + y_1 \rangle \otimes \langle x_2 + y_2 | \rho_{2j} | x_2 - y_2 \rangle \quad (1.41)$$

Redefining the quadrature variable y_2 to be $-y'_2$.

$$\begin{aligned} W^{PT}(x_1, p_1, x_2, p_2) &= \left(\frac{1}{\pi}\right)^2 \int \int dy_1 (-dy'_2) e^{2i(y_1 p_1 - y'_2 p_2)} \times \\ &\quad \sum_j p_j \langle x_1 - y_1 | \rho_{1j} | x_1 + y_1 \rangle \otimes \langle x_2 - y'_2 | \rho_{2j} | x_2 + y'_2 \rangle \\ &= \left(\frac{1}{\pi}\right)^2 \sum_j p_j \int dy_1 (e^{2i(y_1 p_1)}) \langle x_1 - y_1 | \rho_{1j} | x_1 + y_1 \rangle \otimes \\ &\quad \int (-dy'_2) e^{2i(-p_2)y'_2} \langle x_2 - y'_2 | \rho_{2j} | x_2 + y'_2 \rangle \\ &= W(x_1, p_1, x_2, -p_2) \end{aligned} \quad (1.42)$$

Thus, it is evident from the definition of Wigner distribution that the partial transpose operation PT, which takes every ρ to its transpose ρ^{PT} , is equivalent to a mirror reflection

in phase space:

$$\rho \rightarrow \rho^{PT} \iff W(x_1, p_1, x_2, p_2) \rightarrow W(x_1, p_1, x_2, -p_2) \quad (1.43)$$

Thus, according to Peres-Horodecki (PPT) separability criterion for continuous variable: if ρ is separable, then its Wigner distribution necessarily goes over into a Wigner distribution under the phase space mirror reflection .

1.4.4 Uncertainty Principle based Entanglement Criterion

The Uncertainty Principle, formulated by Werner Heisenberg, states that there is a fundamental limit to the precision with which certain pairs of physical properties, such as position and momentum, can be known simultaneously. It implies that the more precisely one property is measured, the less precisely the other property can be known. In other words, there is an inherent trade-off in the precision of simultaneous measurements of certain pairs of physical quantities. For two non commuting observables A and B , mathematical form of Heisenberg uncertainty relation takes the following form:

$$\Delta A \Delta B \geq \frac{1}{2} |\langle [A, B] \rangle| \quad (1.44)$$

where $[A, B] = AB - BA$ is the commutator. According to quantum mechanics, every physical state had to satisfy the above stated uncertainty principle. In fact, Nha and Zubairy shows in [65] that the converse is also true. Therefore, the satisfaction of the uncertainty relation can be used as a separability criterion in a similar way that the positivity of a density matrix does. Uncertainty relation based entanglement criterion are proposed [66, 67, 64, 68, 69]. Here, we review some uncertainty relation based inseparability criterion , particularly for continuous variable, that are relevant to our thesis work. In this direction, Simon et al [64] has derived certain separability inequalities, by employing Peres's criterion of separability, violation of which is sufficient to detect entanglement in

bipartite systems.

Duan et al [68], proposed a simple entanglement criterion for two-mode continuous variable states, which is based on the total variance of a pair of Einstein Podolsky-Rosen (EPR) type operators. The criterion is based on the observation that entangled states exhibit lower variances in certain combinations of observables compared to separable states. Specifically, it focuses on the sum of the variances of the position and momentum operators. Consider the following EPR-like operators

$$\begin{aligned}\hat{u} &= |a|\hat{q}_1 + \frac{1}{a}\hat{q}_2 \\ \hat{v} &= |a|\hat{p}_1 - \frac{1}{a}\hat{p}_2\end{aligned}\tag{1.45}$$

where a is any nonzero real number. Then, according to the Duan criterion [68], for any separable bipartite CV quantum state ρ , the total variance of the above defined EPR-like operators with commutators $[\hat{q}_i, \hat{p}_j] = i\delta_{ij}$ satisfies the following inequality

$$\langle(\Delta\hat{u})^2\rangle_\rho + \langle(\Delta\hat{v})^2\rangle_\rho \geq a^2 + \frac{1}{a^2}\tag{1.46}$$

If the inequality is violated, the state is considered to be entangled; otherwise, it is deemed separable. Thus, for a two-mode CV system, the Duan's criterion states that if the sum of the variances of the position operators and the sum of the variances of the momentum operators are below certain threshold values, then the system is entangled. This threshold is determined by the Heisenberg uncertainty principle, where the product of the variances must exceed a certain value. So, violation of this bound provides a sufficient condition for inseparability of the state. It is then investigated how strong the bound is for the Gaussian states (fully characterized by the first and second moments of the position and momentum operators). And, it turns out necessary and sufficient for all CV Gaussian continuous.

A new sufficient inseparability criterion, involving the product of second-order mo-

ments of continuous observable has been derived by Mancini et al [70]. Define two operators $u = q_1 + q_2$ and $v = p_1 - p_2$ such that $[q_j, p_j] = \iota$, then, according to Mancini et al any separable state will satisfy the following inequality,

$$\langle (\Delta u)^2 \rangle \langle (\Delta v)^2 \rangle \geq 1 \quad (1.47)$$

Thus, any bimodal CV state can be said to be entangled if it violates the inequality (Eq. (1.47)). Further, it was shown in [69] that the criterion proposed by Mancini et al and Duan et al are interrelated with each other. Furthermore, by using some algebraic identity, it is also proved that Mancini's criterion is stronger than Duan criterion. These inequalities are experimentally testable, since these inequalities depend on variances of relative position and total momentum coordinates of the two subsystems.

In another pertinent study, Hillery and Zubairy derived a class of inequalities to detect the presence of entanglement in two-mode systems, where they defined the operators as follows [71]:

$$\begin{aligned} L_1 &= ab^\dagger + a^\dagger b \\ L_2 &= \iota (ab^\dagger - a^\dagger b) \\ L_3 &= a^\dagger a + b^\dagger b \end{aligned} \quad (1.48)$$

They utilized two-mode squeezing and the Cauchy–Schwarz inequality to illustrate entanglement. In this context, the Lie algebra of $SU(2)$, with $J_i = \frac{L_i}{2}$ where $i = 1, 2, 3$, leads to the satisfaction of the commutation relation $[J_1, J_2] = \iota J_3$. Consequently, the general equation for the uncertainty principle of variables must adhere to the condition:

$$(\Delta L_1^2) (\Delta L_2^2) \geq \frac{|[J_1, J_2]|^2}{4} \quad (1.49)$$

The total quadrature variance takes the form of:

$$\begin{aligned} (\Delta L_1^2) + (\Delta L_2^2) &= 2 [\langle (N_a + 1) N_b \rangle + \langle N_a (N_b + 1) \rangle - 2|\langle ab^\dagger \rangle|^2] \\ &\simeq 2 [\langle N_a + 1 \rangle \langle N_b \rangle + \langle N_a \rangle \langle N_b + 1 \rangle - 2|\langle a \rangle \langle b^\dagger \rangle|^2] \end{aligned} \quad (1.50)$$

The expectation values of the two-mode state are expressed as a product of the a mode and b mode. The Schwarz inequality is applied, resulting in $|\langle a \rangle|^2 \leq \langle N_a \rangle$ and $|\langle b \rangle|^2 \leq \langle N_b \rangle$ [71]. It is found that the product state satisfies the following inequality:

$$(\Delta L_1)^2 + (\Delta L_2)^2 \geq 2 (\langle N_a \rangle + \langle N_b \rangle) \quad (1.51)$$

Eq. (1.51) indicates that the state is entangled if it satisfies the condition $\langle N_a N_b \rangle < |\langle ab^\dagger \rangle|^2$. This condition is utilized in the Hillery–Zubairy method [72], using the photon number relation in terms of annihilation and creation operators, $\hat{n} = \hat{a}^\dagger \hat{a}$, in two-mode entanglement to derive the inequality $\langle n_1 \rangle \langle n_2 \rangle < |\langle a_1 a_2 \rangle|^2$. Furthermore, the inequality relation in the Hillery–Zubairy approach is applicable to detect entanglement in the systems of more than two modes.

Although, entanglement is well-established in scientific theory and experimental observations, its underlying mechanisms and implications are still subjects of ongoing research and exploration in the field of quantum physics.

1.5 Outline of Thesis

In the following, we present the outline of the thesis by giving the brief description of the problems tackled in the form of different chapters of the thesis. There are a total five chapters. We present a brief summery about the content of each chapter below.

Chapter 1: This chapter starts with the introduction and motivation of the thesis, with

a brief literature review of the recent developments in the cavity optomechanical systems. It is then followed by a brief discussion of the basic theory of cavity optomechanics. It is then guided through the fundamentals of the current work.

Chapter 2: It is said that synchronization and entanglement are two independent properties which two coupled quantum system may not exhibit simultaneously. In this chapter, we present a systematic study on the interplay between quantum synchronization and entanglement between two indirectly coupled mechanical oscillators in a double cavity optomechanical system. Each mechanical oscillator is suspended inside a cavity and is coupled with the cavity mode via linear and quadratic dependence on its displacement from the equilibrium position. Based on these realizations, first, we show that when both the mechanical oscillators are linearly coupled to the cavity mode, the oscillators are synchronized without entanglement. Also, the level of quantum synchronization is poor. Further, we show that when we consider quadratic coupling as well in our simulation, quantum synchronization increases beyond what was achieved without it. Moreover, entanglement between the oscillators starts appearing with non-zero quadratic coupling. To be more clear, we show that appropriate choice of parameters in the presence of both type of coupling leads to the greatly enhanced quantum synchronization and entanglement between the indirectly coupled oscillators. At the end, we explore the effect of system parameters on quantum synchronization and entanglement.

Chapter 3: This chapter address the issue of generalization of relation between entanglement and quantum synchronization. In this chapter, we present an optomechanical model to show that entanglement can act as booster to achieve near complete quantum synchronization between two mechanical oscillators. In this model, one of oscillator makes the cavity while the other is kept suspended inside the cavity. Both the oscillators are coupled to the same cavity mode via linear and quadratic dependence on their displace-

ment from their respective equilibrium positions. An indirect always-on coupling between the two is also mediated via the same cavity mode. With this realization, we first demonstrate classical synchronization between the oscillator via limit cycle trajectories, which is a precondition for quantum synchronization. Further, we show that when the cavity is strongly amplitude-modulated, the two coupled oscillators are nearly complete quantum synchronized and entangled simultaneously.

Chapter 4: The content of this chapter is motivated by the several proposed entanglement criterion to detect entanglement of mixed states. We observed that these criterion correctly detect the entanglement in pure as well as in mixed states, but they can not reveal the correct domain of the relevant parameters as identified by the Positive Partial Transpose (PPT) criterion. In this chapter, we will address this issue and propose a strong entanglement criterion for bipartite mixed states, which correctly identifies the correct domain of relevant parameters for entanglement. We will show by explicit analysis that our criterion successfully detects entanglement not only in pure states, but also in several generalized mixed states including Werner state. We further show that our criterion reduces to the SRPT inequality for the pure state.

Chapter 5: This chapter contains the summary of the results discussed in the aforementioned main chapters of the thesis. We also consider some future scopes that might aid in gaining a deeper understanding of quantum correlations.

Chapter 2

Quantum synchronization and entanglement between two indirectly coupled oscillators

In the previous chapter, we introduced the cavity optomechanical system and discussed the interaction between the optical field and the mechanical system. In this chapter, we study the simultaneous entanglement and the synchronization between the two indirectly-coupled mechanical oscillators. As a result of quadratic coupling, we show that these oscillators can be quantum synchronized and entangled simultaneously.

2.1 Motivation

Synchronization refers to the ability of a group of self-oscillators to adjust their intrinsic rhythms spontaneously and oscillate in unison. This concept has a long history, dating back to Huygens's observation of synchronized maritime pendulum clocks in the 17th century [7]. After the introduction of the synchronization phenomenon by Huygens, it has been observed in a wide range of classical systems. It has practical applications in

high-precision clocks [73] and information processing [5].

In the last decade, many efforts have been devoted to extending this interesting phenomenon to the quantum regime. As discussed in Chapter 1, Mari et al [14] gave an effective measurement scheme and proposed a figure of merit to measure the degree of quantum synchronization and quantum phase synchronization between the two coupled quantum harmonic oscillators. Recent experiments have demonstrated quantum phase synchronization in spin-1 atoms [74]. This discovery has generated significant interest in exploring quantum synchronization in other quantum systems. Quantum-mechanical self-sustained oscillators are synchronized to the external harmonic drive [47] or a different mechanical oscillator [46]. Marquardt and his coworkers have demonstrated that an array of optomechanical systems can exhibit synchronization [75] that can be described by an effective Kuramoto-type model [76]. Quantum synchronization has also been studied in trapped ions, ensembles of atoms [77, 78, 79], qubits, Van der Pol oscillators [80, 48], and Josephson junctions [81, 82].

One of the distinctive features of quantum correlations is nonlocality, which does not have any classical analog. This refers to the possibility that the measurement of one of the two coupled systems can affect the probability distributions of the other, which may be at a distance apart. There are various prescriptions for identifying nonlocality, including Bell's inequalities and EPR steering. To advocate for the local realism between two particles, Einstein, Podolsky, and Rosen (EPR) proposed that their position and momentum quadratures would maintain the relation $q_1 = q_2$ and $\vec{p}_1 = -\vec{p}_2$ at all times, as these particles are coupled to each other in the stationary center-of-mass limit. In fact, in the classical sense, these particles may be considered synchronized. Moreover, the states of these two particles have been shown to exhibit nonlocality in terms of suitable Bell's inequality violation [83, 84] and to correspond to an ideal quantum correlation - called EPR-correlation.

The local measurement of probability distributions is closely related to the concept of

separability. If a local operation on one of the subsystems changes the quantum probability distributions, then it signals a quantum correlation. For a coupled bosonic system (like that of two harmonic oscillators), the joint variables q_- and p_- (which have been used to quantify synchronization in [14]) satisfy the following uncertainty relation: $\langle(\delta q_-)^2\rangle + \langle(\delta p_-)^2\rangle \geq 1$. If the state of this coupled system is separable, the following inequality is also satisfied, as shown by Duan and his coworkers (DC) [68]:

$$\langle(\delta q_-)^2\rangle + \langle(\delta p_+)^2\rangle \geq 1, \quad (2.1)$$

where the transformation $p_- \rightarrow p_+$ is made using partial transposition, using Peres's prescription [59]. This means that violation of this inequality Eq. (2.1) refers to inseparability. Such an inseparable state is referred to as being entangled.

As clear from the above, both the quantum synchronization and the nonlocality are certain manifestations of quantum correlations and can be described or identified in terms of uncertainties of a set of joint EPR-like quadratures. The Heisenberg uncertainty relation has been used to suitably quantify the quantum synchronization [14] as well as to establish conditions for inseparability (or, entanglement [64]). Therefore, it is natural to expect certain interconnection between them. At least, there must exist a certain regime of parameters, in which two oscillators can simultaneously exhibit quantum synchronization and entanglement. This could happen when $\langle(\delta q_-)^2\rangle \neq 0$ and $\langle(\delta p_-)^2\rangle > \langle(\delta p_+)^2\rangle$. In this chapter, we will explore a coupled oscillator system in this regard.

We note that such interaction has been explored before, as well. For example, it was shown by Manzano *et al.* that two indirectly coupled oscillators, initially prepared in a separable state, can be both classically synchronized and entangled at long times [17]. This could be done by suitably tuning the coupling strength to the rest of the oscillators in the network. It was pointed out that synchronization helps in maintaining the entanglement even in the presence of decoherence. How classical synchronization triggers the entanglement in many-body systems has been studied in [85]. Lee and Cross

have investigated both synchronization and quantum correlation between the two cavities with nonlinear crystals [46]. They have shown in the classical limit that two cavities can exhibit synchronization, while in the quantum limit, they get entangled. However, these works primarily focused on classical synchronization.

To study quantum synchronization and entanglement of two harmonic oscillators indirectly coupled with each other, we can look forward to a cavity optomechanical setup, in which a mechanical oscillator is coupled to a cavity mode. The mesoscopic oscillator can be quantized at low temperatures. So quantum-classical crossover can be studied in such a system, once the temperature is varied. In this chapter, we will investigate if we can entangle such oscillators as well as quantum-synchronize them, at the same time.

In an optomechanical system, the leading order of coupling between the cavity mode and the mechanical mode is proportional to the displacement q of the mechanical oscillator from its equilibrium position - a case of the so-called 'linear coupling'. That such a coupling can lead to cooling the mechanical oscillator to its ground state using dynamical back action has been shown in [86] and demonstrated in [87, 88]. This can also generate cavity-oscillator entanglement [89, 38] and quadrature squeezing of mechanical mode [90, 91]. On the other hand, for specific configurations of the mechanical oscillators, when the quadratic dependence of the cavity-mechanical oscillator coupling on q dominates, one can measure the energy eigenstate of the mechanical mode [92]. Cooling and squeezing of the mechanical oscillator [93] and cavity-mechanical oscillator entanglement [94] have also been explored in such cases. It is further shown that quadratic coupling between a cavity mode and the motional degree of freedom of an atomic ensemble within the cavity can give rise to cavity nonlinearity at high probe laser power [95].

To achieve only the quadrature coupling in an optomechanical system, one is required to carefully place a membrane in the middle of the cavity, at one of the extrema of the cavity mode frequency. If such a constraint is relaxed, both the linear and the quadratic coupling can coexist in the same system. In such situations, one could also demonstrate

squeezing of cavity quadratures [96], cooling of microspheres [97] and of the mechanical oscillator to its ground state [98], and self-sustained oscillations of mechanical oscillator [99]. In this chapter, we show that to attain the quantum synchronization between two oscillators, along with entanglement, one is required to consider the coexistence of both types of coupling, and that quadratic coupling enhances the synchronization.

The chapter is organized as follows. In Section 2.2, we present the model and derive the effective Hamiltonian. In Section 2.3, the relevant equations of motion are derived for the fluctuation terms. In Section 2.4, we present the relevant quantities and numerically investigate how both entanglement and synchronization can be simultaneously achieved between the oscillators. In Section 2.5, we conclude our chapter.

2.2 Model

We consider two optomechanical systems, in each of which a membrane is suspended inside a cavity. In addition, the two optical cavities (with resonance frequency ω_{cj} , $j \in 1, 2$) are directly coupled by an optical fiber between the inside mirrors, with a coupling constant J . We assume that the fundamental frequencies of the cavity modes are equal to $\omega_{cj,n} = n\pi c/L_j$, where L_j is the length of the j th cavity ($j \in 1, 2$), n is a positive integer, and c is the speed of light in vacuum. The leading order of coupling between the cavity mode and the mechanical oscillator is proportional to the displacement of the oscillator from its equilibrium position. We consider, in addition, a coupling quadratically varying with this displacement. One can achieve both orders of coupling in the membrane-in-the-middle setup, as we are considering if the cavity frequency does not exhibit any extremum at the equilibrium position of the membrane [100]. That the suitable position and tilt of the membrane can generate both linear and enhanced quadratic coupling has been demonstrated in experiments with optical cavity [101, 102].

The Hamiltonian of the system can be written as follows:

$$\begin{aligned}
H_{ac} &= H_0 + H_g + H_i + H_p, \\
H_0 &= \sum_{j=1,2} \hbar \omega_{cj} a_j^\dagger a_j + \frac{P_j^2}{2m_j} + \frac{m_j \omega_{mj}^2}{2} Q_j^2, \\
H_g &= \sum_{j=1,2} \left[-\hbar g_L^{(j)} a_j^\dagger a_j Q_j + \hbar g_Q^{(j)} a_j^\dagger a_j Q_j^2 \right], \\
H_i &= -\hbar J (a_1^\dagger a_2 + a_2^\dagger a_1), \\
H_p &= i\hbar E [1 + \eta_D \cos(\Omega_D t)] \sum_{j=1,2} \left(a_j^\dagger e^{-i\omega_{lj}t} - a_j e^{i\omega_{lj}t} \right),
\end{aligned} \tag{2.2}$$

$$\tag{2.3}$$

where H_0 represents the unperturbed Hamiltonian, a_j is the annihilation operator for the j th cavity mode, Q_j and P_j refer to the position and momentum operators for the j th mechanical oscillator with the commutation relation $[Q_j, P_j] = i\hbar$, H_g represents the optomechanical coupling between the mechanical oscillator and the cavity mode, $g_L^{(j)}$ and $g_Q^{(j)}$ are the linear and the quadratic coupling constant between cavity and mechanical resonator. They are defined as $g_L^{(j)} = \frac{\partial \omega_{cj}}{\partial Q_j}$ and $g_Q^{(j)} = \frac{1}{2} \frac{\partial^2 \omega_{cj}}{\partial Q_j^2}$, where all the derivatives are calculated at the equilibrium position $Q_j = 0$. The term J is the coupling constant of cavity modes through an optical fiber. The driving of the cavity mode with external laser field of magnitude E and frequency ω_{lj} is described via the Hamiltonian H_p . Both the cavity are driven by laser fields with frequency ω_{lj} and time-modulated amplitude $\epsilon(t) = E[1 + \eta_D \cos(\Omega_D t)]$, where E is the amplitude of the laser without any modulation, η_D and Ω_D are the amplitude factor and the frequency of the modulating field. In the rotating frame of laser frequencies, the total Hamiltonian H_{ac} takes the following form:

$$\begin{aligned}
H &= \sum_{j=1,2} \left[\hbar \Delta_{cj} a_j^\dagger a_j + \frac{P_j^2}{2m_j} + \frac{m_j \omega_{mj}^2}{2} Q_j^2 - \hbar g_L^{(j)} a_j^\dagger a_j Q_j + \hbar g_Q^{(j)} a_j^\dagger a_j Q_j^2 + i\hbar \epsilon(t) (a_j^\dagger - a_j) \right] \\
&\quad - \hbar J (a_1^\dagger a_2 + a_2^\dagger a_1),
\end{aligned} \tag{2.4}$$

where $\Delta_{cj} = \omega_{cj} - \omega_{lj}$ is the detuning of the j th cavity mode from the respective driving

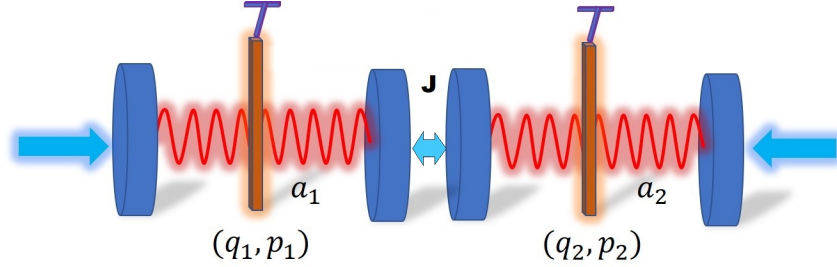


Figure 2.1: Schematic diagram of the two coupled cavity optomechanical systems. Each mechanical oscillator is suspended inside its respective cavity. The two cavity modes are externally coupled with each other via a coupling constant J .

field.

2.3 Langevin equations

Define the dimensionless position and momentum operators q_j and p_j as

$$\begin{aligned} q_j &= \sqrt{\frac{m_j \omega_{mj}}{\hbar}} Q_j, \\ p_j &= \sqrt{\frac{1}{m_j \hbar \omega_{mj}}} P_j, \end{aligned} \quad (2.5)$$

On substituting Eq. (2.5) in Eq. (2.4), we get

$$\begin{aligned} H &= \sum_{j=1,2} \left[\hbar \Delta_{cj} a_j^\dagger a_j + \frac{\hbar \omega_{mj}}{2} (q_j^2 + p_j^2) - \hbar g_1^{(j)} a_j^\dagger a_j q_j + \hbar g_2^{(j)} a_j^\dagger a_j q_j^2 + i \hbar \epsilon(t) (a_j^\dagger - a_j) \right] \\ &\quad - \hbar J (a_1^\dagger a_2 + a_2^\dagger a_1), \end{aligned} \quad (2.6)$$

where $g_1^{(j)} = \frac{\partial \omega_{cj}}{\partial Q_j} \sqrt{\frac{\hbar}{m_j \omega_{mj}}}$ and $g_2^{(j)} = \frac{1}{2} \frac{\partial^2 \omega_{cj}}{\partial Q_j^2} \frac{\hbar}{m_j \omega_{mj}}$ are the scaled linear and quadratic optomechanical coupling constants. We will study the time evolution and the dissipation dynamics of the cavity and mechanical modes. From the above Hamiltonian, the Langevin

equations for the operators in the Heisenberg picture can be obtained as follows:

$$\frac{dq_j}{dt} = \omega_{mj} p_j , \quad (2.7)$$

$$\frac{dp_j}{dt} = -\omega_{mj} q_j + g_1^{(j)} a_j^\dagger a_j - 2g_2^{(j)} a_j^\dagger a_j q_j - \gamma_{mj} p_j + \xi_j(t) , \quad (2.8)$$

$$\frac{da_j}{dt} = -(\kappa_j + i\Delta_{cj}) a_j + ig_1^{(j)} a_j q_j - ig_2^{(j)} a_j q_j^2 + iJ a_{3-j} + \epsilon(t) + \sqrt{2\kappa_j} a_{in}^{(j)} , \quad (2.9)$$

In the large mean field limit [19], we can expand the operators as a sum of their mean values and fluctuations as follows: $a_j \rightarrow \alpha_j + \delta a_j$, $q_j \rightarrow \bar{q}_j + \delta q_j$, $p_j \rightarrow \bar{p}_j + \delta p_j$, here $\alpha_j = \langle a_j \rangle$, $\bar{q}_j = \langle q_j \rangle$ and $\bar{p}_j = \langle p_j \rangle$. From the above equations Eq. (2.7)-Eq. (2.9), the Langevin equations for the mean values can be obtained as follows:

$$\begin{aligned} \frac{d\bar{q}_j}{dt} &= \omega_{mj} \bar{p}_j , \\ \frac{d\bar{p}_j}{dt} &= -\omega_{mj} \bar{q}_j + g_1^{(j)} |\alpha_j|^2 - 2g_2^{(j)} |\alpha_j|^2 \bar{q}_j - \gamma_{mj} \bar{p}_j , \\ \frac{d\alpha_j}{dt} &= -(\kappa_j + i\Delta_{cj}) \alpha_j + ig_1^{(j)} \alpha_j \bar{q}_j - ig_2^{(j)} \alpha_j \bar{q}_j^2 + iJ \alpha_{3-j} + \epsilon(t) , \end{aligned} \quad (2.10)$$

The corresponding noise operators of the above equations satisfy the following correlation relations for all j [36]:

$$\begin{aligned} \langle a_{in}^{(j)}(t) a_{in}^{\dagger(j)}(t') \rangle &= \delta(t - t') , \\ \langle a_{in}^{\dagger(j)}(t) a_{in}^{(j)}(t') \rangle &= 0 , \\ \langle \xi_j(t) \xi_j(t') \rangle &= \frac{\gamma_{mj}}{2\pi\omega_{mj}} \int \omega e^{-i\omega(t-t')} \left[1 + \coth\left(\frac{\hbar\omega}{2k_B T}\right) \right] d\omega , \end{aligned} \quad (2.11)$$

where k_B is the Boltzmann constant. The mechanical mode, coupled to the thermal bath, is affected by a Brownian stochastic force described by $\xi_j(t)$ with zero mean. The thermal bath is assumed to be a thermal equilibrium at a temperature T . For the case of

a large quality factor of the mechanical oscillator, the Brownian noise operator can be approximated in Markov approximation as $\langle \xi_j(t) \xi_j(t') \rangle = \gamma_{mj} (\bar{n}_{mj} + 1) \delta(t - t')$, where $\bar{n}_{mj} = 1 / [\exp(\hbar\omega_{mj}/k_B T) - 1]$ is the mean occupation number of the mechanical oscillators.

Similarly, the Langevin equations for the fluctuations can be obtained as follows:

$$\begin{aligned}
\frac{d}{dt} \delta q_j &= \omega_{mj} \delta p_j, \\
\frac{d}{dt} \delta p_j &= -\omega_{mj} \delta q_j + g_1^{(j)} (\alpha_j \delta a_j^\dagger + \alpha_j^* \delta a_j) - 2g_2^{(j)} \bar{q}_j (\alpha_j^* \delta a_j + \alpha_j \delta a_j^\dagger) - 2g_2^{(j)} |\alpha_j|^2 \delta q_j \\
&\quad - \gamma_{mj} \delta p_j + \xi_j(t), \\
\frac{d}{dt} \delta a_j &= -i[\Delta_{cj} \delta a_j - g_1^{(j)} (\bar{q}_j \delta a_j + \alpha_j \delta q_j) + g_2^{(j)} \bar{q}_j (2\alpha_j \delta q_j + \bar{q}_j \delta a_j)] \\
&\quad - \kappa_j \delta a_j + iJ \delta a_{3-j} + \sqrt{2\kappa_j} a_{in}^{(j)}.
\end{aligned} \tag{2.12}$$

In the next section, we will show that the oscillators do not only get entangled but also get quantum-synchronized. This result further strengthens the fact that quantum synchronization and entanglement are interlinked.

2.4 Simultaneous Entanglement and Synchronization

It is known that the violation of the DC criterion is sufficient to detect entanglement for continuous-variable states. For the variable $q_- = \{q_1(t) - q_2(t)\}/\sqrt{2}$ and $p_+ = \{p_1(t) + p_2(t)\}/\sqrt{2}$, Mancini criterion Eq. (1.47), which is derived from the DC criterion, for separability takes the following form:

$$E_D = \langle (\delta q_-)^2 \rangle \langle (\delta p_+)^2 \rangle \geq \frac{1}{4}, \tag{2.13}$$

the violation of which indicates entanglement. As was shown in [103], the relation Eq. (2.13) is stronger than the DC criterion. To investigate how the system gets entangled with time, we will study the temporal dynamics of E_D . Similarly, to investigate

the quantum synchronization between two mechanical oscillators, we choose to investigate the behavior of the figure of merit S_q given by Eq. (1.37).

To verify the above condition, we calculate the S_q and E_D , by using the covariance matrix of fluctuations. Let us start with the fluctuations equations Eq. (2.12) in the following matrix form by defining the quadrature basis $\delta q_{aj} = \frac{(\delta a_j^\dagger + \delta a_j)}{\sqrt{2}}$, $\delta p_{aj} = \frac{i(\delta a_j^\dagger - \delta a_j)}{\sqrt{2}}$:

$$\dot{U}(t) = BU(t) + V(t) , \quad (2.14)$$

where $U(t)^T = (\delta q_1, \delta p_1, \delta q_{a1}, \delta p_{a1}, \delta q_2, \delta p_2, \delta q_{a2}, \delta p_{a2})$ and

$$V(t)^T = \left(0, \xi_1, \sqrt{2\kappa_1}\delta q_{a1}^{in}, \sqrt{2\kappa_1}\delta p_{a1}^{in}, 0, \xi_2, \sqrt{2\kappa_2}\delta q_{a2}^{in}, \sqrt{2\kappa_2}\delta p_{a2}^{in} \right) \quad (2.15)$$

is the noise vector. Here $\delta q_{aj}^{in} = (a_{in}^{(j)\dagger} + a_{in}^{(j)})/\sqrt{2}$ and $\delta p_{aj}^{in} = i(a_{in}^{(j)\dagger} - a_{in}^{(j)})/\sqrt{2}$, for $j = 1, 2$. The solution of this equation can be written as: $U(t) = B(t)U(0) + \int_0^t ds F(s)V(t-s)$, where $F(t) = \exp(Bt)$ and the matrix B takes the following form:

$$B = \begin{pmatrix} B_1 & B_0 \\ B_0 & B_2 \end{pmatrix} , \quad (2.16)$$

with

$$B_j = \begin{pmatrix} 0 & \omega_{mj} & 0 & 0 \\ -\omega'_{mj} & -\gamma_{mj} & \sqrt{2}G'_j \text{Re}(\alpha_j) & \sqrt{2}G'_j \text{Im}(\alpha_j) \\ -\sqrt{2}G'_j \text{Im}(\alpha_j) & 0 & -\kappa_j & \Delta'_j \\ \sqrt{2}G'_j \text{Re}(\alpha_j) & 0 & -\Delta'_j & -\kappa_j \end{pmatrix} , \quad (2.17)$$

for $j = 1, 2$. The matrix B_0 , as given below, describes the coupling between the cavities:

$$B_0 = \begin{pmatrix} 0 & 0 & 0 & 0 \\ 0 & 0 & 0 & 0 \\ 0 & 0 & 0 & -J \\ 0 & 0 & J & 0 \end{pmatrix}. \quad (2.18)$$

Here $G'_j = g_1^{(j)} - 2g_2^{(j)}\bar{q}_j$, $\omega'_{mj} = \omega_{mj} + 2g_2^{(j)}|\alpha_j|^2$, and $\Delta'_j = \Delta_{cj} - g_1^{(j)}\bar{q}_j + g_2^{(j)}|\bar{q}_j|^2$.

To calculate the entanglement in any two subsystems, we can now calculate the covariance matrix $C(t)$, as a solution of the following linear differential equation,

$$\dot{C}(t) = B(t)C(t) + C(t)B(t)^T + D, \quad (2.19)$$

where the elements of C can be identified as $C_{ij} = (\langle U_i(\infty)U_j(\infty) + U_j(\infty)U_i(\infty) \rangle) / 2$ and the diffusion matrix D is given by

$$D = \text{diag}[0, (2\bar{n}_{m1} + 1)\gamma_{m1}, \kappa_1, \kappa_1, 0, (2\bar{n}_{m2} + 1)\gamma_{m2}, \kappa_2, \kappa_2], \quad (2.20)$$

In the matrix C , every diagonal element represents the 2×2 matrix for the respective mode, and every non-diagonal element C_{ij} represents the 2×2 matrix of inter-mode covariance.

The complete quantum synchronization $S_q(t)$ can be expressed in a concise form as

$$S_q(t) = \left\{ \frac{1}{2} [C_{11}(t) + C_{55}(t) - C_{15}(t) - C_{51}(t) + C_{22}(t) + C_{66}(t) - C_{26}(t) - C_{62}(t)] \right\}^{-1} \quad (2.21)$$

Similar expressions can be found for E_D as well.

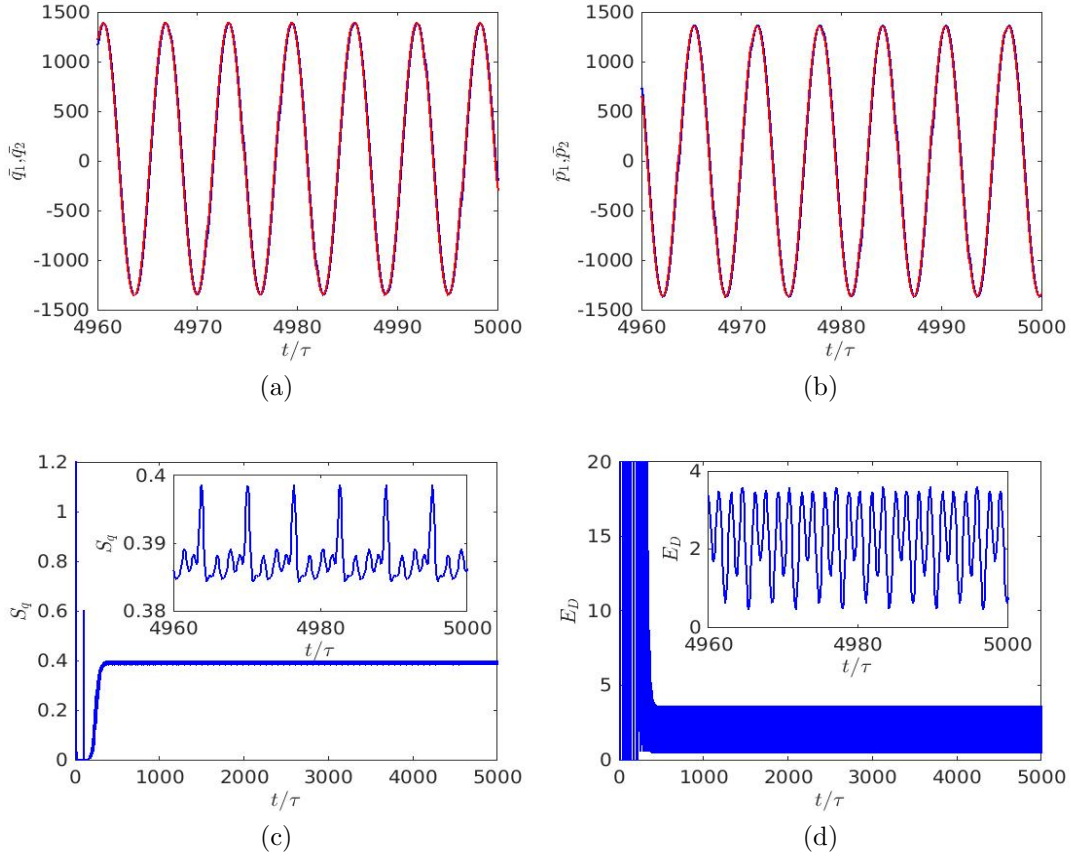


Figure 2.2: Variation of (a) the mean values of \bar{q}_1 (red) and \bar{q}_2 (blue), (b) the mean values of \bar{p}_1 (red) and \bar{p}_2 (blue), (c) complete synchronization S_q , (e) entanglement E_D , with respect to time (in the units of $\tau = 1/\omega_{m1}$). Parameters chosen are $\omega_{m1} = -\Delta_{c1} = 1$, $\omega_{m2} = -\Delta_{c2} = 1.005$, $\bar{n}_{mj} = 0$, $g_1 = 0.005$, $g_2 = 0$, $\gamma_{mj} = 0.005$, $\kappa_j = 0.15$, $E = 100$, $\eta_D = 1$, $\Omega_D = 1$ and $J = 0.04$. The inset shows the steady-state behavior of the oscillation of S_q and E_D .

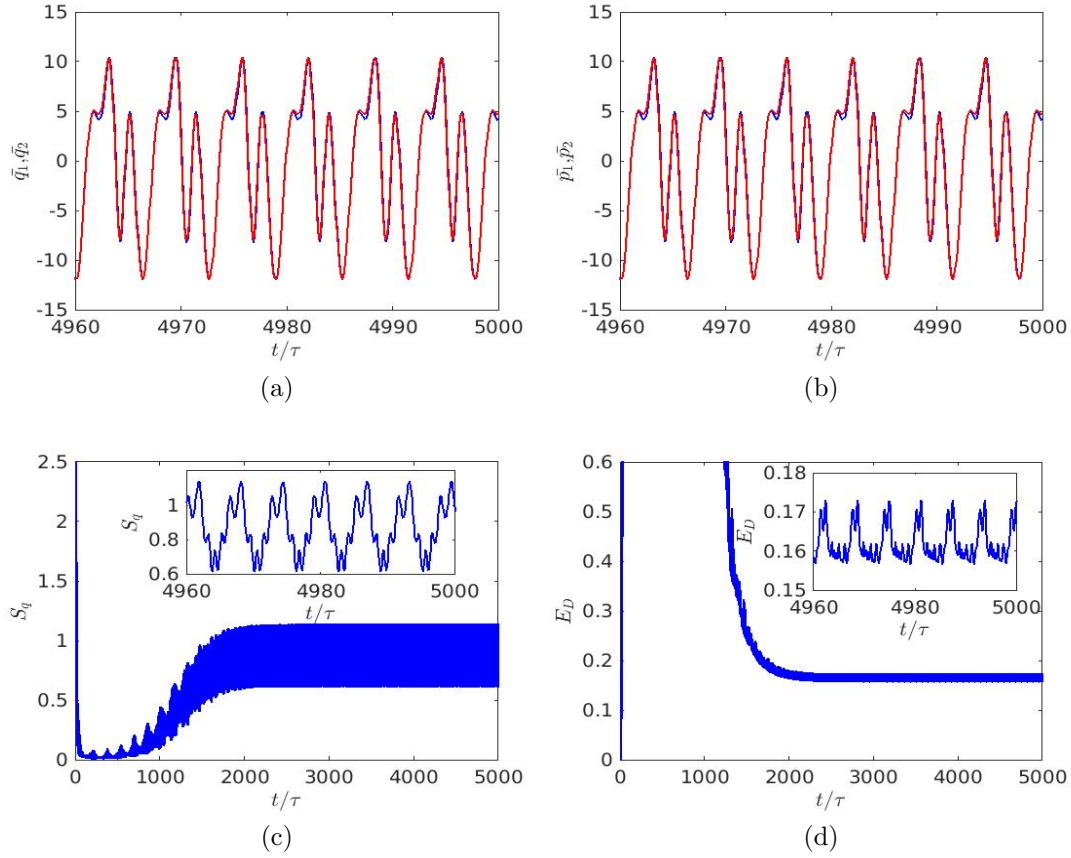


Figure 2.3: Variation of (a) the mean values of \bar{q}_1 (red) and \bar{q}_2 (blue), (b) the mean values of \bar{p}_1 (red) and \bar{p}_2 (blue), (c) synchronization S_q , and (d) entanglement E_D , with respect to time (in the units of $\tau = 1/\omega_{m1}$). Here we have chosen $g_2/g_1 = 1 \times 10^{-2}$, while all the other parameters are the same as in Fig. 2.2. The inset shows the steady-state behavior of the oscillation of S_q and E_D .

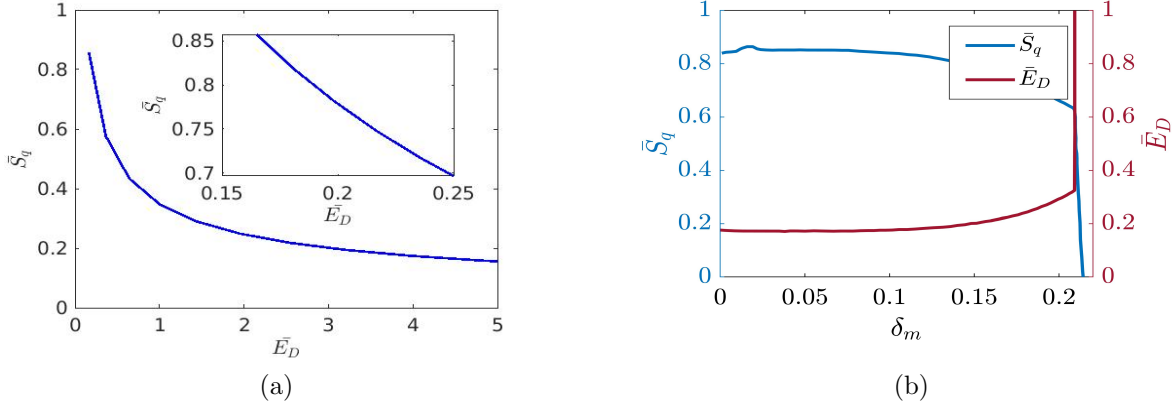


Figure 2.4: (a) A parametric plot of the variation of time-averaged values of synchronization \bar{S}_q with the entanglement \bar{E}_D , when the number of thermal phonons \bar{n}_m varies from 0 to 5. The inset shows the zoomed version of the same plot in the regions of parameters when $\bar{E}_D \leq 0.25$. (b) Variation of time-averaged values of synchronization \bar{S}_q and entanglement \bar{E}_D between the mechanical oscillators with respect to frequency difference $\delta_m = \omega_{m2} - \omega_{m1}$ of the mechanical oscillators. The other parameters are the same as in Fig. 2.3.

2.4.1 Numerical Results and Discussion

In this section, we will show how this entanglement is built up with time and will investigate whether these oscillators get synchronized, as well. We choose here that the optomechanical couplings for both the mechanical oscillators are equal, i.e., $g_1^{(j)} = g_1$ and $g_2^{(j)} = g_2$ for all j .

We first consider the case when there is no quadratic coupling, i.e., $g_2 = 0$. As shown in the Fig. 2.2a and Fig. 2.2b, the system will reach a steady state at long times, when the mean values of the position and momentum vary periodically. This corresponds to the onset of the limit cycles in phase space. In the Fig. 2.2c we show the time evolution of synchronization S_q between the oscillators. The $S_q \sim 0.39$ at the steady state signifies the existence of incomplete quantum synchronization. The small oscillations appearing in this figure are due to sinusoidal variation of the fluctuations in position and momentum at long times. It has been observed that there is no entanglement between the mechanical

oscillators in this case of zero quadratic coupling. This is supported by the Fig. 2.2d, which shows that at long times, the separability criterion Eq. (2.13) is satisfied, as E_D remains greater than 0.25.

When we consider the quadratic coupling as well in our simulation, the synchronization increases beyond what was achieved without it. In the Fig. 2.3a and Fig. 2.3b, we first show the time evolution of limit-cycle trajectories of the mean values \bar{q}_1 , \bar{q}_2 , \bar{p}_1 , and \bar{p}_2 . This shows that the mechanical oscillators are classically completely synchronized. In the Fig. 2.3c, we display the time evolution of quantum synchronization S_q . Even for a value of g_2 as small as $\sim 10^{-2}g_1$, the synchronization increases to a value close to unity, and therefore the mechanical oscillators become nearly completely quantum synchronized. More importantly, the entanglement between the mechanical oscillators starts appearing with $g_2 \neq 0$. The system also violates the standard inseparability criterion Eq. (2.13), as E_D becomes less than 0.25 [see Fig. 2.3d]. A comparison between the Fig. 2.3d and Fig. 2.3c clearly shows that the entanglement and synchronization are achieved, at a time scale of a similar order, and retain their values at long times, even in the presence of decay [refer to Eq. (2.12) and Eq. (2.20)].

The numerical results for $g_2 \neq 0$ suggest that one can get a significant enhancement of quantum synchronization and entanglement simultaneously between mechanical oscillators by choosing appropriate parameters. The direct coupling between the cavity (with a coupling constant J) and the linear coupling mediated by the cavity modes is proportional to q_1 and q_2 , while the effective quadratic coupling between them varies as q_1^2 and q_2^2 . Thus, the coupling proportional to g_2 imparts additional nonlinearity into the fluctuation dynamics, leading to the synchronization. That higher order terms are useful in obtaining synchronization has also been shown in [85].

2.4.2 Effect of indirect coupling and quadratic coupling

From Eq. (2.12), we can notice that the nonlinearity, arising due to coupling constant g_2 , can suppress the oscillation of the two cavities as well as the photon exchange between them. Therefore, the oscillations of the positions and the momenta of the two mechanical oscillators are frozen, unlike the linear cases. This can be attributed to the opposite signs of the terms containing g_1 and g_2 in Eq. (2.12). In this situation, the term containing g_2 tends to reduce the effect of that containing g_1 and the dynamics of the oscillators become more synchronized with each other (albeit with a g_2 -dependent effective frequency). Therefore, the S_q is enhanced and E_D becomes less than 0.25 since the oscillation of the oscillators is suppressed, even for small values of g_2 . Thus, it is the joint effect of the linear coupling and the quadratic coupling of mechanical oscillators with their respective cavity modes, that leads to the simultaneous appearance of synchronization and entanglement between the oscillators. We emphasize that quadratic coupling is essential to build up entanglement and to attain near-complete quantum synchronization for this particular optomechanical system.

Further note that for $g_2 = 0$, one can still have quantum synchronization, albeit not even near-complete and without entanglement. It must be borne in mind that the classical synchronization (and the limit cycle) remains a necessary condition in any case. The above results are valid for a suitable direct coupling constant J . An interesting observation can be made when $J = 0$. In such a case, one cannot have any synchronization between the oscillators (and no limit cycle), as they are not coupled. Indeed, this has been previously noted by Mari *et al.* [14].

We show in the parametric plot Fig. 2.4a, how the synchronization and the entanglement change with the increase in thermal excitation. Clearly, the system remains maximally synchronized ($1 - \bar{S}_q$ is minimum) when it maximally violates Eq. (2.13) [i.e., when $1/4 - \bar{E}_D$ is maximum, see Eq. (2.13)]. This happens at absolute zero, i.e., for $\bar{n}_m = 0$. For larger excitation, the synchronization deteriorates and the entanglement

decreases too, as \bar{E}_D tends to $1/4$ (see Fig. 2.4a). However, the synchronization remains more robust to temperature (or equivalently, the number of thermal phonons \bar{n}_m) as compared to the entanglement. The entanglement vanishes (when \bar{E}_D becomes larger than $1/4$), for $\bar{n}_m \gtrsim 0.2$, while the system still maintains a residual quantum synchronization ~ 0.15 even for \bar{n}_m as large as 5. We further show in the inset of the Fig. 2.4a the domain of simultaneous occurrence of synchronization and entanglement.

We further show in Fig. 2.4b that with the increase in frequency difference $\delta_m = \omega_{m2} - \omega_{m1}$, the synchronization and entanglement decreases similarly up to $\delta_m \sim 0.2$. This means that both synchronization and entanglement are retained even when the frequency of the second oscillator, ω_{m2} , is as large as 20% more than that of the first oscillator, ω_{m1} .

2.5 Conclusion

In conclusion, we have presented a theoretical scheme to study the interplay between quantum synchronization and entanglement of two mechanical oscillators in a double-cavity optomechanical system. As both the criterion for entanglement [70] and the measure of the quantum synchronization [14] can be derived from the same uncertainty principle (in terms of their joint quadratures), we expected that there could be the possibilities of their simultaneous occurrence in the same system. In our model, each mechanical oscillator is suspended inside a cavity and is coupled with the cavity mode via a linear and a quadratic dependence on its displacement from the equilibrium position. Our numerical results show that two coupled harmonic oscillators satisfy both the criteria at the same time and therefore, can be both quantum-synchronised and entangled simultaneously. To be more specific, an appropriate choice of parameters in the presence of quadratic coupling can lead to greatly enhanced quantum synchronization ($S_q > 0.85$) and entanglement between coupled oscillators, at a time much longer than the cavity decay time scale. We have demonstrated classical synchronization via limit cycle trajectories

of the mean quadratures at long times, as a precondition to achieve quantum synchronization. We also investigated the robustness of synchronization and the entanglement against thermal noise and frequency difference.

Though quantum synchronization can be considered to arise out of certain quantum correlation, which could be related to quantum discord [14, 104], there can be certain parameter regimes at which the quantum synchronization can also exist without entanglement (possibly, with nonzero discord). More importantly, the two phenomena (quantum synchronization and entanglement) can be related to quantum fluctuations of a common set of quadrature variables (EPR variables). Precisely speaking, the entanglement criteria based on position and momentum quadratures can provide a suitable marker for quantum synchronization. As discussed in detail in this chapter, entanglement is associated with an enhanced degree of quantum synchronization between two coupled oscillators. Note that entanglement refers to a nonclassical property of coupled bosonic systems, with a close equivalence to the nonlocality. Interestingly, any classical mixture with a bosonic entangled state even exhibits quantum correlation, based on entanglement, as mentioned in the motivation. Thus entanglement can stand, in its merit, as closely related to quantum synchronization, as both arise out of quantum correlations in the quadratures. The existence of entanglement may be considered a stronger criterion for near-complete quantum synchronization. We emphasize that we have put forward a common prescription to relate the two properties. The criteria that we have used can also be verified in experiments, based on quadrature measurements, contrary to quantum discord that cannot be directly verified in experiments.

We also emphasize that our results of quantum synchronization and entanglement are consistent with complete classical synchronization, as both \bar{q}_- and \bar{p}_- tend to zero, corresponding to a time-asymptotic limit cycle in classical phase space. Contrary to what Mari *et al.* conjectured, this is not equivalent to mixed synchronization [105, 106] (that corresponds to $\bar{q}_-, \bar{p}_+ \rightarrow 0$). Though the partial transpose (used to derive the Mancini

criteria) refers to a local time-reversal (and hence counter-rotating trajectory in phase space), our results do not involve any anti-synchronization (i.e., $\bar{p}_+ \rightarrow 0$), as we have $\bar{p}_- \rightarrow 0$ instead.

Chapter 3

Entanglement boosts quantum synchronization between two oscillators

In the previous chapter, we studied the simultaneous occurrence of quantum synchronization and entanglement between two indirectly coupled oscillators in a double cavity optomechanical system. In this chapter, we present a more generic optomechanical model to explore how the entanglement can be related to the quantum synchronization of two mechanical oscillators. We show that entanglement delivers a catalytic effect on the quantum synchronization in the specific system we considered.

3.1 Motivation

Spontaneous synchronization is a natural phenomenon that can be often experienced in avian flight and flashing of fireflies [40]. It has been explored in many different areas, namely, neuron networks [107, 108, 109], chemical reaction [110], nonlinear dynamics [111, 47, 112], and electrical circuits and communications [113, 114].

Classical synchronization between two nonlinearly coupled oscillators occurs due to a rephasing and energy redistribution of their motions. This refers to a limit cycle in phase space, where their respective generalized positions $q_j(t)$ and generalized linear momenta $p_j(t)$ ($j \in 1, 2$) become equal. In quantum regimes, however, one cannot measure these quadratures with certainty at the same time t , according to Heisenberg's uncertainty principle. The best estimate of the quantum synchronization therefore corresponds to a state of two oscillators, for which the total uncertainty of their joint quadratures becomes minimum. In this regard, Mari *et al.* proposed the figure of merit to measure the quantum synchronization in continuous variables [14] in terms of the synchronization errors $q_-(t)$ and $p_-(t)$. Expanding these operators around their mean values, $q_-(t) = Q_-(t) + \delta q_-(t)$, $p_-(t) = P_-(t) + \delta p_-(t)$, and using the limit of zero mean of these quadrature differences, a modified form of the measure of quantum synchronization can be obtained as introduced in the chapter 1 (Eq. (1.37)).

Based on the measure proposed by Mari [14], a more generalized measure of quantum synchronization is introduced, called quantum ϕ synchronization [25], in which the pair of variables have the same amplitude and possess the same phase shift ϕ . We note that a generalized information-theoretic measure of synchronization for quantum systems has also been proposed [115] in terms of the trace distance to the limit cycle.

On the other hand, quantum correlation between the interacting systems can also manifest itself as entanglement. In the context of two oscillators (two bosonic modes), entanglement has been characterized in terms of uncertainties of the joint quadratures. The criterion for entanglement can be derived starting from the uncertainty relation of q_- and p_- and then applying Peres's separability criterion [59] based on the partial transposition. Any bimodal state can be said to be entangled if it violates the partially transposed uncertainty relation Eq. (2.1), as given by [68]. We investigate the entanglement in terms of the well-known Mancini criterion of entanglement which is given by Eq. (2.13).

It can be observed from the above, that both the quantum synchronization measure S_q

and the entanglement criterion E_D are derived from the Heisenberg uncertainty principle for a pair of EPR-like variables. This suggests that both these seemingly different features originate purely from the same class of quantum correlation (namely, the EPR-type) and therefore can appear in the same system at a similar time scale. In fact, in our recent work [116], we have shown that it is indeed possible to both quantum-synchronize and entangle two oscillators in a certain parameter regime, by coupling them with two different cavities. In this chapter, we will explore if such a relation between quantum synchronization and entanglement also exists in a different system. With an always-on nonlinear coupling between two oscillators, we will show that they remain quantum-synchronized as long as they are entangled. More importantly, without the entanglement, the quantum synchronization degrades. Thus, the entanglement can be considered a booster towards complete quantum synchronization.

We note that whether two coupled systems can be simultaneously synchronized and entangled has been investigated in several systems. Manzano *et al.* showed that any two coupled oscillators in a network, initially prepared in a separable state, can be both synchronized and entangled [17], for a suitable choice of the interaction strength to the other oscillators in the network. They further showed that in the presence of synchronization, the entanglement is retained despite the decoherence. It was further shown in [85, 46] that many-body systems can be entangled in the presence of synchronization. In the classical (quantum) limit, two single-mode cavities get synchronized (entangled). However, all the above works dealt only with classical synchronization. On the contrary, it is more meaningful to focus on quantum synchronization, when one looks for its relationship with entanglement, which has no classical analogy. In this chapter, we specifically investigate if there is any inherent quantum correlation that can lead to both quantum synchronization and entanglement. Previous attempts in this regard include the study of quantum discord [117, 17], linear entropy [118], mutual information based on von Neumann entropy [15] and Renyi entropy [119]. Very recently, the relationship between the synchronization

phase, detuning, and quantum correlations has been investigated in a bio-inspired quantum system in [120]. It is shown that quantum discord must be greater than classical information at all times for the emergence of spontaneous quantum synchronization. A minimal model for the emergence of synchronization and possible buildup of quantum correlations during synchronization in the absence of any nonlinear effects, external forcing, or dissipation is introduced in [56]. In this model, two indirectly coupled oscillators, initially prepared in an unentangled state, can get entangled during synchronization. In all of the above works, similar steady-state behavior of these measures of quantum correlation and quantum synchronization was reported. However, their numerical studies could not essentially relate them as arising from the same physical origin. The present work addresses this exact loophole of the earlier reports.

To do the relevant analysis, an optomechanical system poses as a suitable platform. In our model, two mechanical oscillators indirectly interact with each other, via their common coupling to the same cavity mode. One of the oscillators is suspended inside the cavity, while the other is a usual movable mirror of the same cavity. Clearly, their interaction is always on and weakly nonlinear but still leads to near-complete quantum synchronization and entanglement between them. We will specifically show that the quantum correlation manifests itself in the simultaneous existence of the two. This happens at the modulation frequency of the driving field. It is recently reported that the continuous measurement of a single bosonic system can enhance its phase synchronization with the external drive [121], when it is subjected to a squeezed driving field and both negative and nonlinear damping. A feedback control of the system based on the continuous measurement of an additional bath can also enhance synchronization [122]. In this chapter, we however consider a coupled system (not a single system entrained with a drive), and our result suggests an opposite effect upon measurement. If one of the oscillators is measured, it destroys the entanglement and hence the complete quantum synchronization (note that we do not study the phase synchronization in this chapter). In addition, the dynamics of

the oscillators do not involve any two-photon processes, either driving or damping, unlike the van der Pol oscillators considered in [121, 122].

We organize the chapter in the following way. In Section 3.2, we introduce the model and the Hamiltonian and derive all the equations of motion for the fluctuation operators to study how both entanglement and quantum synchronization between the oscillators can arise at a similar time scale. We obtain the analytic expressions of the fluctuations and numerically solve the dynamics of the system in Section 3.3. Finally, we conclude the chapter in Section 3.4.

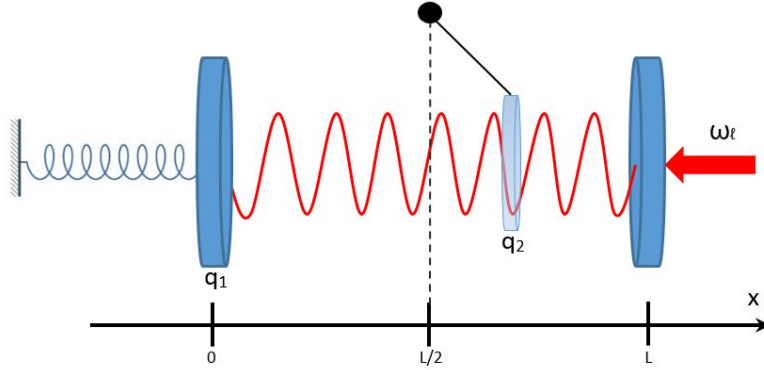


Figure 3.1: Schematic illustration of a driven optical cavity with one oscillating end mirror (acting as a mechanical oscillator) and a membrane in the middle (acting as the second mechanical oscillator). The two oscillators indirectly interact with each other through their common coupling to the same cavity field via radiation pressure force. The optical cavity is driven by a strong amplitude-modulated blue-detuned laser drive to achieve self-sustained oscillations and synchronization of these oscillators.

3.2 Theoretical Model

The optomechanical system under consideration is shown in Fig. 3.1. This system consists of an optical cavity with one mirror fixed, while the other is movable, acting as a mechanical oscillator (with resonance frequency ω_{m1}). Another oscillating membrane is also suspended inside the cavity. The cavity is driven by a laser with frequency ω_l and

time-modulated amplitude $\epsilon(t) = E[1 + \eta_D \cos(\Omega_D t)]$, where E is the amplitude of the laser without any modulation, η_D and Ω_D are the amplitude factor and the frequency of the modulating field. This model is quite different from the other optomechanical setups in which two membranes (or mirrors) are optically coupled to two different cavities [123, 25], while an additional mechanical coupling between them has to be externally introduced to facilitate the synchronization [24, 23]. In our model, the coupling between the mirror and the membrane is always on and there is no need to introduce any additional coupling. Their interaction with the same cavity mode generates an effective photon-number-dependent mirror-membrane coupling, which leads to their synchronization and entanglement as well. Recently, the synchronization effect in this type of optomechanical system where both the mechanical oscillators couple to the same cavity mode has been explored experimentally [124, 125].

The coupling between the optical cavity and membrane depends upon the position of the membrane, placed relative to the nodes and antinodes of the cavity mode. A one-dimensional calculation gives the frequency of the cavity as a function of the mirror displacement q_1 and the membrane displacement q_2 , as follows [92]:

$$\omega_{cav}(q_1, q_2) = \left(\frac{c}{L + q_1} \right) \cos^{-1} \left(r_c \cos \frac{4\pi q_2}{\lambda} \right). \quad (3.1)$$

Here L is the length of the cavity in equilibrium, r_c is the reflectivity of the membrane and λ is the wavelength of the laser field. Expanding $\omega_{cav}(q_1, q_2)$ about the equilibrium positions $q_{10} = 0$ and q_{20} of the respective cavity, up to second order in Taylor series, we have:

$$\omega_{cav}(q_1, q_2) = \omega_c - g_1^{(1)} q_1 - g_1^{(2)} q_2 + g_2^{(1)} q_1^2 + g_2^{(2)} q_2^2 - g_3 q_1 q_2, \quad (3.2)$$

where we can identify

$$\omega_c = \omega_{cav}(0, q_{20}) - \left. \frac{\partial \omega_{cav}}{\partial q_2} \right|_{(0, q_{20})} q_{20} + \frac{1}{2} \left. \frac{\partial^2 \omega_{cav}}{\partial q_2^2} \right|_{(0, q_{20})} q_{20}^2 ,$$

and

$$\begin{aligned} g_1^{(1)} &= \left(- \left. \frac{\partial \omega_{cav}}{\partial q_1} \right|_{(0, q_{20})} + \frac{1}{2} \left. \frac{\partial^2 \omega_{cav}}{\partial q_1 \partial q_2} \right|_{(0, q_{20})} q_{20} \right) q_{zpf} , \\ g_1^{(2)} &= \left(- \left. \frac{\partial \omega_{cav}}{\partial q_2} \right|_{(0, q_{20})} + \left. \frac{\partial^2 \omega_{cav}}{\partial q_2^2} \right|_{(0, q_{20})} q_{20} \right) q_{zpf} , \\ g_2^{(j)} &= \frac{1}{2} \left. \frac{\partial^2 \omega_{cav}}{\partial q_j^2} \right|_{(0, q_{20})} q_{zpf}^2 , \quad j = 1, 2 \\ g_3 &= - \frac{1}{2} \left. \frac{\partial^2 \omega_{cav}}{\partial q_1 \partial q_2} \right|_{(0, q_{20})} q_{zpf}^2 . \end{aligned} \quad (3.3)$$

The Hamiltonian of the system then takes the following form ($\hbar = 1$):

$$H = \omega_{cav}(q_1, q_2) a^\dagger a + \sum_{j=1,2} \frac{\omega_{mj}}{2} (q_j^2 + p_j^2) + \iota \epsilon(t) (a^\dagger - a) , \quad (3.4)$$

where ω_{mj} , q_j , and p_j are the frequency, dimensionless position and momentum operators, respectively, of the j th oscillator, $a^\dagger(a)$ is the creation (annihilation) operator of cavity mode, satisfying the commutation relation $[a, a^\dagger] = 1$, and η_D and Ω_D are the amplitude and the frequency of the modulating field. The quadratures satisfy the following commutation relation: $[q_j, p_{j'}] = \iota \delta_{jj'}$.

On putting the expression Eq. (3.2) of $\omega_{cav}(q_1, q_2)$, the Hamiltonian in the frame rotating with the laser frequency ω_l can be written as

$$H = \Delta a^\dagger a + \sum_{j=1,2} \left[\frac{\omega_{mj}}{2} (q_j^2 + p_j^2) + \left(-g_1^{(j)} q_j + g_2^{(j)} q_j^2 \right) a^\dagger a \right] - g_3 q_1 q_2 a^\dagger a + \iota \epsilon(t) (a^\dagger - a) \quad (3.5)$$

Here $\Delta = \omega_c - \omega_l$ denotes the cavity mode detuning. Considering the dissipation of the

system, we can now obtain the following quantum Langevin equations for the relevant operators

$$\begin{aligned}\frac{dq_j}{dt} &= \omega_{mj} p_j , \\ \frac{dp_j}{dt} &= -\omega_{mj} q_j + g_1^{(j)} a^\dagger a - 2g_2^{(j)} a^\dagger a q_j + g_3 a^\dagger a q_{3-j} - \gamma_{mj} p_j + \xi_j(t) , \\ \frac{da}{dt} &= -(\kappa + \iota \Delta) a + \iota \sum_{j=1,2} \left(g_1^{(j)} q_j - g_2^{(j)} q_j^2 \right) a + \iota g_3 q_1 q_2 a + \epsilon(t) + \sqrt{2\kappa} a_{in} ,\end{aligned}\quad (3.6)$$

where we have used the Hamiltonian Eq. (3.5). Here κ is the decay rate of cavity mode, γ_{mj} is the damping rate of j th mechanical oscillator, and a_{in} is the input noise operator with the following two-time correlation functions: [36]:

$$\left\langle a_{in}(t) a_{in}^\dagger(t') \right\rangle = \delta(t - t') , \quad \left\langle a_{in}^\dagger(t) a_{in}(t') \right\rangle = 0 . \quad (3.7)$$

On the other hand, the thermal bath at an equilibrium temperature T is described by a Brownian noise $\xi_j(t)$ with zero mean and the following two-time correlation function:

$$\langle \xi_j(t) \xi_j(t') \rangle = \frac{\gamma_{mj}}{2\pi\omega_{mj}} \int \omega e^{-i\omega(t-t')} \left[1 + \coth \left(\frac{\hbar\omega}{2k_B T} \right) \right] d\omega , \quad (3.8)$$

where k_B is the Boltzmann constant. For the case of a large quality factor of the mechanical oscillator, the expression above reduces to the following Markovian-approximated form [126]:

$$\langle \xi_j(t) \xi_j(t') \rangle = \gamma_{mj} (2\bar{n}_{mj} + 1) \delta(t - t') , \quad (3.9)$$

where $\bar{n}_{mj} = 1/[\exp(\hbar\omega_{mj}/k_B T) - 1]$ is the mean phonon number of the j th mechanical oscillator.

3.2.1 Solution in mean-field approximation

Since it is difficult to solve equation Eq. (3.6) analytically, we use the mean-field approximation to simplify the calculation by rewriting the operators as the sum of their mean values and quantum fluctuation near mean value, i.e., $a \rightarrow A + \delta a$, $q_j \rightarrow Q_j + \delta q_j$, and $p_j \rightarrow P_j + \delta p_j$, where $A = \langle a \rangle$, $Q_j = \langle q_j \rangle$, and $P_j = \langle p_j \rangle$. Thus, the quantum Langevin equations can be split into two sets of equations, namely, (i) the nonlinear equations for the mean values:

$$\begin{aligned} \frac{dQ_j}{dt} &= \omega_{mj} P_j , \\ \frac{dP_j}{dt} &= -\omega_{mj} Q_j + \left(g_1^{(j)} + g_3 Q_{3-j} \right) |\alpha|^2 - 2g_2^{(j)} Q_j |\alpha|^2 - \gamma_{mj} P_j , \\ \frac{dA}{dt} &= -(\kappa + \iota \Delta) A + \iota \sum_{j=1,2} \left(g_1^{(j)} Q_j - g_2^{(j)} Q_j^2 \right) A + \iota g_3 Q_1 Q_2 A + \epsilon(t) , \end{aligned} \quad (3.10)$$

and (ii) the linearized equations for the quantum fluctuations:

$$\begin{aligned} \frac{d}{dt} \delta q_j &= \omega_j \delta p_j , \\ \frac{d}{dt} \delta p_j &= - \left(\omega_{mj} + 2g_2^{(j)} |A|^2 \right) \delta q_j + g_3 |A|^2 \delta q_{3-j} + G_j \left(A \delta a^\dagger + A^* \delta a \right) - \gamma_{mj} \delta p_j + \xi_j(t) , \\ \frac{d}{dt} \delta a &= -\iota F \delta a + \iota G_1 A \delta q_1 + \iota G_2 A \delta q_2 - \kappa \delta a + \sqrt{2\kappa} a_{in} , \end{aligned} \quad (3.11)$$

where

$$\begin{aligned} G_j &= g_1^{(j)} - 2g_2^{(j)} Q_j + g_3 Q_{3-j} , \\ F &= \Delta - g_1^{(1)} Q_1 - g_1^{(2)} Q_2 + g_2^{(1)} Q_1^2 + g_2^{(2)} Q_2^2 - g_3 Q_1 Q_2 . \end{aligned} \quad (3.12)$$

Here, we have ignored the second and higher-order terms in fluctuations.

In order to calculate the desired markers, S_q and E_D , respectively for quantum synchronization and entanglement, we need to obtain the solutions for the quadrature fluctuations

of the oscillators. Solving the Eq. (3.11) will be convenient if we replace the intra-cavity field and the input noise operators by their quadratures, as well: $\delta x = \frac{1}{\sqrt{2}} (\delta a^\dagger + \delta a)$, $\delta y = \frac{i}{\sqrt{2}} (\delta a^\dagger - \delta a)$, $\delta x_{in} = \frac{1}{\sqrt{2}} (\delta a_{in}^\dagger + \delta a_{in})$, and $\delta y_{in} = \frac{i}{\sqrt{2}} (\delta a_{in}^\dagger - \delta a_{in})$. Therefore, the Eq. (3.11) takes a simpler form, as given by

$$\dot{r}(t) = Sr(t) + n(t), \quad (3.13)$$

where $r(t)^T = (\delta q_1, \delta p_1, \delta q_2, \delta p_2, \delta x, \delta y)$, the vector $n(t)$ as given below contains the noise terms:

$$n(t)^T = \left(0, \xi_1, 0, \xi_2, \sqrt{2\kappa}\delta x_{in}, \sqrt{2\kappa}\delta y_{in} \right), \quad (3.14)$$

and

$$S = \begin{pmatrix} 0 & \omega_{m1} & 0 & 0 & 0 & 0 \\ -\omega_{m1} - 2g_2^{(1)}|A|^2 & -\gamma_{m1} & g_3|A|^2 & 0 & \sqrt{2}G_1 \operatorname{Re}(A) & \sqrt{2}G_1 \operatorname{Im}(A) \\ 0 & 0 & 0 & \omega_{m2} & 0 & 0 \\ g_3|A|^2 & 0 & -\omega_{m2} - 2g_2^{(2)}|A|^2 & -\gamma_{m2} & \sqrt{2}G_2 \operatorname{Re}(A) & \sqrt{2}G_2 \operatorname{Im}(A) \\ -\sqrt{2}G_1 \operatorname{Im}(A) & 0 & -\sqrt{2}G_2 \operatorname{Im}(A) & 0 & -\kappa & F \\ \sqrt{2}G_1 \operatorname{Re}(A) & 0 & \sqrt{2}G_2 \operatorname{Re}(A) & 0 & -F & -\kappa \end{pmatrix} \quad (3.15)$$

is a 6×6 time-dependent coefficient matrix.

The initial states of the oscillators can be best approximated as Gaussian states with the peak at the mean position of the respective oscillators, along with minimum uncertainties in position quadratures. The fluctuation dynamics of the system is governed by a set of linearized equations, and this ensures that the evolved states also remain Gaussian. Since the Gaussian state can be fully characterized by its covariance matrix $C(t)$, we use it to calculate the correlation between the quantum fluctuations of the system variables and to compute all the relevant measures, namely, S_q and E_D . The temporal dynamics

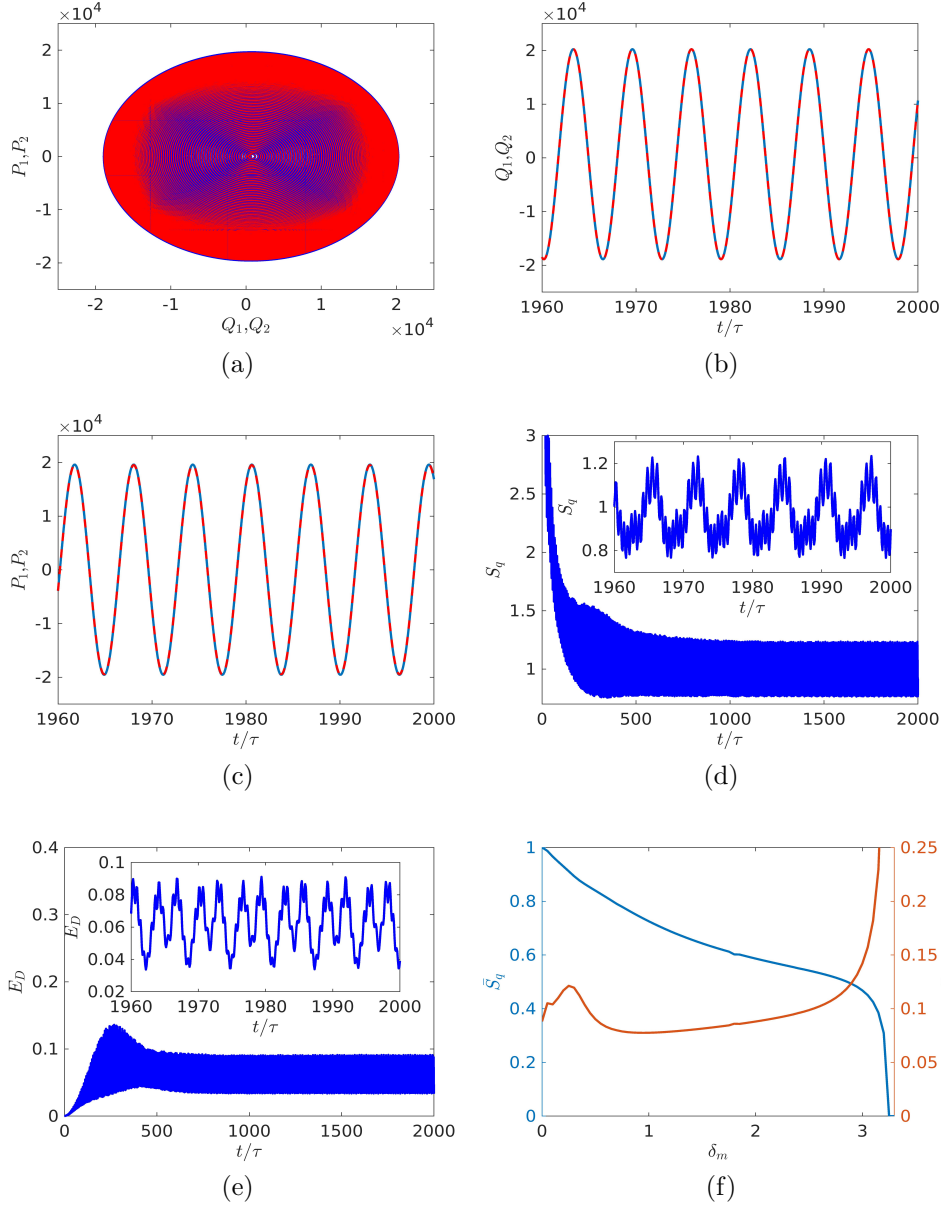


Figure 3.2: (a) Limit-cycle trajectories in the $Q_1 \rightleftharpoons P_1$ (red) and $Q_2 \rightleftharpoons P_2$ (blue) spaces, Variation of (b) the mean values Q_1 (red) and Q_2 (blue), (c) the mean values P_1 (red) and P_2 (blue), (d) synchronization S_q , (e) entanglement E_D , with respect to time (in the units of $\tau = 1/\omega_{m1}$). The parameters chosen are $\omega_{m1} = -\Delta = 1$, $\omega_{m2} = 1.005$, $\bar{n}_{mj} = 0.5$, $g_1 = 5 \times 10^{-5}$, $g_2 = g_1 \times 10^{-2}$, $g_3 = 10^{-6}$, $\gamma_{mj} = 0.009$, $\kappa = 0.1$, $E = 250$, $\eta_D = 4$ and $\Omega_D = 1$. All frequencies are normalized with respect to ω_{m1} . (f) Evolution of time-averaged values of synchronization \bar{S}_q (blue) and entanglement \bar{E}_D (red) with respect to the frequency difference $\delta_m = \omega_{m2} - \omega_{m1}$ of the mechanical oscillators. [all the other parameters are the same as in (a)-(e) above].

3 Entanglement boosts quantum synchronization between two oscillators

of $C(t)$ is governed by the following linear differential equation:

$$\dot{C}(t) = S(t)C(t) + C(t)S(t)^T + D, \quad (3.16)$$

where the elements of C are given by $C_{ij} = [\langle r_i(\infty)r_j(\infty) + r_j(\infty)r_i(\infty) \rangle] / 2$. The matrix D , as below, describes the diffusion of the system:

$$D = \text{diag}[0, (2\bar{n}_{m1} + 1)\gamma_{m1}, 0, (2\bar{n}_{m2} + 1)\gamma_{m2}, \kappa, \kappa]. \quad (3.17)$$

In the matrix C , the diagonal (off-diagonal) element represents the variance of the respective mode (covariance of two modes). The quantum synchronization quantifier $S_q(t)$ can then be expressed as

$$S_q(t) = \left\{ \frac{1}{2} [C_{11}(t) + C_{33}(t) - C_{13}(t) - C_{31}(t) + C_{22}(t) + C_{44}(t) - C_{24}(t) - C_{42}(t)] \right\}^{-1} \quad (3.18)$$

and entanglement marker $E_D(t)$ as

$$E_D(t) = \frac{1}{4} [C_{11}(t) + C_{33}(t) - C_{13}(t) - C_{31}(t)] \times [C_{22}(t) + C_{44}(t) + C_{24}(t) + C_{42}(t)] \quad (3.19)$$

3.2.2 Numerical results

We show in [Fig. 3.2](#), the time-evolution of the quadratures of the oscillators, as obtained by simultaneously solving [Eq. \(3.10\)](#). In [Fig. 3.2a](#), we show how the evolution of $Q_1 \rightleftharpoons P_1$ and $Q_2 \rightleftharpoons P_2$ of the two oscillators tend to an asymptotic periodic orbit and the two limit cycles tend to be consistent with each other. This becomes apparent from the [Fig. 3.2b](#) and [Fig. 3.2c](#), as the mean positions Q_1 and Q_2 and also the mean linear momenta P_1 and P_2 are found to oscillate exactly in phase at the long times. This refers to the complete classical synchronization between mechanical oscillators.

With the classical limit cycle as a pre-condition, we next analyze how the S_q and E_D

vary with time. From the Fig. 3.2d, we can see that S_q reaches a stable value close to unity that refers to complete quantum synchronization. More importantly, we find that this is associated with entanglement. From the Fig. 3.2e, we can see that E_D becomes less than 0.25. This shows that entanglement criterion Eq. (2.13) is violated by the state of the two oscillators. By comparing Fig. 3.2e and Fig. 3.2d, it can be observed that the generation of entanglement and synchronization between the oscillators occur at a similar time scale. This indicates a possible relation between the onset of quantum synchronization and the generation of entanglement between the oscillators. In fact, the long-time behavior, as displayed in the insets of Fig. 3.2d and Fig. 3.2e, clearly reveals that when E_D becomes minimum, the S_q also becomes less than unity and minimum. While the S_q oscillates sinusoidally with an amplitude less than 1, the E_D has two different sinusoidal components, which have the same frequency as S_q , but with a relative phase and different amplitudes. Therefore, E_D exhibits two minima, one of which (the global minimum) appears at the same instances as that of S_q .

We further show in Fig. 3.2f, how the quantum synchronization and entanglement behave with the increase in frequency difference $\delta_m = \omega_{m2} - \omega_{m1}$. The time-averaged values of the respective markers S_q and E_D for quantum synchronization and the entanglement deteriorates with the rise in frequency difference δ_m . One can observe that the quantum complete synchronization (i.e., $\bar{S}_q = 1$) and the maximal violation of entanglement inseparability (i.e., $\bar{E}_D - 1/4$ is minimum) occur around the resonance condition $\delta_m = 0$, i.e., for a pair of identical mechanical oscillators (i.e., $\omega_{m1} = \omega_{m2}$). Interestingly, they stay robust (i.e., S_q remains less than 1 and E_D less than 0.25) and therefore maintain both quantum synchronization and entanglement, against the asymmetry in the oscillator frequencies, as large as $\delta_m \sim 3.2$. As $\delta_m \gtrsim 3.2$, the oscillators no longer remain entangled (as E_D exceeds 0.25) and quantum-synchronized (as S_q becomes 0) and both these features vanish together. This further strengthens our conjecture that quantum synchronization and entanglement must originate from the same type of quantum correlation.

3.3 Analytic solution of fluctuations

In order to have a deeper insight into entanglement and synchronization behavior, we next obtain an analytical solution of the mean square fluctuations in the relative displacement q_- , the total momentum p_+ , and relative momentum p_- . We start with the Eq. (3.6), which can be rewritten for these variables as

$$\begin{aligned}
\frac{dq_-}{dt} &= \omega_m p_- , \\
\frac{dq_+}{dt} &= \omega_m p_+ , \\
\frac{dp_-}{dt} &= -\omega_m q_- - 2g_2 a^\dagger a q_- - g_3 a^\dagger a q_- - \gamma_m p_- + \frac{1}{\sqrt{2}} (\xi_1 - \xi_2) , \\
\frac{dp_+}{dt} &= -\omega_m q_+ + \sqrt{2} g_1 a^\dagger a - 2g_2 a^\dagger a q_+ + g_3 a^\dagger a q_+ - \gamma_m p_+ + \frac{1}{\sqrt{2}} (\xi_1 + \xi_2) , \\
\frac{da}{dt} &= -(\kappa + \iota \Delta) a + \iota \left[\sqrt{2} g_1 q_+ - g_2 (q_1^2 + q_2^2) + g_3 q_1 q_2 \right] a + \epsilon(t) + \sqrt{2\kappa} a_{in} , (3.20)
\end{aligned}$$

where we have assumed $\omega_{m1} = \omega_{m2} = \omega_m$, $g_1^{(j)} = g_1$ and $g_2^{(j)} = g_2$ for all j , for simplicity.

3.3.1 Asymptotic solutions of first moments

We next expand the operators q_\pm and p_\pm as a sum of their mean values and fluctuations as follows: $q_\pm = Q_\pm + \delta q_\pm$, $p_\pm = P_\pm + \delta p_\pm$. The Langevin equations Eq. (3.20) can then be split into two sets: one for the mean values, as listed below, and the other one for the

fluctuation operators, to be discussed later.

$$\begin{aligned}
\frac{dQ_-}{dt} &= \omega_m P_- , \\
\frac{dQ_+}{dt} &= \omega_m P_+ , \\
\frac{dP_-}{dt} &= -\omega_m Q_- - 2g_2|A|^2 Q_- - g_3|A|^2 Q_- - \gamma_m P_- , \\
\frac{dP_+}{dt} &= -\omega_m Q_+ + \sqrt{2}g_1|A|^2 - 2g_2|A|^2 Q_+ + g_3|A|^2 Q_+ - \gamma_m P_+ , \\
\frac{dA}{dt} &= -(\kappa + \iota\Delta)A + \iota \left[\sqrt{2}g_1 Q_+ - g_2(Q_1^2 + Q_2^2) + g_3 Q_1 Q_2 \right] A + \epsilon(t) . \quad (3.21)
\end{aligned}$$

Since the cavity is driven by a modulating field $\epsilon(t)$, which can be rewritten as $E_0 + E_1 e^{i\Omega_D t} + E_{-1} e^{-i\Omega_D t}$. Therefore, the amplitudes of the cavity mode and the mechanical modes would also follow the dynamics of this field at a long-time limit, according to the Floquet theorem, i.e., $\lim_{t \rightarrow \infty} A(t) = A(t + \tau)$, $\lim_{t \rightarrow \infty} Q_{1,2}(t) = Q_{1,2}(t + \tau)$ and $\lim_{t \rightarrow \infty} P_{1,2}(t) = P_{1,2}(t + \tau)$ [127]. We therefore redefine these classical amplitudes in terms of Fourier components to the first harmonic of the modulating frequency Ω_D , as follows.

$$\begin{aligned}
A &= A_{-1} e^{i\Omega_D t} + A_0 + A_1 e^{-i\Omega_D t} , \\
Q_- &= Q_{-1}^- e^{i\Omega_D t} + Q_0^- + Q_1^- e^{-i\Omega_D t} , \\
P_- &= P_{-1}^- e^{i\Omega_D t} + P_0^- + P_1^- e^{-i\Omega_D t} , \\
Q_+ &= Q_{-1}^+ e^{i\Omega_D t} + Q_0^+ + Q_1^+ e^{-i\Omega_D t} , \\
P_+ &= P_{-1}^+ e^{i\Omega_D t} + P_0^+ + P_1^+ e^{-i\Omega_D t} . \quad (3.22)
\end{aligned}$$

3.3.1.1 Obtaining the Fourier coefficients of Q_- and P_-

To find the time-independent coefficients $Q_{-1,0,1}^-$, we first substitute A , Q_- , and P_- from Eq. (3.22) into the Langevin equations Eq. (3.21) for Q_- and P_- . This leads us to the

following set of three coupled nonlinear equations, when $\Omega_D = \omega_m$:

$$\begin{aligned} (\omega_m + W) Q_0^- + W_0 Q_1^- + W_0^* Q_{-1}^- &= 0 , \\ W_0 Q_0^- + W_1 Q_1^- + (\iota\gamma_m + W) Q_{-1}^- &= 0 , \\ W_0^* Q_0^- + (-\iota\gamma_m + W) Q_1^- + W_1^* Q_{-1}^- &= 0 , \end{aligned} \quad (3.23)$$

where

$$\begin{aligned} W_0 &= (2g_2 + g_3)(A_0 A_1^* + A_0^* A_{-1}) , \\ W_1 &= (2g_2 + g_3)(A_1^* A_{-1}) , \\ W &= (2g_2 + g_3)(|A_0|^2 + |A_1|^2 + |A_{-1}|^2) . \end{aligned} \quad (3.24)$$

The trivial solution of the above set of equations [Eq. \(3.23\)](#) is $Q_{-1,0,1}^- = 0$, so that Q_- vanishes. From the equation of P_- , we also have $P_-(t) = \exp(-\gamma_m t) P_-(0)$, which vanishes as $t \rightarrow \infty$. Both the results $Q_- = 0, P_- = 0$ are expected in a synchronized system. This further implies that $Q_1 = Q_2 = Q_+/\sqrt{2}$.

3.3.1.2 Obtaining the Fourier coefficients $A_{-1,0,1}$

Putting the above results of $Q_{1,2}$ in the Langevin equation of A in [Eq. \(3.21\)](#), we find that this reduces to the following equation:

$$\frac{dA}{dt} = -(\kappa + \iota\Delta)A + \iota \left[\sqrt{2}g_1 Q_+ - \left(\frac{2g_2 - g_3}{2} \right) Q_+^2 \right] A + \epsilon(t) , \quad (3.25)$$

which contains only Q_+ . Substituting A and Q_+ from the [Eq. \(3.22\)](#) into [Eq. \(3.25\)](#) and separating the different Fourier components, we obtain the following coupled equations of

the time-independent coefficients $A_{-1,0,1}$:

$$\begin{aligned} U A_0 + U_{-1} A_1 + U_1 A_{-1} &= E_0 , \\ U_1 A_0 + [-\iota \omega_m + U] A_1 + \left[\frac{\iota}{2} (2g_2 - g_3) (Q_1^+)^2 \right] A_{-1} &= E_1 , \\ U_{-1} A_0 + [\iota \omega_m + U] A_{-1} + \left[\frac{\iota}{2} (2g_2 - g_3) (Q_{-1}^+)^2 \right] A_1 &= E_{-1} , \end{aligned} \quad (3.26)$$

where

$$\begin{aligned} U &= (\kappa + \iota \Delta) - \iota \sqrt{2} g_1 Q_0^+ + \iota (2g_2 - g_3) \left(\frac{1}{2} Q_0^{+2} + Q_1^+ Q_{-1}^+ \right) , \\ U_1 &= -\iota \sqrt{2} g_1 Q_1^+ + \iota (2g_2 - g_3) (Q_0^+ Q_1^+) , \\ U_{-1} &= -\iota \sqrt{2} g_1 Q_{-1}^+ + \iota (2g_2 - g_3) (Q_0^+ Q_{-1}^+) . \end{aligned} \quad (3.27)$$

Here we consider the weak optomechanical coupling regime, i.e., $|g_i| \ll \omega_m, \kappa$ ($i \in 1, 2, 3$), such that $U \approx (\kappa + \iota \Delta)$ and $U_{\pm 1}$ may be neglected. Therefore, in the long-time limit, we have

$$A_0 = \frac{E_0}{\kappa + \iota \Delta}, \quad A_1 = \frac{E_1}{\kappa + \iota (\Delta - \omega_m)}, \quad A_{-1} = \frac{E_{-1}}{\kappa + \iota (\Delta + \omega_m)} . \quad (3.28)$$

3.3.1.3 Obtaining the Fourier coefficients of Q_+ and P_+

So far, we have obtained the expressions of the Fourier components of Q_- and A . To find out Q_+ , we again substitute A , Q_+ , and P_+ from [Eq. \(3.22\)](#) into the Langevin equation [Eq. \(3.21\)](#) for Q_+ and P_+ , that leads us to the following set of three coupled nonlinear equations of $Q_{-1,0,1}^+$:

$$\begin{aligned} (\omega_m + V) Q_0^+ + V_0 Q_1^+ + V_0^* Q_{-1}^+ &= \sqrt{2} g_1 (|A_0|^2 + |A_1|^2 + |A_{-1}|^2) , \\ V_0 Q_0^+ + V_1 Q_1^+ + (\iota \gamma_m + V) Q_{-1}^+ &= \sqrt{2} g_1 (A_0 A_1^* + A_0^* A_{-1}) , \\ V_0^* Q_0^+ + (-\iota \gamma_m + V) Q_1^+ + V_1^* Q_{-1}^+ &= \sqrt{2} g_1 (A_0 A_{-1}^* + A_0^* A_1) , \end{aligned} \quad (3.29)$$

where

$$\begin{aligned}
V_0 &= (2g_2 - g_3)(A_0 A_1^* + A_0^* A_{-1}) , \\
V_1 &= (2g_2 - g_3)(A_1^* A_{-1}) , \\
V &= (2g_2 - g_3)(|A_0|^2 + |A_1|^2 + |A_{-1}|^2) .
\end{aligned} \tag{3.30}$$

Using [Eq. \(3.28\)](#), we can find the time-independent coefficients $Q_{-1,0,1}^+$ by algebraically solving the above equations. The expressions of P_+ can then be easily obtained using the equation for Q_+ in [Eq. \(3.21\)](#).

3.3.2 Frequency spectrum of fluctuations

To investigate the quantum synchronization and entanglement between mechanical oscillators, we need to calculate the mean square fluctuations in q_- and p_{\pm} . The dynamical behavior of these fluctuations can be described by the following Langevin equations, as obtained from [Eq. \(3.20\)](#) [see [Section 3.3.1](#)]:

$$\begin{aligned}
\frac{d}{dt}\delta q_- &= \omega_m \delta p_- , \\
\frac{d}{dt}\delta p_- &= -[\omega_m + (2g_2 + g_3)(|A_0|^2 + |A_1|^2 + |A_{-1}|^2)] \delta q_- - \gamma_m \delta p_- + \frac{\xi_1 - \xi_2}{\sqrt{2}} , \\
\frac{d}{dt}\delta q_+ &= \omega_m \delta p_+ , \\
\frac{d}{dt}\delta p_+ &= -F_0 \delta q_+ + F_1 \delta a^\dagger + F_2 \delta a - \gamma_m \delta p_+ + \frac{\xi_1 + \xi_2}{\sqrt{2}} , \\
\frac{d}{dt}\delta a &= -(\kappa + \iota \Delta') \delta a + \iota F_1 \delta q_+ + \sqrt{2\kappa} \delta a_{in} , \\
\frac{d}{dt}\delta a^\dagger &= -(\kappa - \iota \Delta') \delta a^\dagger - \iota F_2 \delta q_+ + \sqrt{2\kappa} \delta a_{in}^\dagger ,
\end{aligned} \tag{3.31}$$

where

$$\begin{aligned}
F_0 &= \omega_m + (2g_2 - g_3) (|A_0|^2 + |A_1|^2 + |A_{-1}|^2) , \\
F_1 &= \sqrt{2}g_1 A_0 - (2g_2 - g_3) (Q_0^+ A_0 + Q_1^+ A_{-1} + Q_{-1}^+ A_1) , \\
F_2 &= \sqrt{2}g_1 A_0^* - (2g_2 - g_3) (Q_0^+ A_0^* + Q_1^+ A_1^* + Q_{-1}^+ A_{-1}^*) , \\
\Delta' &= \Delta - \sqrt{2}g_1 Q_0^+ + \left(\frac{2g_2 - g_3}{2} \right) (Q_0^{+2} + 2Q_1^+ Q_{-1}^+) .
\end{aligned} \tag{3.32}$$

These equations explicitly depend upon the Fourier components of A and Q_+ . Introducing the cavity field quadratures $\delta x = \frac{\delta a + \delta a^\dagger}{\sqrt{2}}$ and $\delta y = \frac{i(\delta a^\dagger - \delta a)}{\sqrt{2}}$, and the input noise quadratures $\delta x_{in} = \frac{\delta a_{in} + \delta a_{in}^\dagger}{\sqrt{2}}$ and $\delta y_{in} = \frac{i(\delta a_{in}^\dagger - \delta a_{in})}{\sqrt{2}}$, the Eq. (3.31) can be reduced to the following matrix form:

$$\dot{f}(t) = H f(t) + G(t) , \tag{3.33}$$

where $f(t)$ is the fluctuation vector and $G(t)$ is the noise vector, with the respective transposes given by,

$$f(t)^T = (\delta q_+, \delta p_+, \delta x, \delta y) , G(t)^T = \left(0, \frac{\xi_1 + \xi_2}{\sqrt{2}}, \sqrt{2\kappa} \delta x_{in}, \sqrt{2\kappa} \delta y_{in} \right) , \tag{3.34}$$

and the matrix H is given by

$$H = \begin{pmatrix} 0 & \omega_m & 0 & 0 \\ -F_0 & -\gamma_m & \frac{F_1 + F_2}{\sqrt{2}} & \frac{i(F_2 - F_1)}{\sqrt{2}} \\ \frac{-i(F_2 - F_1)}{\sqrt{2}} & 0 & -\kappa & \Delta' \\ \frac{F_1 + F_2}{\sqrt{2}} & 0 & -\Delta' & -\kappa \end{pmatrix} . \tag{3.35}$$

Taking the Fourier transformation of each operator in Eq. (3.31) and solving them in

the frequency domain, the fluctuations spectrum of the q_- and p_- can be obtained as

$$\begin{aligned}\delta q_-(\omega) &= \frac{-\omega_m}{d(\omega)} \left(\frac{\xi_1(\omega) - \xi_2(\omega)}{\sqrt{2}} \right), \\ \delta p_-(\omega) &= \frac{\iota\omega}{d(\omega)} \left(\frac{\xi_1(\omega) - \xi_2(\omega)}{\sqrt{2}} \right),\end{aligned}\quad (3.36)$$

where $d(\omega) = \omega^2 + \iota\omega\gamma_m - \omega_m^2 - \omega_m(2g_2 + g_3)(|A_0|^2 + |A_1|^2 + |A_{-1}|^2)$. Similarly, the fluctuation in the total momentum has the following spectrum:

$$\begin{aligned}\delta p_+(\omega) &= \frac{\iota\omega}{D(\omega)} \left[\sqrt{2\kappa} \left\{ F_1[\kappa + \iota(\Delta' - \omega)]\delta a_{in}^\dagger(-\omega) + F_2[\kappa - \iota(\Delta' + \omega)]\delta a_{in}(\omega) \right\} \right] + \\ &\quad \frac{\iota\omega}{D(\omega)} \left[\{(\kappa - \iota\omega)^2 + \Delta'^2\} \frac{\xi_1(\omega) + \xi_2(\omega)}{\sqrt{2}} \right],\end{aligned}\quad (3.37)$$

where $D(\omega) = 2\Delta'\omega_m F_1 F_2 + [\omega^2 + \iota\omega\gamma_m - \omega_m^2 - \omega_m(2g_2 - g_3)(|A_0|^2 + |A_1|^2 + |A_{-1}|^2)][(\kappa - \iota\omega)^2 + \Delta'^2]$. We must emphasize here that the stability of such a system is essential to achieve any synchronization. If all the eigenvalues of the matrix H have negative real parts, the stability can be ensured at long times. Using the Routh-Hurwitz criterion [39], the corresponding conditions can be derived as follows:

$$\begin{aligned}\kappa\gamma_m \left[(\Delta'^2 + \kappa^2)^2 + (F_0\omega_m + \gamma_m\kappa)^2 + 2\gamma_m\kappa(\kappa^2 + \Delta'^2) \right. \\ \left. + 2F_0\omega_m(\kappa^2 - \Delta'^2) + \gamma_m^2\Delta'^2 \right] + F_1F_2\Delta'\omega_m(\gamma_m + 2\kappa)^2 &> 0, \\ F_0\omega_m(\kappa^2 + \Delta'^2) - 2F_1F_2\omega_m\Delta' &> 0.\end{aligned}\quad (3.38)$$

We assume that the system satisfies these stability conditions.

3.3.2.1 Derivation of mean square fluctuations

The mean square fluctuation of an operator $O(t)$ is determined by [128]

$$\langle \delta O(t)^2 \rangle = \frac{1}{4\pi^2} \iint_{-\infty}^{\infty} d\omega d\Omega e^{-\iota(\omega+\Omega)t} \langle \delta O(\omega) \delta O(\Omega) \rangle \quad (3.39)$$

where the $\langle \delta O(\omega) \delta O(\Omega) \rangle$ refers to two-frequency correlation function of the operator O . In the present case, we use Eq. (3.36) and Eq. (3.37) into Eq. (3.39) to obtain the following forms of mean square fluctuations:

$$\langle \delta q_-(t)^2 \rangle = \frac{1}{2\pi} \int_{-\infty}^{\infty} [\omega_m^2 \mu] d\omega, \quad (3.40)$$

$$\langle \delta p_-(t)^2 \rangle = \frac{1}{2\pi} \int_{-\infty}^{\infty} [\omega^2 \mu] d\omega, \quad (3.41)$$

$$\langle \delta p_+(t)^2 \rangle = \frac{1}{2\pi} \int_{-\infty}^{\infty} [\omega^2 \nu] d\omega, \quad (3.42)$$

where

$$\begin{aligned} \mu &= \frac{\gamma_m(2\bar{n}_m + 1)}{d(\omega)d(-\omega)}, \\ \nu &= \frac{1}{D(\omega)D(-\omega)} \left\{ 2\kappa F_1 F_2 [\kappa^2 + (\Delta' + \omega)^2] + \gamma_m(2\bar{n}_m + 1) [(\Delta'^2 + \kappa^2 - \omega^2)^2 + 4\kappa^2 \omega^2] \right\}. \end{aligned} \quad (3.43)$$

In the above derivation of μ and ν , we have used the following non-vanishing frequency-domain correlation functions of the input noise operators, as obtained by Fourier transformation of the Eq. (3.8) and Eq. (3.9):

$$\begin{aligned} \langle \delta a_{in}(\omega) \delta a_{in}^\dagger(-\Omega) \rangle &= 2\pi \delta(\omega + \Omega), \\ \langle \xi_j(\omega) \xi_k(\Omega) \rangle &= 2\pi \delta_{jk} \gamma_m (2\bar{n}_m + 1) \delta(\omega + \Omega). \end{aligned} \quad (3.44)$$

Here we have assumed $\bar{n}_{mj} = \bar{n}_m$ for all j , for simplicity.

According to Wiener-Khintchine theorem [129], the functions $\omega_m^2 \mu$, $\omega^2 \mu$ and $\omega^2 \nu$ represent the spectral density of the random fluctuation of q_- , p_- and p_+ , respectively. We find that they are even and converging functions of ω , and therefore lead to finite values when integrated over frequencies.

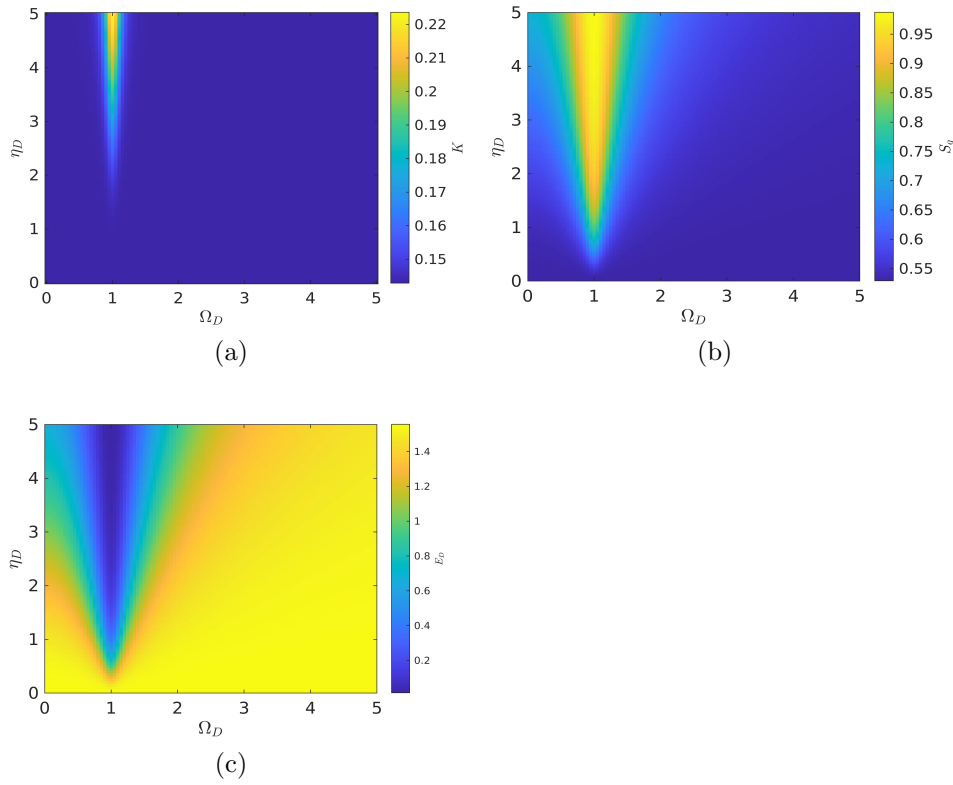


Figure 3.3: Variation of (a) K from Eq. (3.48), (b) quantum synchronization S_q , (c) entanglement E_D between the mechanical oscillators as a function of modulation amplitude η_D and modulation frequency Ω_D with $E = 250$ and $\bar{n}_m = 0.5$. The other parameters are the same as in Fig. 3.2.

3.3.3 Generic relation between entanglement and quantum synchronization

As seen in Eq. (1.37), S_q always remains less than unity according to the uncertainty principle, and therefore, we find a lower limit for $\langle \delta q_-(t)^2 \rangle$, as given by

$$\langle \delta q_-(t)^2 \rangle \geq 1 - \langle \delta p_-(t)^2 \rangle . \quad (3.45)$$

that corresponds to a state with quantum synchronization. In a similar way, we can find out from Eq. (2.13) that there is an upper limit, as well, for $\langle \delta q_-(t)^2 \rangle$, to achieve entanglement. This is given by

$$\langle \delta q_-(t)^2 \rangle < \frac{1}{4\langle \delta p_+(t)^2 \rangle} . \quad (3.46)$$

Therefore, to make the entanglement and quantum synchronization, we must have

$$\frac{1}{4\langle \delta p_+(t)^2 \rangle} > 1 - \langle \delta p_-(t)^2 \rangle , \quad (3.47)$$

which can be simplified to the following analytical condition:

$$K = \frac{1}{4\langle \delta p_+(t)^2 \rangle} + \langle \delta p_-(t)^2 \rangle - 1 > 0 . \quad (3.48)$$

When $K = 0$, the two limits of $\langle \delta q_-(t)^2 \rangle$ become equal, and it suggests a critical set of parameters, that are required for simultaneous occurrence of entanglement and quantum synchronization.

Further, using Eq. (3.46) in Eq. (1.37), we can introduce an upper limit of S_q as

$$S_q = \frac{1}{\langle (\delta q_-)^2 + (\delta p_-)^2 \rangle} < \frac{4\langle (\delta p_+)^2 \rangle}{4E_D - 1 + 4\langle (\delta p_+)^2 \rangle} . \quad (3.49)$$

This upper bound becomes less than unity when $E_D > 1/4$. This means that the oscil-

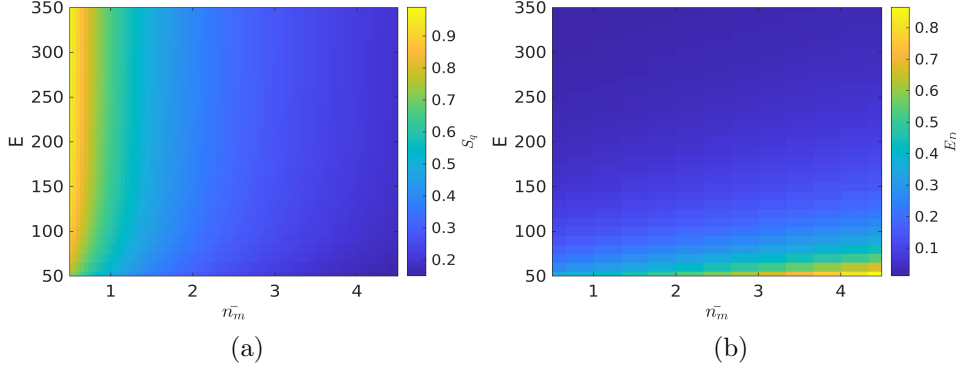


Figure 3.4: Variation of (a) quantum synchronization S_q and (b) entanglement E_D between the mechanical oscillators as a function of the driving field intensity E and the average number of thermal phonons \bar{n}_m with $\eta_D = 4$ and $\Omega_D = 1$. The other parameters are the same as in Fig. 3.2.

lators can never have complete quantum synchronization if they are not entangled. As E_D becomes less than $1/4$, this bound becomes more than unity, referring to the fact that S_q can reach its maximum value of 1, which is otherwise defined by the uncertainty principle. In the present context, this refers to the complete quantum synchronization in the presence of entanglement. Therefore, the entanglement acts as a booster of quantum synchronization. The expression Eq. (3.49) is valid irrespective of any specific details of the systems of interest and therefore poses as a generalized characterization of quantum synchronization in terms of entanglement in coupled bosonic systems.

3.3.4 Numerical results

As noted in Section 3.2.2 and Section 3.3.3, there exists a correlation between quantum synchronization and entanglement. To test this conjecture, we present further numerical results based on the analytical results in Sec. Section 3.3. We choose all the parameters such that they maintain stability in the system, following Eq. (3.38). We first show in Fig. 3.3b and Fig. 3.3c, the variation of the quantum synchronization S_q and entanglement E_D , respectively, as a function of modulation amplitude η_D and modulation frequency Ω_D .

It is observed that both the quantum synchronization and the entanglement trace the classic 'Arnold tongue-like structure', yielding a range of values of η_D and the corresponding values of Ω_D for which synchronization and entanglement are simultaneously achievable. We further find that the tongue is symmetric about $\Omega_D = \omega_m = 1$. The synchronization S_q tends to one and the entanglement E_D decreases further below the upper limit of 0.25, as the modulation strength η_D increases. We note that a similar tongue associated with classical phase synchronization was reported for two dissipatively coupled Van der Pol oscillators [130]. In the quantum regime, frequency entertainment between two such oscillators is however prevented due to quantum noise [49].

We show in Fig. 3.3a the variation of K [Eq. (3.48)] as a function of η_D and Ω_D . This plot also exhibits the classic 'Arnold tongue-like structure' around modulation frequency $\Omega_D = 1$. For larger η_D at $\Omega_D = 1$, the term K increases further. By comparing with the Fig. 3.3b and Fig. 3.3c, we can conclude that with the increase in K the system approaches nearly complete quantum synchronization (i.e., $S_q \lesssim 1$) and larger violation of the inseparability inequality Eq. (2.13) (i.e., $E_D \ll 0.25$). It is also interesting to see that K remains positive for a large range of η_D and Ω_D . Thus, both the quantum synchronization (albeit partial) and entanglement stay robust over a large variation of modulation parameters.

To get further insight into the correlated behavior of synchronization and entanglement, we plot them with respect to the driving field amplitude E and the average number of phonons \bar{n}_m , respectively, in the Fig. 3.4a and Fig. 3.4b, for a fixed modulation amplitude factor $\eta_D = 4$ and modulation frequency $\Omega_D = 1$. It can be seen, for higher E and at lower temperatures of the bath ($\bar{n}_m = 0.5$), the oscillators are nearly complete quantum synchronized, along with maximal violation of separability inequality Eq. (2.13). With the increase in thermal excitation, the synchronization deteriorates and the entanglement decreases too. However, the synchronization stays more robust to temperature as compared to entanglement. This indicates that though some residual synchronization may still ex-

ist without entanglement, the entanglement is always associated with the synchronization and therefore becomes a signature of the latter. In fact, this can also be intuitively understood from the definition [Eq. \(1.37\)](#) of quantum synchronization, which always remains less than unity due to the uncertainty principle, though the quantum state of the system may not exhibit entanglement [i.e., may not violate the [Eq. \(2.13\)](#)]. Moreover, without entanglement (i.e., when $E_D > 0.25$), S_q remains much less than unity, referring to partial synchronization. The above discussion thus suggests that entanglement plays the role of a quantum synchronization booster, as also noted in [Section 3.3.3](#). It must be borne in mind that the entanglement would indicate the existence of quantum synchronization, only in the presence of a limit cycle of mean values of the joint quadratures.

3.4 Conclusion

In conclusion, we have explored the interconnection between quantum synchronization and entanglement between two mechanical oscillators in an optomechanical system. In our model, both mechanical oscillators are coupled with the same cavity mode via linear and quadratic dependence on their displacement from their respective equilibrium positions. An indirect always-on coupling, proportional to $g_3 a^\dagger a$ also arises between the oscillators, which is the key to the generation of the synchronization between them. Since the same uncertainty relation sets the upper limit for quantum synchronization S_q and the lower limit for entanglement marker E_D , so we expected that there could be a correlation between the two. In this regard, we have first demonstrated the classical synchronization via limit cycle trajectories of the mean quadratures at long times, which is a precondition to achieve quantum synchronization. Our numerical results show that the two coupled mechanical oscillators exhibit entanglement and quantum synchronization when the cavity is strongly amplitude-modulated. A nearly complete quantum synchronization and entanglement between the coupled oscillators can be achieved for a large range of modulation parameters. This result leads us to a strong conjecture that they arise from

the same EPR-type correlation. We further show that the entanglement manifests itself as a booster to achieve near-complete quantum synchronization. One can express the quantum synchronization as a function of entanglement when defined in terms of variances of quadratures. We have provided all the relevant analysis, supported by numerical results in this context. Our results open up a newer perspective to interpret quantum synchronization and entanglement on the same footing.

Chapter 4

Strong entanglement criteria for bipartite mixed states

In the previous chapter, we studied the relation between quantum synchronization and entanglement. In this chapter, we will propose another aspect of quantum correlation in mixed states. Precisely speaking, we propose an entanglement criterion for bipartite mixed states by using the Peres-Horodecki partial transposition on a suitable uncertainty relation. This criterion is stronger than any known criteria in this regard, as it correctly detects the entanglement because it can predict the same parameter range for entanglement, as identified by the partial transpose criterion.

4.1 Motivation

Entanglement [18] between two or more subsystems is considered as a resource to deal with quantum information. Several applications like quantum teleportation, quantum metrology, quantum cryptography, and super-dense coding require that the participating subsystems be entangled. Identifying whether these subsystems are entangled or not is therefore an essential step toward quantum information processing.

In the past two decades, several criteria for the detection of entanglement [67] have been developed. The positive partial transpose (PPT) criterion by Peres and Horodecki [59] has been one of the most important ones, which poses a necessary and sufficient condition in certain cases. Peres had proposed that the density matrix of a bipartite entangled state when partially transposed in the basis of one of the parties, exhibits negative eigenvalues. The other criteria include those based on reduction [62], entanglement witness [60, 63] and the computable cross norm [61]. However, to test these criteria in experiments, one would ideally need to reproduce the density matrix using quantum state tomography.

As an alternative approach more suitable for experimental detection of entanglement, criteria based on measurement outcomes of the relevant observables have been derived. For example, the PT criterion has been mapped into uncertainty relations of the relevant quadratures, violation of which would indicate the existence of entangled states [69, 131]. There exist methods based on Bell-type inequalities [132], local uncertainty relations [66], the Schrodinger-Robertson partial transpose (SRPT) inequality [131], as well. These measurement-dependent criteria are often expressed in terms of inequalities, which are satisfied by separable states, and any state violating these inequalities must be entangled.

These criteria are useful to detect entanglement in pure as well as in mixed states. Unfortunately, they cannot reveal the correct domain of the relevant parameters, as prescribed by the PPT criterion, to detect entanglement in mixed states. This can be attributed to the fact that the mixed states involve both classical and quantum probability distributions and the above criteria do not differentiate between these two for evaluation of the expectation values. As the entanglement is a property purely of a quantum nature, to detect this, we need a criterion that considers only the quantum uncertainties of the relevant variables.

In addition to the criteria based on partial transposition, quantum uncertainty of local observables has also been used to characterize non-classical correlations like quantum

discord [133]. Quantum discord can distinguish between classical and quantum probability distributions, inherent in the system. However, it is rather quite cumbersome to calculate the discord, as it requires optimization over many measurements and for the systems with more than two qubits, it becomes more intractable. In this work, we use an alternative strategy.

In this chapter, we consider a Schrodinger-Robertson-type uncertainty relation proposed by Furuichi [134], which includes the Wigner-Yanase skew information. This skew information is known to give a measure of the quantum uncertainty of an operator X with respect to a given state ρ . As mentioned above, for a joint state of two subsystems, the quantum uncertainty of a local variable provides an alternative estimate of the discord. Here, we consider both local and non-local variables of the two subsystems and apply the partial transposition (PT) criterion to the uncertainty relation to detecting entanglement between them. When using the nonlocal variables, we essentially consider the nonlocal correlation of the subsystems. Moreover, the uncertainty relation used for employing the entanglement criterion involves only the terms that do not contain the classical mixing uncertainty. It implies that this criterion is particularly suitable for mixed states. We emphasize that the skew information represents quantum (rather than total) uncertainty which considers both incompatibility and correlation between the relevant observables. Thus our criterion is of purely quantum nature and turns out to be stronger for the mixed states considered in this work. Note that this uncertainty relation reduces to the Schrodinger-Robertson inequality for the pure state. We will apply the inequality to several generalized mixed states including the Werner states. We show that our inequality reveals an ideal domain of the relevant parameter for entanglement, unlike the other criteria based on the Bell inequalities [135, 136], uncertainty relations [137], and the Schrodinger-Robertson inequality [131]. It must be borne in mind that the proposed inseparability inequality requires the full knowledge of the density matrix to be evaluated. So we need quantum state tomography to reproduce the density matrix.

The chapter is organized as follows. In [Section 4.2](#), we review some basic properties of skew information and highlight its relation with variance. In [Section 4.3](#), we will present the entanglement criterion in the form of the Schrodinger-Robertson type inequality in terms of the skew information. In [Section 4.4](#), We demonstrate how the violation of this inequality can detect entanglement for a large class of mixed states, including the two-qubit Werner states and two-qutrit mixed states. In [Section 4.5](#), we conclude the chapter.

4.2 Wigner-Yanase Skew Information

In their seminal paper on quantum measurement, Wigner and Yanase introduced the quantity, the skew information, [\[138\]](#) as

$$I(\rho, X) = -\frac{1}{2}\text{Tr}[\sqrt{\rho}, X]^2 . \quad (4.1)$$

This corresponds to a measure of the amount of information on the values of observable, which is skew to the operator X . Here X is a conserved quantity like Hamiltonian, momentum, etc. of the relevant quantum system, which is in a state described by the density matrix ρ . Note that $I(\rho, X)$ accounts for the non-commutativity between ρ and X .

The skew information satisfies several criteria, suitable for a valid information-theoretic measure, which are as follows:

1. Non-negativity: $I(\rho, X) \geq 0$.
2. Convexity: It is convex with respect to ρ in the sense that

$$I(p_1\rho_1 + p_2\rho_2, X) \leq p_1I(\rho_1, X) + p_2I(\rho_2, X) , \quad (4.2)$$

where $p_1 + p_2 = 1$, $p_1, p_2 \geq 0$. This suggests that the skew information decreases

when two density matrices are mixed.

3. Additivity: This is represented by

$$I(\rho_1 \otimes \rho_2, X_1 \otimes I_2 + I_1 \otimes X_2) = I(\rho_1, X_1) + I(\rho_2, X_2) , \quad (4.3)$$

where ρ_1 and ρ_2 are two density operators describing the two systems, I_i are the density matrices in their respective subspace ($i \in 1, 2$), and X_1 and X_2 are their corresponding conserved quantities.

4. Let U be a unitary operator, then

$$I(U\rho U^{-1}, X) = I(\rho, X) , \quad (4.4)$$

where $U = e^{-i\theta X}$ commutes with X .

i.e., when the state changes according to the Landau-von Neumann equation, the skew information remains constant for isolated systems.

Wigner-Yanase skew information has been used to construct measures of quantum correlations [139] and quantum coherence [140], to detect entanglement [141], to study phase transitions [142] and uncertainty relations [143, 144, 145], and so on.

Skew information is related to the conventional variance, through the following relation:

$$I(\rho, X) = \text{Tr}(\rho X^2) - \text{Tr}(\sqrt{\rho} X \sqrt{\rho} X) . \quad (4.5)$$

This is equal to the variance only if the state ρ is a pure state, i.e., if $\rho = |\psi\rangle\langle\psi|$:

$$I(\rho, X) = V(\rho, X) , \quad (4.6)$$

where $V(\rho, X) = \text{Tr}\rho X^2 - (\text{Tr}\rho X)^2$. On the other hand, for any mixed state ρ , the skew

information is always dominated by the variance:

$$I(\rho, X) \leq V(\rho, X) . \quad (4.7)$$

A mixed state can be considered a classical mixture of quantum states. The variance does not differentiate between the quantum uncertainty (arising out of purely quantum probability distribution) and the classical uncertainty (associated with the classical mixing) in the mixed state. On the contrary, the skew information can be interpreted as equivalent to quantum uncertainty and does not account for the classical mixing. It vanishes if ρ and X commute with each other. Also, the convexity property of I , as mentioned above, suggests that classical mixing cannot increase quantum uncertainty.

The fact that the skew information can be interpreted as a form of quantum uncertainty [146, 147] and the relation Eq. (4.7) above were used to construct an uncertainty relation, which is stronger than the usual Heisenberg uncertainty relation to detecting entanglement in a mixed state. We will discuss this in the next Section.

4.3 Entanglement criteria based on the uncertainty relations

In this Section, we will first discuss the modified uncertainty relations and then will propose how this can be useful as an entanglement criterion.

4.3.1 Modified uncertainty relations

Usual uncertainty relation, due to Heisenberg, sets a fundamental limit on the simultaneous measure of two non-commuting observables [148]. For the measurement of any two

observables A and B in a quantum state ρ , this is given by

$$V(\rho, A)V(\rho, B) \geq \frac{1}{4}|\text{Tr}(\rho[A, B])|^2, \quad (4.8)$$

where $V(\rho, A)$ and $V(\rho, B)$ are the variances of A and B , as defined above, and $\text{Tr}(\rho[A, B])$ is the average of commutator $[A, B] = AB - BA$ in the state ρ . It is noticeable that the commutator, which is so fundamental in quantum mechanics, makes its appearance in Heisenberg's relation. In addition to this commutator, one also considers the correlation between the observables, which is usually expressed in terms of anti-commutator in quantum mechanics. This was included by Schrodinger [149] into the following canonical form of the uncertainty relation:

$$V(\rho, A)V(\rho, B) \geq \frac{1}{4}|\text{Tr}(\rho[A, B])|^2 + \frac{1}{4}|\text{Tr}(\rho\{A_0, B_0\})|^2. \quad (4.9)$$

Here $\text{Tr}[\rho\{A_0, B_0\}]$ denotes the average of the anti-commutator $\{A_0, B_0\} = A_0B_0 + B_0A_0$, where $A_0 = A - \langle A \rangle_\rho I$ and $B_0 = B - \langle B \rangle_\rho I$ can be interpreted as the fluctuation operators about their respective expectation values, calculated for the state ρ .

As discussed in the Section 4.2, the skew information can be considered as quantum uncertainty. Luo therefore proposed [143] that Heisenberg's uncertainty relation might be modified, as follows, in terms of the skew information, for any two observables A, B and the quantum state ρ :

$$I(\rho, A)I(\rho, B) \geq \frac{1}{4}|\text{Tr}(\rho[A, B])|^2. \quad (4.10)$$

This relation is defined in the spirit of the relation $0 \leq I(\rho, A) \leq V(\rho, A)$. However, this does not distill the right essence of the uncertainty relation, as when the quantum uncertainties I vanish for two non-commuting operators A and B , the above inequality Eq. (4.10) gets violated, even if the state ρ has non-classical correlations.

It was later observed that the Heisenberg uncertainty relation is of purely quantum nature for the pure state and is of "mixed" flavor for the mixed state because $V(\rho, A)$ is a hybrid of classical and quantum uncertainty for these states. Motivated by this simple observation, Luo then introduced [145] the quantity $U(\rho, A)$, as follows, by decomposing the variance into classical and quantum parts i.e., $V(\rho, A) = C(\rho, A) + I(\rho, A)$:

$$\begin{aligned} U(\rho, A) &= \sqrt{V^2(\rho, A) - C^2(\rho, A)} \\ &= \sqrt{V^2(\rho, A) - [V(\rho, A) - I(\rho, A)]^2} . \end{aligned} \quad (4.11)$$

Luo then successfully introduced a new Heisenberg-type uncertainty relation based on $U(\rho, A)$ (which suitably takes care of the exclusion of classical mixing, especially for mixed state) as follows:

$$U(\rho, A)U(\rho, B) \geq \frac{1}{4}|\text{Tr}(\rho[A, B])|^2 . \quad (4.12)$$

The three quantities $V(\rho, A)$, $I(\rho, A)$, and $U(\rho, A)$ have the following ordering:

$$0 \leq I(\rho, A) \leq U(\rho, A) \leq V(\rho, A) . \quad (4.13)$$

Clearly, for pure states, we have the classical correlation $C = 0$ and thus, $U = V$ and the above relation Eq. (4.12) becomes the same as the original uncertainty relation Eq. (4.8).

The above uncertainty relation Eq. (4.12) is improved by Furuichi [134], who proposed a stronger Schrodinger-type uncertainty relation, by improving the upper bound, for the quantity U , as

$$U(\rho, A)U(\rho, B) - |\text{Re}\{C_\rho(A, B)\}|^2 \geq \frac{1}{4}|\text{Tr}(\rho[A, B])|^2 , \quad (4.14)$$

where $C_\rho(A, B)$ is called the Wigner-Yanase correlation between two observables and can

be written as

$$C_\rho(A, B) = \text{Tr}(\rho A^* B) - \text{Tr}(\sqrt{\rho} A^* \sqrt{\rho} B) , \quad (4.15)$$

where A^* is the complex conjugate of the operator A . Note that, if $A = B$ are self-adjoint, this simplifies to

$$C_\rho(A, A) = \text{Tr}(\rho A^2) - \text{Tr}(\sqrt{\rho} A \sqrt{\rho} A) , \quad (4.16)$$

which becomes the same as the skew information. It can be shown that

$$|\text{Im}\{C_\rho(A, B)\}|^2 = \frac{1}{4} |\text{Tr}(\rho[A, B])|^2 . \quad (4.17)$$

So the inequality [Eq. \(4.14\)](#) can be finally written as

$$U(\rho, A)U(\rho, B) \geq |C_\rho(A, B)|^2 . \quad (4.18)$$

4.3.2 Relation to the entanglement criteria

As mentioned in the motivation, entanglement criteria based on partial transpose in the uncertainty relations do not differentiate between the quantum and classical probabilities and also the correlations of the observables. Thus they fail to indicate the correct domain of the relevant variables for the states to be entangled, as prescribed by the PPT criteria, in the mixed states. As the uncertainty relation [Eq. \(4.18\)](#) includes both the quantum uncertainty and correlations while excluding the classical uncertainty, it is expected that the entanglement criterion based on [Eq. \(4.18\)](#) would prove to be much stronger compared to the older versions of such criteria when mixed states are involved. In the following, we therefore propose a new criterion, particularly useful for detecting entanglement in bipartite mixed states.

$$U(\rho^{PT}, A)U(\rho^{PT}, B) \geq |C_{\rho^{PT}}(A, B)|^2 , \quad (4.19)$$

where A and B are the operators in the joint Hilbert space and ρ^{PT} represents the partial transpose of the joint density matrix ρ in terms of one of the subsystems. Violation of the above inequality is a sufficient condition for entanglement because Peres criterion is sufficient to detect entanglement in a bipartite system.

4.4 Examples

4.4.1 Two qubit pure states

In this Section, we first consider a case of two-qubit non-maximally pure entangled state $|\psi\rangle$ of the following form:

$$|\psi\rangle = c_0|00\rangle + c_1|11\rangle, \quad (4.20)$$

where c_0, c_1 are the complex coefficients and unequal in magnitude. Note that when $c_0 = c_1$, the state becomes one of the Bell states, which are maximally entangled. For $A = \sigma_z \otimes \sigma_z$ and $B = \sigma_x \otimes \sigma_x$, the inequality [Eq. \(4.9\)](#) with ρ^{PT} leads to

$$0 \geq |c_0^*c_1 + c_0c_1^*|^2, \quad (4.21)$$

which is always violated for any nonzero c_0 and c_1 . This is maximally violated when $c_0 = c_1$. Thus, the violation of inequality [Eq. \(4.9\)](#) can be reliably used to detect entanglement in this state.

But for mixed states, this is not true. For different classes of mixed states, the inequality [Eq. \(4.9\)](#) indicates separability for a large range of parameters, for which these states are known to be entangled. We show below all these cases, where, the criterion [Eq. \(4.19\)](#) turns out to be useful.

4.4.2 Two qubit mixed states

4.4.2.1 Werner state

To illustrate the utility of the criterion [Eq. \(4.19\)](#), we start with a two-qubit Werner state, which is a mixture of a maximally entangled state and a maximally mixed state. The Werner state for a two-qubit system is given by

$$\rho = \frac{1-p}{4} I_1 \otimes I_2 + p |\psi_-\rangle \langle \psi_-|, \quad (4.22)$$

where $|\psi_-\rangle = \frac{1}{\sqrt{2}}(|01\rangle - |10\rangle)$ is a maximally entangled state (one of the four celebrated Bell states) and $0 \leq p \leq 1$. In the computational basis ($|00\rangle, |01\rangle, |10\rangle, |11\rangle$) of two qubits, we can write ρ as follows:

$$\rho = \frac{1}{4} \begin{pmatrix} 1-p & 0 & 0 & 0 \\ 0 & 1+p & -2p & 0 \\ 0 & -2p & 1+p & 0 \\ 0 & 0 & 0 & 1-p \end{pmatrix}. \quad (4.23)$$

With the partial transpose with respect to the second qubit, this transforms into

$$\rho^{PT} = \frac{1}{4} \begin{pmatrix} 1-p & 0 & 0 & -2p \\ 0 & 1+p & 0 & 0 \\ 0 & 0 & 1+p & 0 \\ -2p & 0 & 0 & 1-p \end{pmatrix}, \quad (4.24)$$

the eigenvalues of which are $(1+p)/4$ (triply degenerate) and $(1-3p)/4$. The Werner state is entangled (inseparable) for $p > \frac{1}{3}$ (as one of the eigenvalues becomes negative), according to the PT criterion and maximally entangled when $p = 1$. But, if we use the uncertainty relation [Eq. \(4.9\)](#) with ρ^{PT} , we find the following condition for separability: $p \leq 1$, which is always satisfied. Thus, the violation of this inequality cannot be reliably

used to detect entanglement in this state. If one would perform the partial transposition on the relevant observables A and B , instead of on ρ , the relation [Eq. \(4.9\)](#) becomes the SRPT inequality. However, not all observables are suitable to demonstrate the violation of the SRPT inequality. They have to satisfy a general condition to be eligible. The SRPT inequality detects the entanglement of Werner state for a particular choice of observables A and B when $p > \frac{1}{2}$. This lower bound is however larger than $p = \frac{1}{3}$. We show below that the present criterion [Eq. \(4.19\)](#) reveals the entanglement even in the domain $(\frac{1}{3}, \frac{1}{2})$.

In this regard, we first obtain

$$\sqrt{\rho^{PT}} = \begin{pmatrix} P & 0 & 0 & Q \\ 0 & R & 0 & 0 \\ 0 & 0 & R & 0 \\ Q & 0 & 0 & P \end{pmatrix}, \quad (4.25)$$

where $P = \sqrt{1+p}/2$, $Q = [\sqrt{1-3p} - \sqrt{1+p}]/4$, and $R = [\sqrt{1+p} + \sqrt{1-3p}]/4$.

It is now important to suitably choose the observables A and B , such that they do not commute with ρ^{PT} .

Case I: Following [\[133\]](#), we first choose a set of local observables $A = \sigma_z \otimes I_2$ and $B = I_1 \otimes \sigma_z$. For these operators, we found that

$$\begin{aligned} V(\rho^{PT}, A) &= V(\rho^{PT}, B) = 1, \\ I(\rho^{PT}, A) &= I(\rho^{PT}, B) = \frac{1}{2}(1 - p - \sqrt{1+p}\sqrt{1-3p}), \\ U(\rho^{PT}, A) &= U(\rho^{PT}, B) = \sqrt{\frac{1}{2} \left\{ 1 + p^2 - (1+p)^{3/2} \sqrt{1-3p} \right\}}, \\ C_{\rho^{PT}}(A, B) &= \frac{1}{2} \left(1 - p - \sqrt{1+p}\sqrt{1-3p} \right). \end{aligned} \quad (4.26)$$

For $0 \leq p \leq \frac{1}{3}$, the state ρ^{PT} is positive, which implies that it describes some physical state and therefore satisfies the inequality [Eq. \(4.19\)](#). For $p > \frac{1}{3}$, however, the term

$\sqrt{1-3p}$ is complex. Therefore, we can rewrite $U(\rho^{PT}, A)$ and $U(\rho^{PT}, B)$ as

$$\sqrt{\frac{1}{2} \left\{ 1 + p^2 - \iota(1+p)^{3/2} \sqrt{3p-1} \right\}}. \quad (4.27)$$

There are several forms of the square root Eq. (4.27). By choosing $U(\rho^{PT}, A) = \iota\sqrt{b-a} + \sqrt{a+b}$, and $U(\rho^{PT}, B) = \iota\sqrt{b-a} - \sqrt{a+b}$ (where $a = (1+p^2)/4$ and $b = p\sqrt{p^2+2p+2}/2$), and by using Eq. (4.26), we have the following condition from Eq. (4.19):

$$p[\sqrt{p^2+2p+2} + p] \leq 0. \quad (4.28)$$

It should be remembered that the above condition is obtained in the domain $p > 1/3$ and is obviously violated for all $p \in (1/3, 1]$.

Case II: Usually, measurement of local observables bypasses the issue of nonlocal correlations that exist between two subsystems when they are entangled. Accordingly, if we choose a set of global observables $A = \sigma_z \otimes \sigma_z$ and $B = \sigma_x \otimes \sigma_x$, we find that they commute with ρ^{PT} , and thus the skew information vanishes, i.e., $I(\rho^{PT}, A) = I(\rho^{PT}, B) = 0$. The correlation between these operators also vanishes $C_{\rho^{PT}}(A, B) = 0$. Clearly, for such choices of global observables, we cannot clearly say anything about the inseparability of the Werner state using Eq. (4.19).

But if we choose a different set of operators, say, $A = \sigma_x \otimes \sigma_y$ and $B = \sigma_y \otimes \sigma_x$, which do not commute with ρ^{PT} , we have the same expressions of V , I , and U as in Eq. (4.26), and the correlation term becomes

$$C_{\rho^{PT}}(A, B) = \frac{1}{2}(-1 + p + \sqrt{1+p}\sqrt{1-3p}). \quad (4.29)$$

Using these expressions, we find that, for $p > \frac{1}{3}$, the condition Eq. (4.19) for separability is violated, i.e., the Werner state is entangled for $p > \frac{1}{3}$. This result indicates that the criterion Eq. (4.19) identifies the same lower bound as obtained from the PPT criteria, unlike all the other known criteria for entanglement. For example, the Bell's inequalities

[135, 136] lead to $p > \frac{1}{\sqrt{2}}$ for entanglement, while the uncertainty relation in [137] sets the lower limit as $p > \frac{1}{\sqrt{3}}$ and the Schrodinger-Robertson inequality based on local variables [131] suggests $p > \frac{1}{2}$. Thus, the criterion Eq. (4.19) turns out to be stronger than all other known criteria based on uncertainties and Bell's inequalities for the Werner state and gives the same lower bound as obtained using the PPT criterion.

As clear from the two cases discussed above, the separability criterion Eq. (4.19) affirms the correct limit for entanglement, which is the same as that obtained from the Peres criteria. Interestingly, both local and global sets of operators can reveal this limit. One only needs to choose the set of operators that do not commute with the ρ^{PT} .

4.4.2.2 Werner derivative

An important generalized class of Werner states is Werner derivative [150], which is a mixture of non-maximally pure entangled states and the maximally mixed state. This can be written in the form

$$\rho_{WD} = \frac{1-p}{4} I_1 \otimes I_2 + p |\psi\rangle\langle\psi|, \quad (4.30)$$

where $|\psi\rangle = \sqrt{a}|00\rangle + \sqrt{1-a}|11\rangle$ is the Schmidt decomposition of the state obtained by a nonlocal unitary rotation of the Bell state $|\psi_{-}\rangle$, and $\frac{1}{2} \leq a \leq 1$. It is worth noting the difference between the states Eq. (4.30) and Eq. (4.22). In the computational basis of two qubits, ρ_{WD} takes the following form:

$$\rho_{WD} = \frac{1}{4} \begin{pmatrix} 1-p+4ap & 0 & 0 & 4p\sqrt{a(1-a)} \\ 0 & 1-p & 0 & 0 \\ 0 & 0 & 1-p & 0 \\ 4p\sqrt{a(1-a)} & 0 & 0 & 1+3p-4ap \end{pmatrix}, \quad (4.31)$$

According to the PT criterion, the state described by Eq. (4.30) is entangled if

$$\frac{1}{2} \leq a < \frac{1}{2} \left(1 + \frac{1}{2p} \sqrt{(3p-1)(p+1)} \right), \quad (4.32)$$

which further restricts p as $\frac{1}{3} \leq p \leq 1$. Clearly, for different values of p , the parameter a has an upper and a lower bound, such that the state ρ_{WD} parameterized by a becomes entangled. But when using the standard uncertainty relation Eq. (4.9), one finds that the state is separable for all $p \in [0, 1]$. This can be seen by using ρ_{WD}^{PT} along with the observables, $A = \sigma_z \otimes I_2$ and $B = I_1 \otimes \sigma_z$ in the inequality Eq. (4.9), which leads to $p \leq 1$. This means, according to Eq. (4.9), the state ρ_{WD} should be always separable, which is not the case. We show below, how the inequality Eq. (4.19) can successfully detect entanglement in this state.

To employ the criterion Eq. (4.19), we choose the same set of local operators, as above and we obtain the following inequality:

$$\left[\frac{3 + p - 4(2a - 1)^2 p^2 + D}{2} \right] \times \left(\frac{1 - p - D}{2} \right) \geq \left| \left(\frac{1 - p - D}{2} \right) \right|^2,$$

where

$$D = \sqrt{16p^2 a^2 - 16p^2 a + (1 - p)^2}. \quad (4.33)$$

We find that the above inequality is violated in the domain when D is imaginary. This happens in the following range of a :

$$\frac{1}{2} - \frac{1}{4p} \sqrt{(3p-1)(p+1)} \leq a \leq \frac{1}{2} + \frac{1}{4p} \sqrt{(3p-1)(p+1)}. \quad (4.34)$$

The upper limit of a thus matches with the one obtained by directly applying the PT criterion [see Eq. Eq. (4.32)]. By definition of the Schmidt decomposition, one further requires a to be real positive, and therefore $p \geq 1/3$ [else, a would be complex; see Eq. (4.34)]. Note that p cannot be greater than unity, as it defines the probability of the

state $|\psi\rangle$ in the mixture ρ_{WD} . Interestingly, for $p = 1/3$, the state ρ_{WD} is entangled only for $a = 1/2$. For higher values of p , the Werner derivative is entangled for a range of values a , including $a = 1/2$ (corresponding to the maximally entangled Bell state) and $a \neq 1/2$ (corresponding to a non-maximally entangled state $|\psi\rangle$).

4.4.2.3 An example of mixed non-maximally entangled state

Finally, we consider a non-maximally entangled mixed state ρ_{new} [151], which is a convex combination of a separable density matrix $\rho_{12}^G = \text{Tr}_3(|GHZ\rangle_{123})$ and an inseparable density matrix $\rho_{12}^W = \text{Tr}_3(|W\rangle_{123})$. Here $|GHZ\rangle_{123}$ and $|W\rangle_{123}$ are the GHZ state and W-state, respectively, of three qubits 1, 2, and 3. The state ρ_{new} can be explicitly written as

$$\rho_{new} = (1 - p)\rho_{12}^G + p\rho_{12}^W, \quad (4.35)$$

where $0 \leq p \leq 1$. Note that the Werner state is also a convex sum of a maximally entangled pure state and a maximally mixed state. On the contrary, the state ρ_{12}^W is not a pure state (though entangled) and the ρ_{12}^G is also not maximally mixed (though separable).

In the computational basis of two qubits, ρ_{new} and ρ_{new}^{PT} take the following forms:

$$\rho_{new} = \begin{pmatrix} \frac{3-p}{6} & 0 & 0 & 0 \\ 0 & \frac{p}{3} & \frac{p}{3} & 0 \\ 0 & \frac{p}{3} & \frac{p}{3} & 0 \\ 0 & 0 & 0 & \frac{1-p}{2} \end{pmatrix} \quad (4.36)$$

and

$$\rho_{new}^{PT} = \begin{pmatrix} \frac{3-p}{6} & 0 & 0 & \frac{p}{3} \\ 0 & \frac{p}{3} & 0 & 0 \\ 0 & 0 & \frac{p}{3} & 0 \\ \frac{p}{3} & 0 & 0 & \frac{1-p}{2} \end{pmatrix}. \quad (4.37)$$

According to the PT criterion, that ρ_{new} is entangled for $p > 0.708$ can be easily verified by finding the eigenvalues of the ρ_{new}^{PT} . But this cannot be revealed by using the Eq. (4.9) with ρ_{new}^{PT} and the following set of local operators: $A = \sigma_z \otimes I_2$ and $B = I_1 \otimes \sigma_z$. This leads to the following inequality: $p \geq 0$, which means that, according to Eq. (4.9), the state ρ_{new} is separable for all p . On the contrary, as we show below, the inequality Eq. (4.19) can successfully detect the entanglement in this state, as well.

To evaluate the condition Eq. (4.19), we choose the same set of local operators, as above and obtain the following inequality:

$$\left(\frac{-18 - 2p^2 + 24p + 12E}{9} \right) \times \left(\frac{12 - 8p - 4E}{3} \right) \geq \left| \frac{12 - 8p - 4E}{3} \right|^2 .$$

$$E = \sqrt{-p^2 - 12p + 9} . \quad (4.38)$$

We find that this is always violated for $p > 0.708$, which correctly matches with the result obtained by directly using the Peres criterion.

4.4.3 Two qutrit mixed states

While the PT criterion is a necessary and sufficient condition for the detection of entanglement for two-qubit and qubit-qutrit states, for higher-dimensional systems, this criterion is only sufficient. To illustrate the utility of the criterion Eq. (4.19), we now consider two-qutrit Werner state [152].

4.4.3.1 Two-qutrit Werner state

This state is a mixture of a maximally entangled state and the maximally mixed state, which can be expressed for two-qutrits as

$$\rho = \frac{1-p}{9} I_{ab} + p |\psi\rangle_{ab} \langle \psi| \quad (4.39)$$

where I_{ab} is 9×9 identity matrix; $|\psi\rangle_{ab} = \frac{1}{\sqrt{3}}(|00\rangle + |11\rangle + |22\rangle)$ is the Bell state composed of subsystems A and B and $0 \leq p \leq 1$. In the computational basis of two qutrit, ρ and ρ^{PT} takes the following forms:

$$\rho = \begin{pmatrix} \frac{1+2p}{9} & 0 & 0 & 0 & \frac{p}{3} & 0 & 0 & 0 & \frac{p}{3} \\ 0 & \frac{1-p}{9} & 0 & 0 & 0 & 0 & 0 & 0 & 0 \\ 0 & 0 & \frac{1-p}{9} & 0 & 0 & 0 & 0 & 0 & 0 \\ 0 & 0 & 0 & \frac{1-p}{9} & 0 & 0 & 0 & 0 & 0 \\ \frac{p}{3} & 0 & 0 & 0 & \frac{1+2p}{9} & 0 & 0 & 0 & \frac{p}{3} \\ 0 & 0 & 0 & 0 & 0 & \frac{1-p}{9} & 0 & 0 & 0 \\ 0 & 0 & 0 & 0 & 0 & 0 & \frac{1-p}{9} & 0 & 0 \\ 0 & 0 & 0 & 0 & 0 & 0 & 0 & \frac{1-p}{9} & 0 \\ \frac{p}{3} & 0 & 0 & 0 & \frac{p}{3} & 0 & 0 & 0 & \frac{1+2p}{9} \end{pmatrix} \quad (4.40)$$

$$\rho^{PT} = \begin{pmatrix} \frac{1+2p}{9} & 0 & 0 & 0 & 0 & 0 & 0 & 0 & 0 \\ 0 & \frac{1-p}{9} & 0 & \frac{p}{3} & 0 & 0 & 0 & 0 & 0 \\ 0 & 0 & \frac{1-p}{9} & 0 & 0 & 0 & \frac{p}{3} & 0 & 0 \\ 0 & \frac{p}{3} & 0 & \frac{1-p}{9} & 0 & 0 & 0 & 0 & 0 \\ 0 & 0 & 0 & 0 & \frac{1+2p}{9} & 0 & 0 & 0 & 0 \\ 0 & 0 & 0 & 0 & 0 & \frac{1-p}{9} & 0 & \frac{p}{3} & 0 \\ 0 & 0 & \frac{p}{3} & 0 & 0 & 0 & \frac{1-p}{9} & 0 & 0 \\ 0 & 0 & 0 & 0 & 0 & \frac{p}{3} & 0 & \frac{1-p}{9} & 0 \\ 0 & 0 & 0 & 0 & 0 & 0 & 0 & 0 & \frac{1+2p}{9} \end{pmatrix}. \quad (4.41)$$

The eigenvalues of ρ^{PT} are $\frac{1+2p}{9}$ (six times) and $\frac{1-4p}{9}$ (three times). According to the PT criterion, the two-qutrit Werner state is entangled for $p > \frac{1}{4}$ and maximally entangled when $p = 1$. Using [Eq. \(4.9\)](#) with ρ^{PT} and the following set of local operators $A = I_1 \otimes S_z$

and $B = S_z \otimes I_2$, where

$$S_z = \begin{pmatrix} 1 & 0 & 0 \\ 0 & 0 & 0 \\ 0 & 0 & -1 \end{pmatrix}, \quad (4.42)$$

the following inequality is obtained: $p \leq 1$, which implies that, according to Eq. (4.9), the state ρ is separable for all p . On the other hand, we show below, the inequality Eq. (4.19) can successfully detect the entanglement in this state.

To evaluate the condition Eq. (4.19), we choose the same set of local operators as above and obtain the following inequality in the domain $p > \frac{1}{4}$:

$$3p + \sqrt{9p^2 + 8p + 8} \leq 0. \quad (4.43)$$

which is violated for all $p \in (1/4, 1]$. As clear from above, the separability criterion Eq. (4.19) detects the correct domain for entanglement, as one gets from PT criteria.

4.4.4 Discussions

It is worth noting that the usefulness of the criterion Eq. (4.19) becomes more prominent when the state under consideration is mixed in nature. In fact, when ρ is pure, the classical mixing is zero, and therefore $I(\rho, A) = V(\rho, A)$ and similarly for B . So, we have $U(\rho, A) = V(\rho, A)$ and $U(\rho, B) = V(\rho, B)$. The left-hand side of Eq. (4.18) becomes the same as that in Eq. (4.9). On the right-hand side also, $C_\rho(A, B)$ becomes equal to the covariance $Cov_\rho(A, B)$ for the pure state, which is defined by, for any ρ ,

$$Cov_\rho(A, B) = \text{Tr}(\rho AB) - (\text{Tr}\rho A)(\text{Tr}\rho B). \quad (4.44)$$

In this way, the criterion Eq. (4.9) becomes enough to identify the entanglement in two-qubit pure states. But it fails to identify the entanglement in the two-qubit and two-qutrit mixed state as we have shown above that it is satisfied by all the two-qubit and two-qutrit

mixed states, considered in this chapter.

Note that if the partial transpose is taken on the operators A and B instead of on ρ , the inequality Eq. (4.18) reduces to the SRPT inequality [131], as given by

$$(\Delta A^{PT})^2(\Delta B^{PT})^2 \geq \frac{1}{4}|\langle[A, B]^{PT}\rangle|^2 + \frac{1}{4}|\langle\{A, B\}^{PT}\rangle - 2\langle A^{PT}\rangle\langle B^{PT}\rangle|^2.$$

This inequality can detect entanglement in any pure entangled state of bipartite and tripartite systems, by experimentally measuring mean values and variances of different observables [131]. For mixed states, however, the above inequality cannot detect the entanglement of bipartite Werner states, for the entire range of the probability p , though works better than the Bell inequalities.

Note that, the criterion Eq. (4.19) cannot be experimentally verified, as it involves terms like $\text{Tr}(\sqrt{\rho}A\sqrt{\rho}A)$, which cannot be measured by usual quantum measurements. However, it is possible to set a nontrivial lower bound, that is experimentally measurable. For all ρ and A , we have $\frac{1}{2}\text{Tr}[\rho, A]^2 \geq \text{Tr}[\sqrt{\rho}, A]^2$ [153]. This implies that $I(\rho, A) \geq I^L(\rho, A) \geq 0$, i.e., the skew information has a non-negative lower bound. For the spectral decomposition, $\rho = \sum_i \lambda_i |\phi_i\rangle\langle\phi_i|$, putting $A_{ij} = \langle\phi_i|A|\phi_j\rangle$, we have $I(\rho, A) = \frac{1}{2} \sum_{ij} (\sqrt{\lambda_i} - \sqrt{\lambda_j})^2 |A_{ij}|^2$, with the lower bound $I^L(\rho, A) = \frac{1}{4} \sum_{ij} (\lambda_i - \lambda_j)^2 |A_{ij}|^2$.

4.5 Conclusions

In conclusion, we have formulated a strong entanglement criterion for mixed states. This criterion uses the Peres-Horodecki partial transposition applied to a suitable uncertainty relation. We show by explicit analysis that this criterion can be useful for not only the pure states but also several generalized forms of mixed states. For example, it can correctly reveal the lower bound of the mixing probability (i.e., $p > 1/3$) of the Bell state in the Werner state. Thus it turns out to be stronger, for the Werner state, than any other known criteria, based on, e.g., the Bell inequality, the uncertainty relation proposed

in [137] or the Schrodinger-Robertson inequality. More interestingly, this has been useful for two-qutrit mixed states as well. The strength of our criterion lies in the fact that it suitably takes care of the quantum share of the uncertainties (the Wigner-Yanase skew information) and correlations of the relevant observables. We further conjecture that the results could also be valid for all the two-qubit and two-qutrit mixed states as it has applied to certain canonical forms of these states, as shown in this chapter.

Chapter 5

Summary and Outlook

This thesis primarily focuses on the study of quantum correlations. The issues raised in this thesis are principally inspired by the conjecture that quantum synchronization and entanglement are two independent properties that are not exhibited simultaneously by two coupled quantum systems. The phenomenon of spontaneous synchronization is universal and only recent advances have been made in the quantum domain. Being synchronization a kind of temporal correlation between subsystems, it is interesting to understand its connection with other quantum correlations, specifically entanglement. It has also been observed that both the quantum synchronization measure and entanglement criterion for continuous variables are derived from the Heisenberg uncertainty principle for a set of EPR-like pairs of joint quadrature. So it is natural to expect that there can be a correlation between the two. An optomechanical system is best suited to address this issue. In this thesis, we have systematically explored the interplay between entanglement and quantum synchronization in optomechanical systems. The models that are proposed in Chapters 2 and 3 provide extensive information about the interconnection between quantum synchronization and entanglement. In Chapter 3, we have proposed a strong entanglement criterion for bipartite mixed states. In the following, we provide a comprehensive chapter-wise summary of our results.

In Chapter 1, we introduced the readers to the basics of cavity optomechanics with a brief literature survey and discussed a little bit about the various aspects of entanglement and quantum synchronization which are relevant to our thesis work.

In Chapter 2, we proposed a double cavity optomechanical model to study the interconnection between quantum synchronization and entanglement between two indirectly coupled mechanical oscillators. Each mechanical oscillator is coupled with cavity mode via a linear and quadratic dependence of their displacement from the equilibrium position. In this work, two sets of numerical results are discussed, one when the oscillators are coupled only via linear coupling to the cavity mode i.e., the quadratic coupling constant is zero, and the second when the oscillators are both linearly and quadratically coupled to their respective cavity mode. It has been found that depending on these configurations, both quantum synchronization and entanglement behave in a very distinctive manner. For instance, in the linear coupling case, we found that the oscillators are quantum synchronized with a poor degree of quantum synchronization but without entanglement. In the presence of both coupling (linear as well as quadratic), we found that the oscillators became nearly complete quantum synchronized $S_q > 0.85$ and more importantly, entanglement between the oscillators starts appearing (as E_D becomes less than 0.25) even for a very small value of quadratic coupling constant. We have also demonstrated classical synchronization, via limit cycle trajectories of the mean quadratures at long times, between the oscillator, which is a precondition to achieve quantum synchronization. We found that synchronization is more robust than entanglement with the increase in thermal excitation. We further showed that both synchronization and entanglement decrease in a similar way up to a frequency difference of 0.2 between the oscillators.

In Chapter 3, we have shown that both oscillators can be synchronized and entangled at the same time, but this feature depends on the choice of configuration of the system. In Chapter 3, we further investigated such a possibility in a different optomechanical system. We presented a more generic optomechanical system in which both the mechanical

oscillators are coupled to the same cavity mode via linear and quadratic dependence on their displacement from their respective equilibrium positions and an indirect always-on coupling also arises between the oscillators. With this realization, it has been found that when the cavity is strongly amplitude modulated with the same frequency as that of the oscillators, oscillators are nearly completely quantum synchronized and entangled at the same time. Moreover, we found that both the synchronization and entanglement exhibit a tongue, which is a quantum analog of classic Arnold tongue-like behavior. We further showed that the entanglement manifests itself as a booster to achieve near-complete quantum synchronization. We provided an analytic expression of the generalized characterization of quantum synchronization in terms of entanglement in coupled bosonic systems. This expression is valid irrespective of any specific details of the systems of interest.

In Chapter 4, we proposed a strong entanglement criterion for bipartite mixed states. Our criterion uses Peres-Horodecki partial transposition applied to a suitable uncertainty relation. The variances in this uncertainty relation do not involve any classical mixing uncertainty and are therefore purely of a quantum mechanical nature. Using the proposed criterion, we detected entanglement in pure as well as in several generalized mixed states and we found that the proposed criterion correctly reveals the parameter, as identified by the PPT criterion, detecting the entanglement of considered state. Moreover, the proposed criterion is reduced to the SRPT inequality for pure states.

Cavity optomechanics is a highly interdisciplinary field that deals with the interaction between optical and mechanical systems. The hybrid optomechanical system is created from an optomechanical system by coupling mechanical systems in the quantum regime to atoms, qubits, and ions. Such hybrid systems offer new avenues for quantum control and sensing. Probing quantum correlations in a hybrid optomechanical system is an emerging field and constantly opens up new opportunities for applications in quantum information processing. Further, this has implications for quantum information processing, precision

measurement, and quantum-enhanced technologies. Spin is an intrinsic property of quantum particles, like electrons or nuclei, and it can be thought of as a quantum analog of angular momentum. When multiple quantum particles with spin are coupled, their collective behavior can exhibit unique and non-classical characteristics. This can lead to intriguing phenomena such as entanglement and quantum correlations. So another important aspect could be the study of synchronization in coupled spin-chain systems which has no classical analogy. Exploring quantum synchronization in coupled spin-chain systems provides a platform for investigating many-body quantum dynamics.

Bibliography

- [1] G. Adesso, T. R. Bromley, and M. Cianciaruso, “Measures and applications of quantum correlations,” *Journal of Physics A: Mathematical and Theoretical*, vol. 49, no. 47, p. 473001, 2016.
- [2] Q. Zhuang, Z. Zhang, and J. H. Shapiro, “Distributed quantum sensing using continuous-variable multipartite entanglement,” *Physical Review A*, vol. 97, no. 3, p. 032329, 2018.
- [3] N. Aslam, H. Zhou, E. K. Urbach, M. J. Turner, R. L. Walsworth, M. D. Lukin, and H. Park, “Quantum sensors for biomedical applications,” *Nature Reviews Physics*, vol. 5, no. 3, pp. 157–169, 2023.
- [4] S. E. Crawford, R. A. Shugayev, H. P. Paudel, P. Lu, M. Syamlal, P. R. Ohodnicki, B. Chorpening, R. Gentry, and Y. Duan, “Quantum sensing for energy applications: Review and perspective,” *Advanced Quantum Technologies*, vol. 4, no. 8, p. 2100049, 2021.
- [5] K. Makino, Y. Hashimoto, J.-i. Yoshikawa, H. Ohdan, T. Toyama, P. van Loock, and A. Furusawa, “Synchronization of optical photons for quantum information processing,” *Science Advances*, vol. 2, no. 5, p. e1501772, 2016.

- [6] Q. Xie, G. Chen, and E. M. Bollt, “Hybrid chaos synchronization and its application in information processing,” *Mathematical and Computer Modelling*, vol. 35, no. 1-2, pp. 145–163, 2002.
- [7] C. Huygens, *Oeuvres complètes*, vol. 7. M. Nijhoff, 1897.
- [8] A. Pikovsky, M. Rosenblum, and J. Kurths, “Synchronization: a universal concept in nonlinear science,” 2002.
- [9] S. Strogatz, “Sync: The emerging science of spontaneous order,” 2004.
- [10] S. Bregni *et al.*, *Synchronization of digital telecommunications networks*. John Wiley & Sons, 2002.
- [11] T. Womelsdorf, J.-M. Schoffelen, R. Oostenveld, W. Singer, R. Desimone, A. K. Engel, and P. Fries, “Modulation of neuronal interactions through neuronal synchronization,” *science*, vol. 316, no. 5831, pp. 1609–1612, 2007.
- [12] J. Buck and E. Buck, “Mechanism of rhythmic synchronous flashing of fireflies: Fireflies of southeast asia may use anticipatory time-measuring in synchronizing their flashing,” *Science*, vol. 159, no. 3821, pp. 1319–1327, 1968.
- [13] M. Toiya, H. O. González-Ochoa, V. K. Vanag, S. Fraden, and I. R. Epstein, “Synchronization of chemical micro-oscillators,” *The Journal of Physical Chemistry Letters*, vol. 1, no. 8, pp. 1241–1246, 2010.
- [14] A. Mari, A. Farace, N. Didier, V. Giovannetti, and R. Fazio, “Measures of quantum synchronization in continuous variable systems,” *Physical Review Letters*, vol. 111, no. 10, p. 103605, 2013.
- [15] V. Ameri, M. Eghbali-Arani, A. Mari, A. Farace, F. Kheirandish, V. Giovannetti, and R. Fazio, “Mutual information as an order parameter for quantum synchronization,” *Physical Review A*, vol. 91, no. 1, p. 012301, 2015.

- [16] A. Roulet and C. Bruder, “Quantum synchronization and entanglement generation,” *Physical review letters*, vol. 121, no. 6, p. 063601, 2018.
- [17] G. Manzano, F. Galve, G. L. Giorgi, E. Hernández-García, and R. Zambrini, “Synchronization, quantum correlations and entanglement in oscillator networks,” *Scientific Reports*, vol. 3, p. 1439, 2013.
- [18] R. Horodecki, P. Horodecki, M. Horodecki, and K. Horodecki, “Quantum entanglement,” *Reviews of modern physics*, vol. 81, no. 2, p. 865, 2009.
- [19] M. Aspelmeyer, T. J. Kippenberg, and F. Marquardt, “Cavity optomechanics,” *Reviews of Modern Physics*, vol. 86, no. 4, p. 1391, 2014.
- [20] A. A. Clerk and F. Marquardt, “Basic theory of cavity optomechanics,” *Cavity Optomechanics: Nano-and Micromechanical Resonators Interacting with Light*, pp. 5–23, 2014.
- [21] V. Braginski and A. Manukin, “Ponderomotive effects of electromagnetic radiation,” *Sov. Phys. JETP*, vol. 25, no. 4, pp. 653–655, 1967.
- [22] W. Li, C. Li, and H. Song, “Quantum synchronization in an optomechanical system based on lyapunov control,” *Physical Review E*, vol. 93, no. 6, p. 062221, 2016.
- [23] H. Geng, L. Du, H. Liu, and X. Yi, “Enhancement of quantum synchronization in optomechanical system by modulating the couplings,” *Journal of Physics Communications*, vol. 2, no. 2, p. 025032, 2018.
- [24] G.-j. Qiao, H.-x. Gao, H.-d. Liu, and X. Yi, “Quantum synchronization of two mechanical oscillators in coupled optomechanical systems with kerr nonlinearity,” *Scientific Reports*, vol. 8, no. 1, p. 1, 2018.

- [25] G. Qiao, X. Liu, H. Liu, C. Sun, and X. Yi, “Quantum ϕ synchronization in a coupled optomechanical system with periodic modulation,” *Physical Review A*, vol. 101, no. 5, p. 053813, 2020.
- [26] R.-G. Yang, N. Li, J. Zhang, J. Li, and T.-C. Zhang, “Enhanced entanglement of two optical modes in optomechanical systems via an optical parametric amplifier,” *Journal of Physics B: Atomic, Molecular and Optical Physics*, vol. 50, no. 8, p. 085502, 2017.
- [27] D. Aoune, N. Benrass, N. Habiballah, and M. Nassik, “Entanglement between mechanical modes of an optomechanical system according to simon and mancini,” *Materials Today: Proceedings*, vol. 66, pp. 181–186, 2022.
- [28] Y. Li, L. Deng, T. Yin, and A. Chen, “Entanglement between two mechanical oscillators in a dual-coupling optomechanical system,” *Frontiers in Physics*, vol. 10, p. 908205, 2022.
- [29] J. M. Dobrindt, I. Wilson-Rae, and T. J. Kippenberg, “Parametric normal-mode splitting in cavity optomechanics,” *Physical Review Letters*, vol. 101, no. 26, p. 263602, 2008.
- [30] S. Huang and G. Agarwal, “Normal-mode splitting and antibunching in stokes and anti-stokes processes in cavity optomechanics: radiation-pressure-induced four-wave-mixing cavity optomechanics,” *Physical Review A*, vol. 81, no. 3, p. 033830, 2010.
- [31] S. Weis, R. Rivière, S. Deléglise, E. Gavartin, O. Arcizet, A. Schliesser, and T. J. Kippenberg, “Optomechanically induced transparency,” *Science*, vol. 330, no. 6010, pp. 1520–1523, 2010.
- [32] H. Xiong and Y. Wu, “Fundamentals and applications of optomechanically induced transparency,” *Applied physics reviews*, vol. 5, no. 3, 2018.

- [33] C. Law, “Interaction between a moving mirror and radiation pressure: A hamiltonian formulation,” *Physical Review A*, vol. 51, no. 3, p. 2537, 1995.
- [34] W. P. Bowen and G. J. Milburn, *Quantum optomechanics*. CRC press, 2015.
- [35] C. W. Gardiner and M. J. Collett, “Input and output in damped quantum systems: Quantum stochastic differential equations and the master equation,” *Physical Review A*, vol. 31, no. 6, p. 3761, 1985.
- [36] D. Walls and G. J. Milburn, “Input–output formulation of optical cavities,” *Quantum optics*, pp. 127–141, 2008.
- [37] D. Walls and G. J. Milburn, “Quantum information,” in *Quantum Optics*, pp. 307–346, Springer, 2008.
- [38] D. Vitali, S. Gigan, A. Ferreira, H. Böhm, P. Tombesi, A. Guerreiro, V. Vedral, A. Zeilinger, and M. Aspelmeyer, “Optomechanical entanglement between a movable mirror and a cavity field,” *Physical review letters*, vol. 98, no. 3, p. 030405, 2007.
- [39] E. X. DeJesus and C. Kaufman, “Routh-hurwitz criterion in the examination of eigenvalues of a system of nonlinear ordinary differential equations,” *Physical Review A*, vol. 35, no. 12, p. 5288, 1987.
- [40] S. Strogatz, “Nonlinear dynamics and chaos: with applications to physics, biology, chemistry, and engineering (cambridge, ma,” 1994.
- [41] S. J. Aton and E. D. Herzog, “Come together, right... now: synchronization of rhythms in a mammalian circadian clock,” *Neuron*, vol. 48, no. 4, pp. 531–534, 2005.
- [42] R. Adler, “A study of locking phenomena in oscillators,” *Proceedings of the IEEE*, vol. 61, no. 10, pp. 1380–1385, 1973.

- [43] Y. Kuramoto, “Cooperative dynamics of oscillator communitya study based on lattice of rings,” *Progress of Theoretical Physics Supplement*, vol. 79, pp. 223–240, 1984.
- [44] J. A. Acebrón, L. L. Bonilla, C. J. P. Vicente, F. Ritort, and R. Spigler, “The kuramoto model: A simple paradigm for synchronization phenomena,” *Reviews of modern physics*, vol. 77, no. 1, p. 137, 2005.
- [45] K. Wiesenfeld, P. Colet, and S. H. Strogatz, “Frequency locking in josephson arrays: Connection with the kuramoto model,” *Physical Review E*, vol. 57, no. 2, p. 1563, 1998.
- [46] T. E. Lee and H. Sadeghpour, “Quantum synchronization of quantum van der pol oscillators with trapped ions,” *Physical review letters*, vol. 111, no. 23, p. 234101, 2013.
- [47] S. Walter, A. Nunnenkamp, and C. Bruder, “Quantum synchronization of a driven self-sustained oscillator,” *Physical review letters*, vol. 112, no. 9, p. 094102, 2014.
- [48] T. E. Lee, C.-K. Chan, and S. Wang, “Entanglement tongue and quantum synchronization of disordered oscillators,” *Physical Review E*, vol. 89, no. 2, p. 022913, 2014.
- [49] S. Walter, A. Nunnenkamp, and C. Bruder, “Quantum synchronization of two van der pol oscillators,” *Annalen der Physik*, vol. 527, no. 1-2, pp. 131–138, 2015.
- [50] G. L. Giorgi, F. Galve, G. Manzano, P. Colet, and R. Zambrini, “Quantum correlations and mutual synchronization,” *Physical Review A*, vol. 85, no. 5, p. 052101, 2012.
- [51] G. Manzano, F. Galve, and R. Zambrini, “Avoiding dissipation in a system of three quantum harmonic oscillators,” *Physical Review A*, vol. 87, no. 3, p. 032114, 2013.

- [52] S. Boccaletti, J. Kurths, G. Osipov, D. Valladares, and C. Zhou, “The synchronization of chaotic systems,” *Physics reports*, vol. 366, no. 1-2, pp. 1–101, 2002.
- [53] S. Lorenzo, B. Militello, A. Napoli, R. Zambrini, and G. M. Palma, “Quantum synchronisation and clustering in chiral networks,” *New Journal of Physics*, vol. 24, no. 2, p. 023030, 2022.
- [54] G. L. Giorgi, F. Plastina, G. Francica, and R. Zambrini, “Spontaneous synchronization and quantum correlation dynamics of open spin systems,” *Physical Review A*, vol. 88, no. 4, p. 042115, 2013.
- [55] G. L. Giorgi, F. Galve, and R. Zambrini, “Probing the spectral density of a dissipative qubit via quantum synchronization,” *Physical Review A*, vol. 94, no. 5, p. 052121, 2016.
- [56] C. Benedetti, F. Galve, A. Mandarino, M. G. Paris, and R. Zambrini, “Minimal model for spontaneous quantum synchronization,” *Physical Review A*, vol. 94, no. 5, p. 052118, 2016.
- [57] A. K. Ekert, “Quantum cryptography based on bell’s theorem,” *Physical review letters*, vol. 67, no. 6, p. 661, 1991.
- [58] C. H. Bennett, G. Brassard, C. Crépeau, R. Jozsa, A. Peres, and W. K. Wootters, “Teleporting an unknown quantum state via dual classical and einstein-podolsky-rosen channels,” *Physical review letters*, vol. 70, no. 13, p. 1895, 1993.
- [59] A. Peres, “Separability criterion for density matrices,” *Physical Review Letters*, vol. 77, no. 8, p. 1413, 1996.
- [60] M. Horodecki, P. Horodecki, and R. Horodecki, “Separability of mixed quantum states: necessary and sufficient conditions phys,” 1996.

- [61] O. Rudolph, “Some properties of the computable cross-norm criterion for separability,” *Physical Review A*, vol. 67, no. 3, p. 032312, 2003.
- [62] M. Horodecki and P. Horodecki, “Reduction criterion of separability and limits for a class of distillation protocols,” *Physical Review A*, vol. 59, no. 6, p. 4206, 1999.
- [63] B. M. Terhal, “Bell inequalities and the separability criterion,” *Physics Letters A*, vol. 271, no. 5-6, pp. 319–326, 2000.
- [64] R. Simon, “Peres-horodecki separability criterion for continuous variable systems,” *Physical Review Letters*, vol. 84, no. 12, p. 2726, 2000.
- [65] H. Nha and M. S. Zubairy, “Uncertainty inequalities as entanglement criteria for negative partial-transpose states,” *Physical review letters*, vol. 101, no. 13, p. 130402, 2008.
- [66] H. F. Hofmann and S. Takeuchi, “Violation of local uncertainty relations as a signature of entanglement,” *Physical Review A*, vol. 68, no. 3, p. 032103, 2003.
- [67] O. Gühne and G. Tóth, “Entanglement detection,” *Physics Reports*, vol. 474, no. 1-6, pp. 1–75, 2009.
- [68] L.-M. Duan, G. Giedke, J. I. Cirac, and P. Zoller, “Inseparability criterion for continuous variable systems,” *Physical Review Letters*, vol. 84, no. 12, p. 2722, 2000.
- [69] G. S. Agarwal and A. Biswas, “Inseparability inequalities for higher order moments for bipartite systems,” *New Journal of Physics*, vol. 7, no. 1, p. 211, 2005.
- [70] S. Mancini, V. Giovannetti, D. Vitali, and P. Tombesi, “Entangling macroscopic oscillators exploiting radiation pressure,” *Physical Review Letters*, vol. 88, no. 12, p. 120401, 2002.

- [71] M. Hillery and M. S. Zubairy, “Entanglement conditions for two-mode states,” *Physical review letters*, vol. 96, no. 5, p. 050503, 2006.
- [72] E. A. Sete and C. R. Ooi, “Continuous-variable entanglement and two-mode squeezing in a single-atom raman laser,” *Physical Review A*, vol. 85, no. 6, p. 063819, 2012.
- [73] D. Antonio, D. H. Zanette, and D. López, “Frequency stabilization in nonlinear micromechanical oscillators,” *Nature communications*, vol. 3, no. 1, p. 806, 2012.
- [74] A. W. Laskar, P. Adhikary, S. Mondal, P. Katiyar, S. Vinjanampathy, and S. Ghosh, “Observation of quantum phase synchronization in spin-1 atoms,” *Physical review letters*, vol. 125, no. 1, p. 013601, 2020.
- [75] G. Heinrich, M. Ludwig, J. Qian, B. Kubala, and F. Marquardt, “Collective dynamics in optomechanical arrays,” *Physical review letters*, vol. 107, no. 4, p. 043603, 2011.
- [76] Y. Kuramoto, “International symposium on mathematical problems in theoretical physics,” *Lecture notes in Physics*, vol. 30, p. 420, 1975.
- [77] M. R. Hush, W. Li, S. Genway, I. Lesanovsky, and A. D. Armour, “Spin correlations as a probe of quantum synchronization in trapped-ion phonon lasers,” *Physical Review A*, vol. 91, no. 6, p. 061401, 2015.
- [78] M. Xu and M. Holland, “Conditional ramsey spectroscopy with synchronized atoms,” *Physical Review Letters*, vol. 114, no. 10, p. 103601, 2015.
- [79] M. Xu, D. A. Tieri, E. Fine, J. K. Thompson, and M. J. Holland, “Synchronization of two ensembles of atoms,” *Physical review letters*, vol. 113, no. 15, p. 154101, 2014.
- [80] O. Zhirov and D. Shepelyansky, “Quantum synchronization and entanglement of two qubits coupled to a driven dissipative resonator,” *Physical Review B*, vol. 80, no. 1, p. 014519, 2009.

- [81] G. Xue, M. Gong, H. Xu, W. Liu, H. Deng, Y. Tian, H. Yu, Y. Yu, D. Zheng, S. Zhao, *et al.*, “Observation of quantum stochastic synchronization in a dissipative quantum system,” *Physical Review B*, vol. 90, no. 22, p. 224505, 2014.
- [82] S. E. Nigg, “Observing quantum synchronization blockade in circuit quantum electrodynamics,” *Physical Review A*, vol. 97, no. 1, p. 013811, 2018.
- [83] L. Praxmeyer, B.-G. Englert, and K. Wódkiewicz, “Violation of bell’s inequality for continuous-variable epr states,” *The European Physical Journal D-Atomic, Molecular, Optical and Plasma Physics*, vol. 32, pp. 227–231, 2005.
- [84] A. Ferraro and M. G. Paris, “Nonlocality of two-and three-mode continuous variable systems,” *Journal of Optics B: Quantum and Semiclassical Optics*, vol. 7, no. 6, p. 174, 2005.
- [85] D. Witthaut, S. Wimberger, R. Burioni, and M. Timme, “Classical synchronization indicates persistent entanglement in isolated quantum systems,” *Nature communications*, vol. 8, no. 1, p. 1, 2017.
- [86] I. Wilson-Rae, N. Nooshi, W. Zwerger, and T. J. Kippenberg, “Theory of ground state cooling of a mechanical oscillator using dynamical backaction,” *Physical review letters*, vol. 99, no. 9, p. 093901, 2007.
- [87] O. Arcizet, P.-F. Cohadon, T. Briant, M. Pinard, and A. Heidmann, “Radiation-pressure cooling and optomechanical instability of a micromirror,” *Nature*, vol. 444, no. 7115, pp. 71–74, 2006.
- [88] J. Chan, T. M. Alegre, A. H. Safavi-Naeini, J. T. Hill, A. Krause, S. Gröblacher, M. Aspelmeyer, and O. Painter, “Laser cooling of a nanomechanical oscillator into its quantum ground state,” *Nature*, vol. 478, no. 7367, pp. 89–92, 2011.

- [89] T. Palomaki, J. Teufel, R. Simmonds, and K. W. Lehnert, “Entangling mechanical motion with microwave fields,” *Science*, vol. 342, no. 6159, pp. 710–713, 2013.
- [90] A. Szorkovszky, A. C. Doherty, G. I. Harris, and W. P. Bowen, “Mechanical squeezing via parametric amplification and weak measurement,” *Physical review letters*, vol. 107, no. 21, p. 213603, 2011.
- [91] K. Jähne, C. Genes, K. Hammerer, M. Wallquist, E. Polzik, and P. Zoller, “Cavity-assisted squeezing of a mechanical oscillator,” *Physical Review A*, vol. 79, no. 6, p. 063819, 2009.
- [92] J. Thompson, B. Zwickl, A. Jayich, F. Marquardt, S. Girvin, and J. Harris, “Strong dispersive coupling of a high-finesse cavity to a micromechanical membrane,” *Nature*, vol. 452, no. 7183, pp. 72–75, 2008.
- [93] A. Nunnenkamp, K. Børkje, J. Harris, and S. Girvin, “Cooling and squeezing via quadratic optomechanical coupling,” *Physical Review A*, vol. 82, no. 2, p. 021806, 2010.
- [94] J.-Q. Liao and F. Nori, “Single-photon quadratic optomechanics,” *Scientific reports*, vol. 4, no. 1, pp. 1–9, 2014.
- [95] T. P. Purdy, D. Brooks, T. Botter, N. Brahms, Z.-Y. Ma, and D. M. Stamper-Kurn, “Tunable cavity optomechanics with ultracold atoms,” *Physical review letters*, vol. 105, no. 13, p. 133602, 2010.
- [96] S. Sainadh and M. A. Kumar, “Effects of linear and quadratic dispersive couplings on optical squeezing in an optomechanical system,” *Physical Review A*, vol. 92, no. 3, p. 033824, 2015.
- [97] A. Xuereb and M. Paternostro, “Selectable linear or quadratic coupling in an optomechanical system,” *Physical Review A*, vol. 87, no. 2, p. 023830, 2013.

- [98] T. Rocheleau, T. Ndukum, C. Macklin, J. Hertzberg, A. Clerk, and K. Schwab, “Preparation and detection of a mechanical resonator near the ground state of motion,” *Nature*, vol. 463, no. 7277, pp. 72–75, 2010.
- [99] L. Zhang and H.-Y. Kong, “Self-sustained oscillation and harmonic generation in optomechanical systems with quadratic couplings,” *Physical Review A*, vol. 89, no. 2, p. 023847, 2014.
- [100] H. Shi and M. Bhattacharya, “Quantum mechanical study of a generic quadratically coupled optomechanical system,” *Physical Review A*, vol. 87, no. 4, p. 043829, 2013.
- [101] J. C. Sankey, C. Yang, B. M. Zwickl, A. M. Jayich, and J. G. Harris, “Strong and tunable nonlinear optomechanical coupling in a low-loss system,” *Nature Physics*, vol. 6, no. 9, pp. 707–712, 2010.
- [102] N. Flowers-Jacobs, S. Hoch, J. Sankey, A. Kashkanova, A. Jayich, C. Deutsch, J. Reichel, and J. Harris, “Fiber-cavity-based optomechanical device,” *Applied Physics Letters*, vol. 101, no. 22, p. 221109, 2012.
- [103] G. S. Agarwal and A. Biswas, “Inseparability inequalities for higher order moments for bipartite systems,” *New Journal of Physics*, vol. 7, p. 211, 2005.
- [104] S. Chakraborty and A. K. Sarma, “Quantum synchronization and correlation in bidirectionally and unidirectionally coupled optomechanical oscillators,” *arXiv preprint arXiv:1908.07296*, 2019.
- [105] A. Prasad, “Universal occurrence of mixed-synchronization in counter-rotating nonlinear coupled oscillators,” *Chaos, Solitons & Fractals*, vol. 43, no. 1-12, pp. 42–46, 2010.

- [106] A. Sharma and M. Dev Shrimali, “Experimental realization of mixed-synchronization in counter-rotating coupled oscillators,” *Nonlinear Dynamics*, vol. 69, pp. 371–377, 2012.
- [107] M. J. Leone, B. N. Schurter, B. Letson, V. Booth, M. Zochowski, and C. G. Fink, “Synchronization properties of heterogeneous neuronal networks with mixed excitability type,” *Physical Review E*, vol. 91, no. 3, p. 032813, 2015.
- [108] G. Tang, K. Xu, and L. Jiang, “Synchronization in a chaotic neural network with time delay depending on the spatial distance between neurons,” *Physical Review E*, vol. 84, no. 4, p. 046207, 2011.
- [109] J. Cao and R. Li, “Fixed-time synchronization of delayed memristor-based recurrent neural networks,” *Science China Information Sciences*, vol. 60, no. 3, p. 1, 2017.
- [110] S. Vaidyanathan, “Dynamics and control of tokamak system with symmetric and magnetically confined plasma,” *Int J ChemTech Res*, vol. 8, no. 6, p. 795, 2015.
- [111] T. E. Lee and H. Sadeghpour, “Quantum synchronization of quantum van der pol oscillators with trapped ions,” *Physical Review Letters*, vol. 111, no. 23, p. 234101, 2013.
- [112] S. Shirasaka, N. Watanabe, Y. Kawamura, and H. Nakao, “Optimizing stability of mutual synchronization between a pair of limit-cycle oscillators with weak cross coupling,” *Physical Review E*, vol. 96, no. 1, p. 012223, 2017.
- [113] B. Van der Pol and J. Van der Mark, “Frequency demultiplication,” *Nature*, vol. 120, no. 3019, p. 363, 1927.
- [114] L. M. Pecora and T. L. Carroll, “Synchronization in chaotic systems,” *Physical Review Letters*, vol. 64, no. 8, p. 821, 1990.

- [115] N. Jaseem, M. Hajdušek, P. Solanki, L.-C. Kwek, R. Fazio, and S. Vinjanampathy, “Generalized measure of quantum synchronization,” *Physical Review Research*, vol. 2, no. 4, p. 043287, 2020.
- [116] D. Garg, Manju, S. Dasgupta, and A. Biswas, “Quantum synchronization and entanglement of indirectly coupled mechanical oscillators in cavity optomechanics: A numerical study,” *Physics Letters A*, vol. 457, p. 128557, 2023.
- [117] G. L. Giorgi, F. Galve, G. Manzano, P. Colet, and R. Zambrini, “Quantum correlations and mutual synchronization,” *Physical Review A*, vol. 85, p. 052101, 2012.
- [118] D. Viennot and L. Aubourg, “Quantum chimera states,” *Physics Letters A*, vol. 380, p. 678683, 2016.
- [119] V. M. Bastidas, I. Omelchenko, A. Zakharova, E. Schöll, and T. Brandes, “Quantum signatures of chimera states,” *Physical Review E*, vol. 92, p. 062924, 2015.
- [120] S. Siwiak-Jaszek, T. P. Le, and A. Olaya-Castro, “Synchronization phase as an indicator of persistent quantum correlations between subsystems,” *Physical Review A*, vol. 102, no. 3, p. 032414, 2020.
- [121] Y. Shen, H. Yi Soh, W. Fan, and L.-C. Kwek, “Enhancing quantum synchronization through homodyne measurement and squeezing,” *arXiv:2302.13465*, 2023.
- [122] Y. Kato and H. Nakao, “Enhancement of quantum synchronization via continuous measurement and feedback control,” *New Journal of Physics*, vol. 23, p. 013007, 2021.
- [123] L. Du, C.-H. Fan, H.-X. Zhang, and J.-H. Wu, “Synchronization enhancement of indirectly coupled oscillators via periodic modulation in an optomechanical system,” *Scientific Reports*, vol. 7, no. 1, p. 1, 2017.

- [124] J. Sheng, X. Wei, C. Yang, and H. Wu, “Self-organized synchronization of phonon lasers,” *Physical review letters*, vol. 124, no. 5, p. 053604, 2020.
- [125] P. Piergentili, W. Li, R. Natali, N. Malossi, D. Vitali, and G. Di Giuseppe, “Two-membrane cavity optomechanics: non-linear dynamics,” *New Journal of Physics*, vol. 23, no. 7, p. 073013, 2021.
- [126] V. Giovannetti and D. Vitali, “Phase-noise measurement in a cavity with a movable mirror undergoing quantum brownian motion,” *Physical Review A*, vol. 63, no. 2, p. 023812, 2001.
- [127] A. Mari and J. Eisert, “Gently modulating optomechanical systems,” *Physical Review Letters*, vol. 103, no. 21, p. 213603, 2009.
- [128] S. Huang and G. Agarwal, “Entangling nanomechanical oscillators in a ring cavity by feeding squeezed light,” *New Journal of Physics*, vol. 11, no. 10, p. 103044, 2009.
- [129] L. Mandel and E. Wolf, *Optical coherence and quantum optics*. Cambridge University Press, New York, 1995.
- [130] T. E. Lee, C.-K. Chan, and S. Wang, “Entanglement tongue and quantum synchronization of disordered oscillators,” *Physical Review E*, vol. 89, p. 022913, 2014.
- [131] J. Gillet, T. Bastin, and G. S. Agarwal, “Multipartite entanglement criterion from uncertainty relations,” *Physical Review A*, vol. 78, no. 5, p. 052317, 2008.
- [132] J. F. Clauser and A. Shimony, “Bell’s theorem. experimental tests and implications,” *Reports on Progress in Physics*, vol. 41, no. 12, p. 1881, 1978.
- [133] D. Girolami, T. Tufarelli, and G. Adesso, “Characterizing nonclassical correlations via local quantum uncertainty,” *Physical Review Letters*, vol. 110, no. 24, p. 240402, 2013.

- [134] S. Furuichi, “Schrödinger uncertainty relation with Wigner-Yanase skew information,” *Physical Review A*, vol. 82, no. 3, p. 034101, 2010.
- [135] J. S. Bell, “On the Einstein Podolsky Rosen paradox,” *Physics Physique Fizika*, vol. 1, no. 3, p. 195, 1964.
- [136] J. F. Clauser, M. A. Horne, A. Shimony, and R. A. Holt, “Proposed experiment to test local hidden-variable theories,” *Physical Review Letters*, vol. 23, no. 15, p. 880, 1969.
- [137] O. Gühne, P. Hyllus, D. Bruß, A. Ekert, M. Lewenstein, C. Macchiavello, and A. Sanpera, “Detection of entanglement with few local measurements,” *Physical Review A*, vol. 66, no. 6, p. 062305, 2002.
- [138] E. P. Wigner and M. M. Yanase, “Information contents of distributions,” in *Part I: Particles and Fields. Part II: Foundations of Quantum Mechanics*, pp. 452–460, Springer, 1997.
- [139] S. Luo, S. Fu, and C. H. Oh, “Quantifying correlations via the Wigner-Yanase skew information,” *Physical Review A*, vol. 85, no. 3, p. 032117, 2012.
- [140] C.-s. Yu, “Quantum coherence via skew information and its polygamy,” *Physical Review A*, vol. 95, no. 4, p. 042337, 2017.
- [141] Z. Chen, “Wigner-Yanase skew information as tests for quantum entanglement,” *Physical Review A*, vol. 71, no. 5, p. 052302, 2005.
- [142] S. Lei and P. Tong, “Wigner-Yanase skew information and quantum phase transition in one-dimensional quantum spin-1/2 chains,” *Quantum Information Processing*, vol. 15, no. 4, pp. 1811–1825, 2016.
- [143] S. Luo, “Wigner-Yanase skew information and uncertainty relations,” *Physical Review Letters*, vol. 91, no. 18, p. 180403, 2003.

- [144] S. Luo and Q. Zhang, “On skew information,” *IEEE Transactions on information theory*, vol. 50, no. 8, pp. 1778–1782, 2004.
- [145] S. Luo, “Heisenberg uncertainty relation for mixed states,” *Physical Review A*, vol. 72, no. 4, p. 042110, 2005.
- [146] S. Luo, “Quantum versus classical uncertainty,” *Theoretical and mathematical physics*, vol. 143, no. 2, pp. 681–688, 2005.
- [147] S. Luo, “Quantum uncertainty of mixed states based on skew information,” *Physical Review A*, vol. 73, no. 2, p. 022324, 2006.
- [148] A. S. Holevo, *Probabilistic and statistical aspects of quantum theory*, vol. 1. Springer Science & Business Media, 2011.
- [149] E. Schrödinger, “About Heisenberg uncertainty relation,” *arXiv preprint quant-ph/9903100*, 1999.
- [150] T. Hiroshima and S. Ishizaka, “Local and nonlocal properties of Werner states,” *Physical Review A*, vol. 62, no. 4, p. 044302, 2000.
- [151] S. Adhikari, A. S. Majumdar, S. Roy, B. Ghosh, and N. Nayak, “Teleportation via maximally and non-maximally entangled mixed states,” *arXiv preprint arXiv:0812.3772*, 2008.
- [152] H. Wang and K. He, “Quantum tomography of two-qutrit werner states,” in *Photonics*, vol. 9, p. 741, MDPI, 2022.
- [153] D. Girolami, “Observable measure of quantum coherence in finite dimensional systems,” *Physical Review Letters*, vol. 113, no. 17, p. 170401, 2014.

List of Publications

Peer-reviewed Journals:

1. D. Garg, **Manju**, S. Dasgupta and A. Biswas, “*Quantum synchronization and entanglement of indirectly coupled mechanical oscillators in cavity optomechanics: A numerical study*”, Phys. Lett. A **457**, 128557 (2022). <https://doi.org/10.1016/j.physleta.2022.128557>
2. **Manju**, S. Dasgupta and A. Biswas, “*Entanglement boosts quantum synchronization between two oscillators in an optomechanical setup*”, Phys. Lett. A **482**, 129039 (2023). <https://doi.org/10.1016/j.physleta.2023.129039>
3. **Manju**, A. Biswas and S. Dasgupta “*Strong entanglement criteria for mixed states, based on uncertainty relations*”, Journal of Physics A: Mathematical and Theoretical **56**, 025304 (2023). <https://doi.org/10.1088/1751-8121/acb4c9>

Presentations and Conferences

Conference Attended:

1. **QIQT 2019**, The Summer School on quantum information and quantum technology, June 13-July 23, 2019, at IISER, Kolkata.

Poster Presentation:

1. **COPaQ-2022**, Quantum synchronization and entanglement of two mechanical oscillators, using parametric interactions, in coupled optomechanical systems, November 10-13, 2022, at IIT Roorkee.
2. **Physics Day**, Quantum synchronization and entanglement of indirectly coupled mechanical oscillators in cavity optomechanics: A numerical study, March 4, 2023, at IIT Ropar.
3. **OPTIQ-2023**, An uncertainty relation based study of quantum correlations in optomechanical systems, December 11-13, 2023, at Cochin University, Kerala.

Oral Presentation:

1. **Photonics 2023**, An Uncertainty-Based Unified Approach Towards Quantum Synchronization and Entanglement in Optomechanical Systems, July 5-8, 2023, at IISc Bengaluru.
2. **OPTIQ 2023**, An Uncertainty Relation Based Study of Quantum Correlations, December 11-13, 2023, at Cochin University, Kerala.